This is to certify that the
dissertation entitled

Improving the Durability and Mechanical Properties of Wood-Plastic Composites Through Coextrusion

presented by

Shan Jin

has been accepted towards fulfillment
of the requirements for the

Ph.D. degree in Forestry

Laurent Matuana
Major Professor's Signature

July 29, 2010
Date

IMPROVING THE DURABILITY AND MECHANICAL PROPERTIES OF WOOD-PLASTIC COMPOSITES THROUGH COEXTRUSION

By

Shan Jin

A DISSERTATION

Submitted to
Michigan State University
in partial fulfillment of the requirements
for the degree of

DOCTOR OF PHILOSOPHY

Forestry

2010

ABSTRACT

IMPROVING THE DURABILITY AND MECHANICAL PROPERTIES OF WOOD-PLASTIC COMPOSITES THROUGH COEXTRUSION

By

Shan Jin

Wood-plastic composites (WPCs) can absorb moisture in a humid environment due to the hydrophilic nature of the wood in the composites, making products susceptible to microbial growth and loss of mechanical properties. This study tested the concept of using coextrusion technology to manufacture two-layer coextruded wood-plastic composites encapsulated with a plastic surface-rich cap layer for improving their water resistance, mechanical performance, and weathering resistance. The results indicated that WPCs can be encapsulated by a neat rigid PVC or HDPE cap layer, or a PVC-based composites (wood flour or carbon nanotube filled rigid PVC) cap layer in a coextrusion process. The moisture uptake rate was lower when a PVC surface-rich cap layer was applied in the composites, and the extent of the decrease was a strong function of the amount of wood flour in the cap layer but insensitive to cap layer thickness. Coextruding PVC surface-rich cap layers on WPCs significantly increased the flexural strength but decreased the flexural modulus as compared with those of control samples. The changes in bending properties were sensitive to both cap layer thickness and wood flour content in the cap. In order to obtain coextruded WPCs with better flexural properties than uncapped WPCs, a two-level factorial design was used to evaluate the statistical effects of material compositions and processing conditions on these properties. Material composition variables were the wood flour content in the core layer and the carbon nanotube (CNT) content in the cap layer of coextruded composites. The processing condition variable

was the processing temperature profile for the core layer. Factors leading to a fast fusion of the PVC-wood flour composites in the core layer, i.e. low wood flour content and high processing temperature, improved the flexural properties of coextruded composites. Reinforcing the cap layer with CNTs produced a significant improvement in the flexural properties of the coextruded composites, insensitive to the core layer composition and the processing temperature condition. Moreover, this study also examined the effect of coextruding a clear HDPE cap layer onto HDPE/wood-flour composites on the discoloration of coextruded composites exposed to accelerated UV weathering tests. Two separate discoloration characteristics occurred in the discoloration of composites. For uncapped WPCs, chemical changes due to photooxidation resulted in darkening followed by physical changes, including loss of colored wood components from the surface, as well as increased roughness on the surface, which led to lightening of WPCs. By contrast, because a hydrophobic cap layer prevented the loss of colored components from the surface, coextruding a clear hydrophobic HDPE cap layer over WPCs significantly decreased the discoloration upon weathering. Photooxidation of wood components at the interface accounted for the discoloration of coextruded WPCs before the failure of cap layer. As the cap layer absorbed a specified amount of UV light and reduced oxygen available to interface, it decreased the photooxidation rate at the interface compared to that at the WPCs surface.

Dedicated to my parents

WEI yueming and JIN jiazhen

ACKNOWLEDGEMENTS

First and foremost, I am grateful to my advisor, Dr. Laurent Matuana, for giving me this great opportunity to further my education in the field of composites materials, and for all of his support, guidance, and encouragement. I also thank my other committee members, Dr. Donatien Pascal Kamdem, Dr. Pascal Nzokou, and Dr. Maria Rubino. Their advice helped me expand my understanding of research.

Assistance with FTIR from Dr. Ruth Smith, Dr. Rui Huang, and Dr. Faai Zhang in the Department of Chemistry as well as UV/VIS from Kelby Thayer in the School of Packaging is appreciated. I am thankful for the following staffs in the Department of Forestry for their assistance throughout my graduate program: Juli Kerr, Carol Graysmith, Barb Anderson, and Karen Ellerhorst. I am also grateful to all my colleagues (Dr. Omar Faruk, Carlos Diaz, Kojo Afrifah, etc.) in the Biocomposites Manufacturing Laboratory for their continued help and support.

This work was financially supported by the USDA-CSREES Grant-Advanced Technology Applications to Eastern Hardwood Utilization (Grant No: 2006-34158-17581 and 2008-34158-19510). An additional thank you to the companies listed in the text of chapters 3, 4, and 5 for generously donating the materials used in the research.

TABLE OF CONTENTS

CHAPTER 3

CHAPTER 4

CHAPTER 5

Ultraviolet Weathering of HDPE/Wood-Flour Composites Coextruded with a Clear HDPE Cap Layer 155

CHAPTER 6

LIST OF TABLES

LIST OF FIGURES

Images in this thesis/dissertation are presented in color.

LIST OF ABBREVIATIONS

BP -- Hydroxybenzophenone

BTZ -- Hydroxyphenylbenzotriazole

CNT -- Carbon Nanotube

EMC -- Equilibrium Moisture Content

FTIR -- Fourier Transform Infrared Spectrometer

HALS -- Hindered Amine Light Stabilizers

HDPE -- High Density Polyethylene

HPT -- Hydroxyphenyl-s-triazine

LDPE -- Low Density Polyethylene

LLDPE -- Linear Low Density Polyethylene

MC -- Moisture Content

MFI -- Melt Flow Index

MOR -- Modulus of Rupture (strength)

MOE -- Modulus of Elasticity (stiffness)

MUR -- Moisture Uptake Rate

PE -- Polyethylene (high-density or low-density)

phr -- Parts Per Hundred Parts of Resin

PVC -- Polyvinyl Chloride

RH -- Relative Humidity

SEM -- Scanning Electron Microscopy

UV -- Ultraviolet (rays or light)

UVA	--	UV Absorbers
WPCs	--	Wood-Plastic Composites
XPS	--	X-ray Photoelectron Spectroscopy

CHAPTER 1

Introduction

1.1 Introduction

Wood-plastic composites (WPCs) are manufactured by mixing wood fiber and plastics through plastic processing procedures such as compression, extrusion or injection molding [1-5]. Wood residue and recycled plastics can be used to produce WPCs, saving waste disposals and reducing the raw material cost [6-7].

Wood-plastic composites combine the excellent properties of both wood and plastics. They are stiffer and more environmentally friendly compared to unfilled plastic owing to the greater stiffness and degradability of wood fibers compared to plastics [4-5]. Wood-plastic composites also require less maintenance than solid wood due to their hydrophobic polymer phase [8].

Due to these attributes, wood-plastic composites have experienced significant market expansion in recent years as a replacement for solid wood, mainly in outdoor applications such as railings, decking, fences, and window and door frames [9-10]. These products are marketed as low-maintenance and weather-resistant compared to solid wood, because the wood fiber in WPCs can be encapsulated in a hydrophobic polymer matrix [11-12]. Moreover, most of current WPC manufacturers are offering 15 to 20 years of warranty on their products. However, as WPCs are exposed to an outdoor environment of moisture and ultraviolet light (UV), the expectation that the products would maintain their new appearance without maintenance is not realistic [13].

When in ground contact, WPCs can be damaged by biological agents such as fungi and termites. Microbial degradation results in surface stains and loss in both weight and mechanical properties [14-17]. In an aboveground outdoor environment, moisture and UV result in degradation of WPCs [18-23]. Moisture absorption reduces the adhesion between the wood fiber and the polymer matrix, leading to loss of mechanical properties [18-19]. Photodegradation can result in breakdown of both wood fiber and polymer chains, causing loss in appearance and mechanical properties [20-23].

In addition, water absorption is a critical factor in both microbial degradation and photodegradation. Wood decay fungi require wood moisture contents in excess of fiber saturation to propagate, thus moisture content of 25-30% is necessary for fungal decay [14]. In a photodegradation process, the presence of water accelerates oxidation reactions, removes degraded components, and swells the wood fiber facilitating light penetration, all of which would accelerate color fading and/or mechanical properties loss [24]. Therefore, improving the water resistance of WPCs is key to enhance the durability. It is necessary to reduce or delay the moisture uptake of WPCs to prolong their long term performance.

Many researchers have investigated the moisture/water absorption behaviors of natural fiber–plastic composites. Marcovich et al. investigated moisture diffusion in polyester-(wood flour) composites and found that the equilibrium moisture content of the composites was dependent on the size and shape of the wood flour [25]. Stark studied the influence of moisture absorption on the mechanical properties of (wood flour)-

polypropylene composites and reported that incomplete encapsulation of wood flour by the polypropylene matrix occurs in both 20% and 40% wood flour composites [18]. In addition, she demonstrated that more moisture was absorbed by the composites with higher wood flour loading, a situation that resulted in a significant decrease of both flexural and tensile properties. Similar results were reported by Bledzki and Faruk, who found that the impact properties of (wood fiber)–polypropylene composites were affected by moisture content [19]. Hygrothermal aging behavior of injection-molded (rice husk)-filled polypropylene composites also has been examined by immersing the specimens in distilled water at 30°C and 90°C [26]. It was found that both the tensile strength and the modulus deteriorated after immersion in water, the extent of the deterioration being dependent on the immersion temperature. This reduction in tensile properties was attributed to the interfacial degradation in the composites.

Although several authors have investigated the moisture/water absorption, biological degradation and photodegradation behaviors of (natural fiber)-plastic composites, only a few provided the methods to alleviate these problems. Current approaches to improving the durability of WPCs focus on the bulk of WPCs, i.e., incorporation of additives into the entire product. For example, adding coupling agents improves the adhesion between the wood fiber and the polymer matrix [19]; adding photostabilizers and pigments provides UV protection [24, 27-28]; adding biocides prevents fungi and termite attacks [29]. However, the weathering effect primarily occurs at the material surface [20-24, 30]. Adding preservatives to the bulk of material is an expensive way to cope with weathering. WPCs with weathering protection on the surface only will be a cost-effective way to improve durability. There are several methods for providing a surface that can withstand weathering.

Coating is one of the methods widely used to improve the durability of wood composites [31-33]. However, due to low surface energy of plastic it is difficult to coat the plastic components at the surface of WPCs. Also, coating involves solvent evaporation, which often causes environmental concerns. Furthermore, drying stages require extra time and reduce efficiency of assembly line.

Lamination is another method for providing a protective surface. Through melt fusion or an adhesive layer, a surface layer can be laminated over substrate. But, when those laminated composites are bent, delamination often occurs [34]. Moreover, it is difficult to use lamination technology to manufacture a fully encapsulated structure other than a planar layered structure.

Coextrusion is another method for providing a protective surface since coextrusion technology can produce a multilayered product with different properties at outer and inner layers, thus offering different properties between surface and bulk [35-36]. The benefit of coextrusion is that each layer of coextruded material offers a particular property, including impermeability or resistance to moisture uptake and improved mechanical properties, such as stiffness, depending on the compositions of the outer and inner layers. For example, when composites are bent, one side suffers maximum compressive stress, and the other side suffers maximum tensile stress [37]. Therefore, the composition of the outer layer will influence not only the durability, but also the flexural properties of the overall composites.

Coextrusion technology is a promising method to manufacture WPCs with a durable surface since the additives involved in durability improvement will only be incorporated into the outer layer of WPCs rather than into the entire product. As a result, the durability of WPCs product could be improved in a cost-effective way. Similarly, flexural properties of coextruded products are related to the surface property of materials. Thus, if the surface layer is reinforced with nanofillers such as nanoclays or carbon nanotubes [38-39], the flexural properties of the composites would be increased accordingly.

Although the coextrusion process has been extensively studied for polymers to manufacture multilayer films, sheet, and tubing [40-42], there is no published work on the use of this innovative technology for the development of wood-plastic composites with enhanced mechanical performance and durability, which is the main goal of this research.

1.2 Hypotheses

In this project, we plan to test the following hypotheses:

1. Coextruding a plastic rich outer layer on WPCs is an effective way to improve the durability of WPCs in terms of water/vapor and weathering resistance;
2. Coextruding a reinforced outer layer on WPCs will enhance the flexural properties of WPCs.

1.3 Objectives

This project tests the idea of using coextrusion technology to make two-layer coextruded encapsulated WPCs for improving their mechanical performance and durability in a cost-effective way. The following specific objectives will be addressed:

a. Investigate the effects of cap layer compositions (cap layer type and wood flour content) and processing conditions (affecting cap layer thickness) on the water/vapor absorption behaviors of both noncoextruded WPCs (control) and coextruded WPCs with the ultimate goal of identifying the moisture resistant WPC formulations;

b. Analyze the effects of cap layer formulation (unfilled vs. carbon nanotube filled), core layer formulation (wood flour content) and melt rheology (high and low temperature profile for the core layer) on the flexural properties of both control and coextruded WPCs in order to statistically model and optimize the material compositions-processing conditions-properties relationships;

c. Investigate the effects of cap layer types (noncoextruded vs. coextruded) and weathering conditions on the UV degradation of both control and coextruded WPCs to understand the role of the cap layer in the mechanisms involved in weathering of WPCs.

Coextruded WPCs that will improve the durability (in terms of resistance to moisture absorption and weathering) and mechanical performance of WPCs in an effective way is expected to result from this project. Moreover, reduced cost of weathering protection and enhanced performance will spur the application of WPCs and utilization of wood from forest products industry.

1.4 Structure of Dissertation

The first chapter introduces the rationale of this research. A broad background on wood-plastic composites was reviewed in the second chapter. The influence of the cap layer types on the flexural properties and water resistance of WPCs was discussed in Chapter 3. The material composition-processing condition-flexural property relationships for coextruded WPCs were analyzed and modeled in Chapter 4. Chapter 5 examined the ultraviolet weathering of HDPE/wood-flour composites coextruded with a clear HDPE cap layer in order to gain an in-depth understanding of the role of transparent HDPE cap layer on the UV resistance of WPCs. Finally, Chapter 6 provides the overall conclusions and future work on the role of coextruding a plastic rich cap layer on the durability of WPCs.

1.5 References

1. C.M. Clemons, Wood-plastic composites in the United States: the interfacing of two industries, *Forest Products Journal*, **52**(6): 10-18 (2002).
2. A.K. Bledzki, J. Gassan, and S. Theis, Wood-filled thermoplastic composites, *Mechanics of Composite Materials*, **34**(6): 563-568 (1998).
3. D.N. Saheb and J.P. Jog, Natural fiber polymer composites: a review, *Advances in Polymer Technology*, **18** (4): 351–363 (1999).
4. M. Bengtsson and K. Oksman, Silane crosslinked wood plastic composites: Processing and properties, *Composites Science and Technology*, **66**(13): 2177-2186 (2006).
5. A. Ashori, Wood–plastic composites as promising green-composites for automotive industries, *Bioresource Technology,* **99**(11): 4661-4667 (2008).
6. S.K. Najafi, A. Kiaefar, and E. Hamidina, Water absorption behavior of composites from sawdust and recycled Plastics, *Journal of Reinforced Plastics and Composites,* **26**(3): 341-348 (2007).
7. Y Lei, Q. Wu, F Yao, and Y. Xu, Preparation and properties of recycled HDPE/natural fiber composites, *Composites Part A: Applied Science and Manufacturing*, **38**(7): 1664-1674 (2007).
8. J.J. Morrell, N.M. Stark, D.E. Pendleton, and A.G. McDonald, Durability of wood-plastic composites, *Wood Design Focus*, **16**(3): 7-10 (2006).
9. A. Jacob, WPC industry focuses on performance and cost, *Reinforced Plastics*, **50**(5): 32-33 (2006).
10. J. Markarian, Outdoor living space drives growth in wood-plastic composites, *Reinforced Plastics*, **10**(4): 20-25 (2008).
11. J.M. Pilarski and L.M. Matuana, Durability of wood flour-plastic composites exposed to accelerated freeze-thaw cycling. Part I. Rigid PVC matrix, *Journal of Vinyl & Additive Technology*, **11**(1): 1-8 (2005).
12. J.M. Pilarski and L.M. Matuana, Durability of wood flour-plastic composites exposed to accelerated freeze-thaw cycling. Part II. High density polyethylene matrix, *Journal of Applied Polymer Science*, **100**(35): 35-39 (2006).
13. J. Markarian, Wood-plastic composites need protection, *Plastics Engineering*, **63**(7): 54-56 (2007).
14. C.M. Clemons and E.R. Ibach, Application of laboratory fungal resistance tests to solid wood and wood-plastic composite, *Plastics in Building Construction*, **27**(2): 7-14 (2003).

15. A. Schirp and M.P. Wolcott, Influence of fungal decay and moisture absorption on mechanical properties of extruded wood-plastic composites, *Wood and Fiber Science*, **37**(4): 643-652 (2005).

16. B. Dawson-Andoh, L.M. Matuana, and J. Harrison, Susceptibility of high density polyethylene/wood-flour composite to mold discoloration, *Journal of the Institute of Wood Science*, **17**(2): 114-119 (2005).

17. B. Dawson-Andoh, L.M. Matuana, and J. Harrison, Mold susceptibility of rigid PVC/wood-flour composites, *Journal of Vinyl & Additive Technology*, **10**(4): 179-186 (2004).

18. N.M. Stark, Influence of moisture absorption on mechanical properties of wood flour-polypropylene composites, *Journal of Thermoplastic Composite Materials*, **14**(5): 421-432 (2001).

19. A.K. Bledzki and O. Faruk, Creep and impact properties of wood fibre–polypropylene composites: Influence of temperature and moisture content, *Composites Science and Technology*, **64**(5): 693-700 (2004).

20. L.M. Matuana and D.P. Kamdem, Accelerated ultraviolet weathering of PVC/wood-flour composites, *Polymer Engineering and Science*, **42**(8): 1657-1666 (2002).

21. N.M. Stark and L.M. Matuana, Surface chemistry and mechanical property changes of wood-flour/high-density-polyethylene composites after accelerated weathering, *Journal of Applied Polymer Science*, **94**(6): 2263-2273 (2004).

22. N.M. Stark and L.M. Matuana, Surface chemistry changes of weathered HDPE/wood-flour composites studied by XPS and FTIR spectroscopy, *Polymer Degradation and Stability*, **86**(1): 1-9 (2004).

23. N.M. Stark and L.M. Matuana, Characterization of weathered wood–plastic composite surfaces using FTIR spectroscopy, contact angle, and XPS, *Polymer Degradation and Stability*, **92**(10): 1883-1890 (2007).

24. N.M. Stark and L.M. Matuana. Influence of photostabilizers on wood flour-HDPE composites exposed to xenon-arc radiation with and without water spray, *Polymer Degradation and Stability*, 91 (12): 3048-3056 (2006).

25. N.E. Marcovich, M.M. Reboredo, and M.I. Aranguren, Moisture diffusion in polyester–woodflour composites, *Polymer*, **40**(26): 7313–7320 (1999).

26. Z.A. M. Ishak, B.N. Yow, B.L. Ng, H.P.S.A. Khalil, and H.D. Rozman, Hygrothermal aging and tensile behavior of injection-molded rice husk-filled polypropylene composites, *Journal of Applied Polymer Science*, **81**(3): 742-753 (2001).

27. N.M. Stark and L.M. Matuana, Ultraviolet weathering of photostabilized wood-flour-filled high density polyethylene composites, *Journal of Applied Polymer Science*, **90**(10): 2609-2617 (2003).

28. M. Muasher and M. Sain, The efficacy of photostabilizers on the color change of wood filled plastic composites, *Polymer Degradation and Stability*, **91**(5): 1156-1165 (2006).

29. D.E. Pendleton, T.A. Hoffard, T. Adcock, B. Woodward, and M.P. Wolcott, Durability of extruded HDPE/wood composites, *Forest Products Journal*, **52**(6): 21-27 (2002).

30. D.N. -S Hon, *Wood and Cellulose Chemistry*, Marcel Dekker, New York, (2001).

31. S.T. Chang and P.L. Chou, Photo-discoloration of UV-curable acrylic coatings and the underlying wood, *Polymer Degradation and Stability*, **63** (3): 435-439 (1999).

32. S.T. Chang and P.L. Chou, Photodiscoloration inhibition of wood coated with UV-curable acrylic clear coatings and its elucidation, *Polymer Degradation and Stability*, **69**(3): 355-360 (2000).

33. P.L. Chou, H.T. Chang, T.F. Yeh, and S.T. Chang, Characterizing the conservation effect of clear coatings on photodegradation of wood, *Bioresource Technology*, **99**(5): 1073-1079 (2008).

34. L. Long, M.P. Wolcott, J. Zhang, and K. Englund, Flexural properties of surface reinforced wood/plastic deck board, *Polymer Engineering and Science*, **47**(3): 281-288 (2007).

35. C. Rauwendaal, *Understand Extrusion*, Hanser/Gardner, Cincinnati, (1998).

36. H.J. Giles Jr., J.R. Wagner Jr., and E.M. Mount III, *Extrusion: The Definitive Processing Guide and Handbook*, William Andrew Publishing, New York, (2004).

37. Z. Gürdal, R.T. Haftka, and P. Hajela, *Design and Optimization of Laminated Composite Materials*, John Wiley & Sons, New York, (1999).

38. S.C. Tjong. Structural and mechanical properties of polymer nanocomposites, *Materials Science and Engineering R-Reports*, **53**(3-4): 73-197 (2006).

39. O. Faruk and L.M. Matuana, Reinforcement of rigid PVC/wood-flour composites with multi-walled carbon nanotubes, *Journal of Vinyl and Additive Technology*, **14**(2): 60-64 (2008).

40. M. Panico, L.D. Maio, V. Nicolais, and L. Incarnato, Experimental set-up and characterization of a mLLDPE-PP co-extruded bilayer system, *Polymer Engineering and Science*, **46**(7): 874-881 (2006).

41. P. Dole, L. Avérous, C. Joly, G.D. Valle, and C. Bliard, Evaluation of starch-PE multilayers: processing and properties, *Polymer Engineering and Science*, **45**(2): 217-224 (2005).

42. S. Elkoun, M. A. Huneault, K. McCormick, F. Puterbaugh and L. Kale, LLDPE-based mono- and multilayer blown films: property enhancement through coextrusion, *Polymer Engineering and Science*, **45**(9): 1222-1230 (2005).

43. L.M. Matuana and Q. Li, Statistical modeling and response surface optimization of extruded HDPE/wood-flour composite foams, *Journal of Thermoplastic Composite Materials*, **17**(2): 185-199 (2004).

44. J.W. Kim, K. Carlborn, L.M. Matuana, and P.A. Heiden, Thermoplastic modification of urea-formaldehyde wood adhesives for increased moisture resistance, *Journal of Applied Polymer Science*, **101**(6): 4222-4229 (2006).

45. L.M. Matuana and J.W. Kim, Fusion characteristics of wood-flour filled rigid PVC by torque rheometry, *Journal of Vinyl & Additive Technology*, **13**(1): 7-13 (2007).

CHAPTER 2

Background and Literature Review

WPCs is manufactured by mixing wood and plastics similar to plastic processing procedures such as compression, extrusion, or injection molding [1-4].Wood refers to various kinds of natural fibers in different amounts and geometries (fiber, flour, etc.), whereas plastic is mainly thermoplastics.

2.1 Polymer

2.1.1 General properties

Polymers are large molecules (macromolecules) composed of repeating structural units connected by covalent chemical bonds to form long chains. The composition of a repeat unit, the number of repeat units, the spatial arrangement of repeat units on the long chains, and chain linearity determine physical, chemical, and rheological properties of polymers.

Polymers fall into two categories: thermoset and thermoplastic. The manufacture of thermoset materials employs curing, a cross-linking process. In this process, the molecular chains react at chemically active sites, linking into a rigid, 3-D structure [5]. This results in a melting point of material higher than the decomposition temperature. Therefore, after curing, melting and remolding of a thermoset material cannot occur. In contrast, thermoplastics have no limit to repeated melting and solidifying through heating and cooling. Thermoplastics instead of thermosets are primarily used as polymer matrices for WPCs. Thermoplastics mostly used in the manufacturing of WPCs include polyethylene (PE), polypropylene (PP), and polyvinyl chloride (PVC) (Figure 2.1).

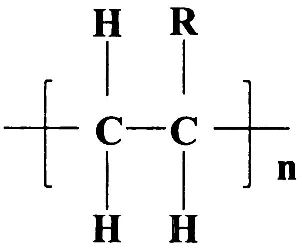

Figure 2.1. Repeating structural units of a polymer. R=H for PE; R=CH_3 for PP; R=Cl for PVC.

About 600 million pounds of thermoplastics in 2005 were used for the manufacturing of WPCs in North America [4]. PE accounts for about 90% of the volume, and PP and PVC occupy the remaining of 10% [4]. Polyethylene and Polyvinyl chloride will be described in detail because they are the two main polymers used in this study.

2.1.2 Polyethylene

Polyethylene (PE) is the most popular plastic in the world [6]. PE consists of long chains of the monomer ethylene. The mechanical properties of PE largely depend on variables such as the extent and type of branching, the crystal structure, and the molecular weight. Classification of polyethylene is mainly based on its density and branching. The main categories are high density polyethylene (HDPE), low density polyethylene (LDPE), and linear low density polyethylene (LLDPE). HDPE typically has a density in the range of 0.94-0.97 g/cm^3 [6]. HDPE has a low degree of branching, leading to stronger intermolecular forces and strength, and a higher degree of crystallinity. The densities of LDPE are between 0.91-0.94 g/cm^3 [6]. LDPE has a high degree of short and long chain branching responsible for the weak intermolecular force and a lower degree of crystallinity, which induces a lower tensile strength and higher ductility compared to those of HDPE. The densities of LLDPE are in the range of 0.915–0.925 g/cm^3 [7]. LLDPE, a substantially linear polymer, has a pronounced amount of short branches but does not have long chain branches. Therefore, properties of LLDPE such as tensile and flexural properties are often between those of HDPE and LDPE.

HDPE is the major category of PE used as a polymer matrix in WPCs because there are several advantages of HDPE over LDPE and LLDPE in terms of WPCs application. HDPE has a higher degree of crystallinity than that of LDPE and LLDPE, thus the properties of HDPE related to crystallinity such as modulus, strength, hardness, and creep resistance override those of LDPE and LLDPE [4].

Besides density, another criterion to differentiate the polymers is the melt flow index (MFI), which is a measure of the ease of flow of the melt of a thermoplastic polymer [5]. It is defined as the rate of extrusion of molten polymers through a die of a specified length and diameter under prescribed conditions of temperature, load, and piston position in the barrel. MFI depends on average molecular weight, molecular weight distribution, and the degree of chain branching. It provides a critical consideration in terms of material selection for manufacturing WPCs. Generally, injection molding needs higher MFI polymers, while extrusion processes can perform with lower MFI polymers [8].

2.1.3 Poly(vinyl chloride)

Polyvinyl chloride (PVC) is the third widely used thermoplastic polymer, after polyethylene and polypropylene.

PVC resin is a major component in PVC formulation among other ingredients. The K-value of PVC resin, related to the average number of molecules, reflects the inherent viscosity. The K-value of PVC resin affects the processing and properties of the final product. In general, a lower K-value means lower melt viscosity and easier processing at a given temperature, while a higher K-value relates to better mechanical properties [9]. As a result, the properties of PVC-based WPCs depend on the K-value of PVC resin in PVC formulation.

PVC resin requires additional additives, such as plasticizers, heat stabilizers and processing aids. Plasticizers decrease the interaction among the PVC chains and thus decrease the strength and modulus of PVC compounds. Flexible PVC compounds contain plasticizers, while rigid PVC compounds do not contain plasticizers. Thus rigid PVC has superior strength and modulus than flexible PVC, which make rigid PVC preferable as polymer matrix in WPCs.

Heat stabilizers are added to PVC formulation to improve thermal stability at processing temperatures. Processing aids are added to change the melt-processing behaviors of PVC such as fusion, melt strength, and melt viscosity. Lubricants are added to loosen the internal friction between materials and external friction between materials and processing equipment. Impact modifiers are added to improve the toughness [9].

The suspension polymerization process is the principal commercial route to produce PVC resins in industry. Thus PVC resin is granular in nature. PVC resin is composed of powder particles that are irregular in shape and about 100-200 μm in diameter. These PVC powder particles are composed of microparticles that are on the order of 10 to 15 microns in diameter. The primary particle agglomerates are composed of submicroparticles, which have diameters of 1 micron [9, 10].

Melting of PVC compounds, generally referred to as PVC fusion, is the thermal reduction of resin particle boundaries by heat and shearing and the compound approaches a unified homogeneous structure. The procedure of PVC fusion includes the following steps: The first step is a breakdown of the powder particles and part of the microparticles. Then grain boundaries must be eliminated, and the microparticles must be compacted together. After further interdiffusion of PVC polymer chains, the boundaries of submicroparticles disappear, and polymer is in a molten state [11, 12]. Since fusion is involved in the breakdown of the particles and the interdiffusion of the polymer chains, shearing force and energy are required.

Fusion behavior is described by fusion curve shown in Figure.2.2. Fusion curve illustrates the changes of viscosity related to torque, temperature, and torque versus time. The viscosity-related torque curve shows three different points.

When the PVC compound is loaded into the system, the first point A is generated. Then, the torque begins to decrease sharply, and this generates the second point B because of free material flow before the materials begin to compact. After that, the torque begins to increase, and this generates the third point. At this point, X, the material reaches a void-free state and starts to melt at the interface between the compacted material and the hot metal surface [12]. The time spent between the loading point (A) and the fusion point (X) is defined as fusion time.

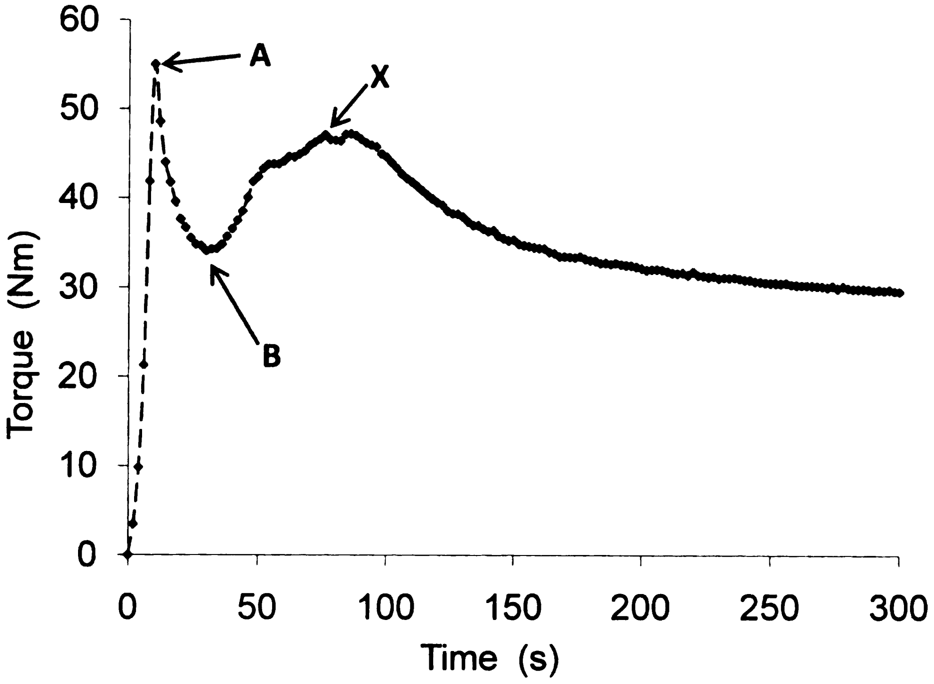

Figure 2.2. Fusion curve of neat rigid PVC compound [12].

Fusion behavior is a linkage between processing conditions and end-use properties. A lot of research shows an inadequate fusion could lead to poor properties of PVC compounds. It has been reported that the tensile strength of rigid PVC increased with increasing fusion and then leveled off at the higher levels of fusion [10]. The effect of fusion level on the brittle-ductile behavior and stiffness of rigid PVC has also been investigated. While the brittle-ductile behavior was found to achieve an optimum value and then decrease, the stiffness increased with fusion level in the whole range [10].

2.1.4 Photodegradation of PE and PVC

Photodegradation is a degradation of a molecule caused by the absorption of photons, which are from ultraviolet (UV) radiation, visible light, and infrared radiation (IR) [13-16]. The photodegradation rate of polymer relies on sunlight intensity, temperature, humidity, oxygen pressure, and the type of polymer [13]. Photodegradation cannot occur without chromophores which absorb photo-energy [14]. Although PE does not contain chromophores inherently, introduction of chromophores such as hydroperoxide and carbonyl groups occurs during polymer manufacturing, processing and storage [13-16]. On the other hand, the photodegradation of PVC is due to the unsaturation site (conjugated double bond), low dissociation energy of C-Cl linkage, and hydroperoxide groups and carbonyl groups introduced during manufacturing, processing and storage [13].

There are two major mechanisms responsible for the photodegradation of polymer. One is initiated by photolysis of hydroperoxides and occurs in three stages, as shown in Figure 2.3 [13]. The first step is the initiation of free radicals generated by photolysis of hydroperoxides. The second step, propagation, contains free polymer alkyl radicals reacting with oxygen and producing the polymer peroxy radicals whereupon the energy of polymer peroxy radicals can transfer to another polymer, generating secondary polymer radicals. Polymer peroxy radicals undergo various kinds of reactions, which results in chain scission. The third step, termination, incorporates two free radicals combining together, thereby leading to crosslinking.

Initiation: $\mathrm{POOH} \xrightarrow{hv} \mathrm{P\bullet, PO\bullet, HO\bullet, HO_2\bullet}$

Propagation: $\mathrm{P\bullet + O_2 \rightarrow PO_2\bullet}$

$\mathrm{PO_2\bullet + PH \rightarrow P\bullet + POOH}$

$\mathrm{PO_2\bullet \rightarrow -CHO + CH_2{=}CH- + \bullet OH}$

Termination: $\mathrm{PO_2\bullet + PO_2\bullet \rightarrow P{=}O + P\text{-}OH + O_2}$

$\mathrm{PO_2\bullet + HO_2\bullet \rightarrow P{=}O + H_2O + O_2}$ or $\mathrm{POOH + O_2}$

$\mathrm{HO_2\bullet + HO_2\bullet \rightarrow HOOH + O_2}$

Figure 2.3. Photodegradation of polymers initiated by photolysis of hydroperoxides (PH: polymer) [13].

The other photodegradation mechanism of polymer is initiated by photolysis of ketone [13]. The photodegradation proceeds through Norrish I and II reactions, as shown in Figure 2.4. Both Norrish I and II reactions result in the scission of polymer backbone. In Norrish I reaction, a carbon-carbon bond is broken to form one alkyl free radical and one carbonyl free radical. As a result, carbon monoxide is easily lost from carbonyl free radical. Thus, two alkyl free radicals are generated via Norrish I. These radicals readily react with oxygen to generate alkyl peroxy radicals and propagate the reaction [13]. Free radical reaction may terminate via crosslinking. In Norrish II reaction, a carbon-carbon bond is broken. Methyl ketone and alkene are generated. Therefore, both Norrish I and II reactions result in the scission of polymer backbone. Norrish I also can leads to crosslinking.

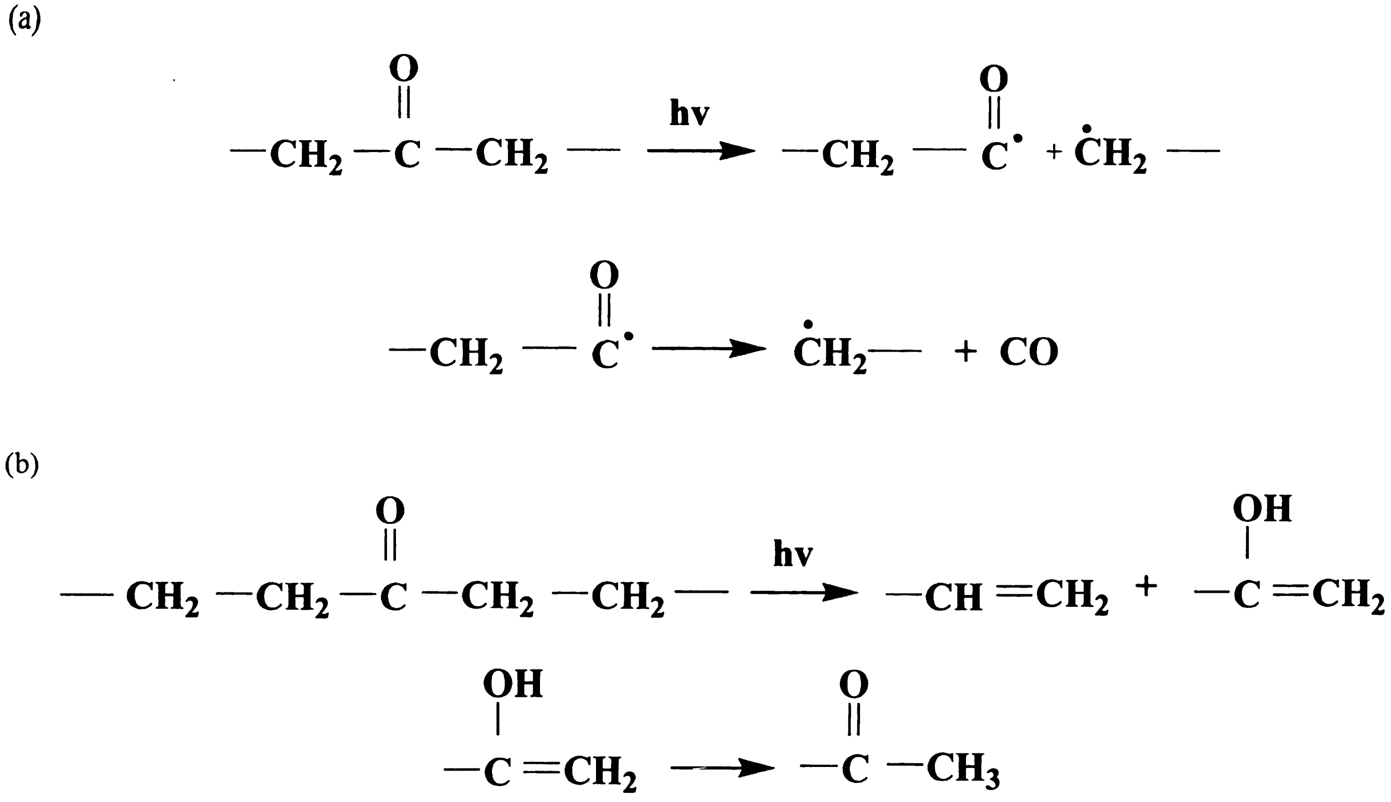

$$-CH_2-\overset{\overset{O}{\|}}{C}-CH_2- \xrightarrow{hv} -CH_2-\overset{\overset{O}{\|}}{C^{\bullet}} + \dot{C}H_2-$$

$$-CH_2-\overset{\overset{O}{\|}}{C^{\bullet}} \longrightarrow \dot{C}H_2- + CO$$

$$-CH_2-CH_2-\overset{\overset{O}{\|}}{C}-CH_2-CH_2- \xrightarrow{hv} -CH=CH_2 + -\overset{\overset{OH}{|}}{C}=CH_2$$

$$-\overset{\overset{OH}{|}}{C}=CH_2 \longrightarrow -\overset{\overset{O}{\|}}{C}-CH_3$$

Figure 2.4. Photodegradation of polymers initiated by photolysis of ketone. (a) Norrish I and (b) Norrish II [13].

Although both chain scission and crosslinking occurs as the result of photodegradation, chain scission is the dominant mechanism in polyethylene and PVC [17]. Chain scission decreases molecular weight, leading to increase the chain mobility and surface cracks [17-20]. Consequently, crystallinity increases but impact resistance and elongation decrease [18]. Increasing crystallinity also affects optical properties, as the crystalline region is translucent and the amorphous region is transparent [5]. Thus polyethylene became whiten after photodegradation.

2.1.5 Protection against photodegradation

UV absorbers (UVA) and hindered amine light stabilizers (HALS) are primarily light stabilizers for Polyolefin and PVC [21-25]. The corresponding protection mechanisms prevent the initial reaction and delay the propagation reaction by consumption of the free radicals.

The protection mechanism of UV absorbers is based on the absorption of the UV radiation and dissipation of radiation as heat. The UV absorption follows the Lambert-Beer's law [21, 22]:

$$\log \frac{I}{I_o} = -\varepsilon \cdot l \cdot c \qquad \text{(Equation 2.1)}$$

where I_0 represents the light energy of monochromatic light incident per unit time on a substrate with a single absorbing species of concentration c (mole per L), I the energy past through the substrate, l the thickness, and ε the molar extinction coefficient of the absorbing species. Since UV absorption by UVA is thickness dependent, UVA may fail to provide adequate surface protection for thin portion.

Hydroxybenzophenone (BP), hydroxyphenylbenzotriazole (BTZ), and hydroxyphenyl-s-triazine (HPT) are three main classes of UVA commercially used in polymers and coatings [22, 23]. The typical protection mechanism of benzotriazoles and benzophenones are illustrated in the Figure 2.5. Hydrogen bonding in the o-hydroxy groups pronouncedly influences photochemical properties [22]. Different classes of UVA have different UV absorption spectra, as shown in Figure 2.6. While BP mainly provides protection against UVB radiation (280-320 nm), HPT and BTZ provide protection against both UVB and UVA radiation (320-400 nm).

Pigments absorb or reflect UV radiation and can be considered as another type of UV stabilizer. The major difference between UVA and pigments is that while UVA primarily absorb radiation in the UV region, pigments absorb light in both UV and VIS area. Thus materials often change color or decrease transparency after the addition of pigments. Titanium dioxide, carbon black, and zinc oxide are pigments used frequently as UV stabilizers.

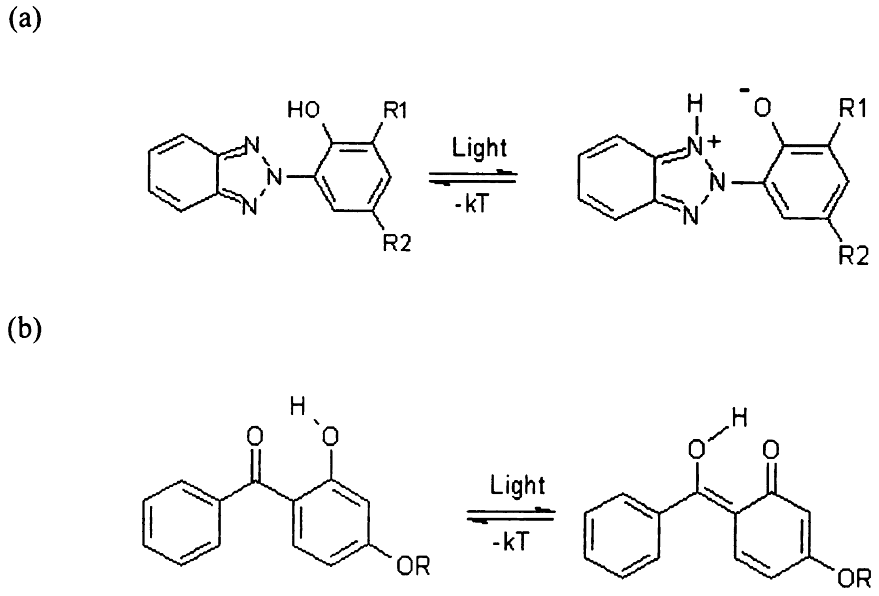

Figure 2.5. Protection mechanisms of (a) benzotriazoles and (b) benzophenones [22].

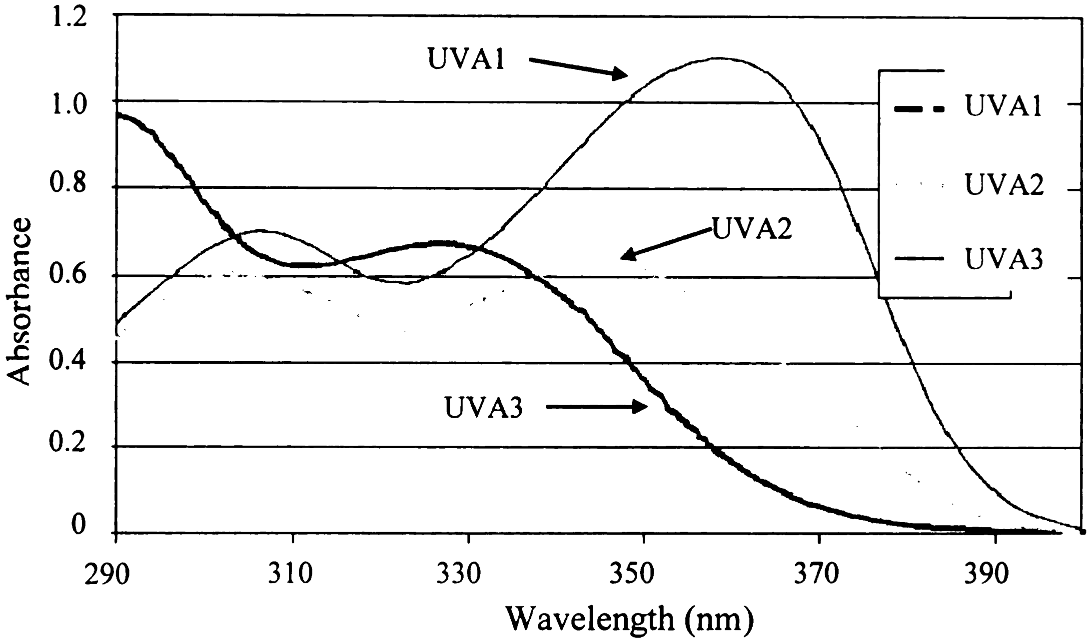

Figure 2.6. UV absorption spectra of HPT (UVA1), BTZ (UVA2), and BP (UVA3) [23].

Hindered amine light stabilizers (HALS), derivatives of 2,2,6,6-tetramethyl piperidine, protect the polymer from UV radiation via free radical termination. The stabilization mechanism of HALS is believed to be a cyclic chain-breaking antioxidant process, shown in Figure 2.7. In the first step, in the presence of oxygen and radiation, the HALS compound (1) is converted into the corresponding nitroxyl radical (2), then nitroxyl radical traps a free radical to form an alkoxy amine (NOR) (3). The alkoxy amine reacts with a peroxide radical under formation of the intermediate structures (4) which then decompose into harmless alcohols and ketones. At the same time, the nitroxyl radical (2) is regenerated, which can repeat the cycle [24, 25]. Moreover, since HALS, unlike UVA, is independent on sample thickness, HALS can be used in applications with high surface-to-volume ratios such as films, tapes, and fibers [24]. Polymers often require a lower addition level of HALS than UV absorbers [22, 24].

In order to achieve optimum UV protection, various types of UV stabilizers are often used together [22, 24]. The selection of light stabilizers is dependent on the characteristics of the polymer matrix (especially its absorption spectrum), application, and dimension etc.

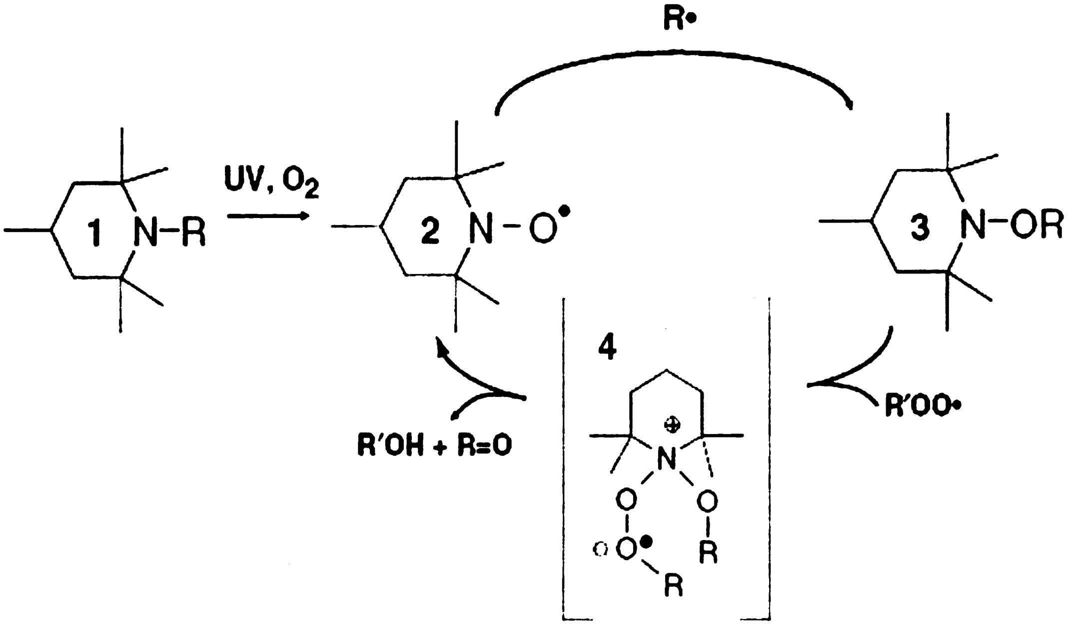

Figure 2.7. The stabilization mechanism of HALS [25].

2.2 Wood

2.2.1 Chemical composition of wood

Cellulose, lignin, hemicelluloses, and minor amounts of extraneous materials (ash and extractives) are the main components of dry wood. Each of these components contributes to the properties of wood and wood derived products.

Cellulose

Cellulose, the primary component, constitutes approximately 40-50% of wood substance on an oven-dry basis [26]. As a high-molecular-weight, stereoregular, and linear polymer, cellulose consists of chains of repeating (1,4)-β-D-glucopyranose units (Figure 2.8). With the empirical formula for cellulose represented as $(C_6H_{10}O_5)_n$, the degree of polymerization (DP) ranges from 1000 to 10000. Hydroxyl groups in the cellulose molecules are the cause of water sorption of wood. Through intra- and intermolecular hydrogen bonds, cellulose molecules crystallize. Cellulose is highly crystalline and may contain up to 65% crystalline regions [27]. The surfaces of crystalline cellulose are accessible to moisture sorption and chemical modification, but the bulk of the crystalline cellulose is not accessible. In contrast, most of the amorphous cellulose is accessible to moisture sorption and chemical modification except for regions covered by hemicelluloses and lignin.

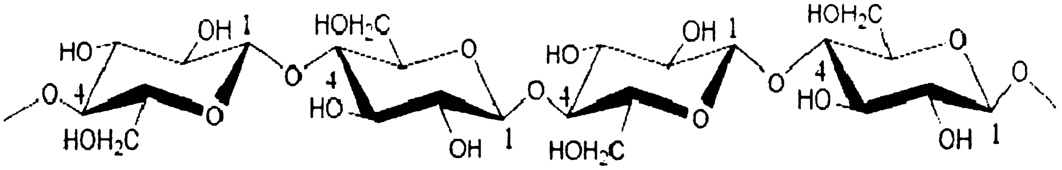

Figure 2.8. The structure of cellulose [27].

Hemicelluloses

Hemicelluloses account for approximately 20% of wood substance. While cellulose is mainly composed of glucose units, hemicelluloses contain various kinds of sugar units with a lower DP (100-200) than cellulose. Moreover, while cellulose is highly crystalline and resistant to hydrolysis, hemicelluloses are amorphous and easily hydrolyzed [27].

Lignin

Lignin, a three-dimensional phenylpropanol amorphous polymer, accounts for 18 to 25% of the wood substance in hardwoods and 25 to 33% in softwoods [27]. The precursors of lignin biosynthesis are paracoumaryl alcohol, coniferyl alcohol, and sinapyl alcohol (Figure 2.9). Paracoumaryl alcohol is a minor precursor of both softwood and hardwood lignins. Coniferyl alcohol is the dominant precursor of softwood lignins. Both coniferyl alcohol and sinapyl alcohols are precursors of hardwood lignin. These three basic units are linked by ether and carbon to carbon linkages, forming lignin. The structure of lignin is shown in Figure 2.10. It is relatively hydrophobic compared to holocellulose (cellulose and hemicelluloses). Although lignin occurs in wood throughout the cell wall, concentrations are highest towards the outside of and between the cells. Lignin commonly acts as the cementing agent responsible for binding individual cells together [26].

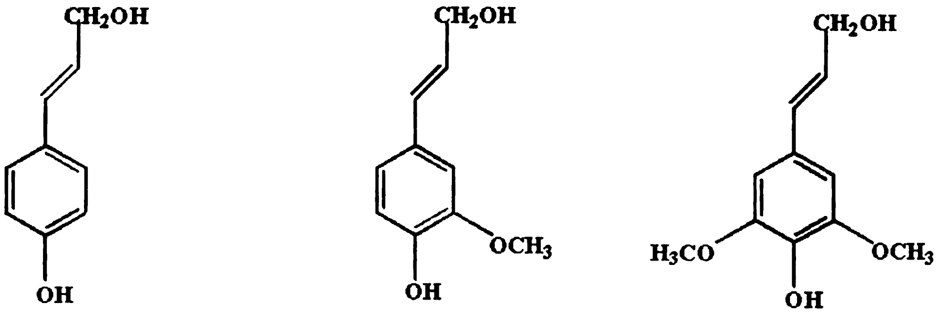

(1) (2) (3)

Figure 2.9. The structure of lignin precursors: (1) paracoumaryl alcohol, (2) coniferyl alcohol, and (3) sinapyl alcohol [27].

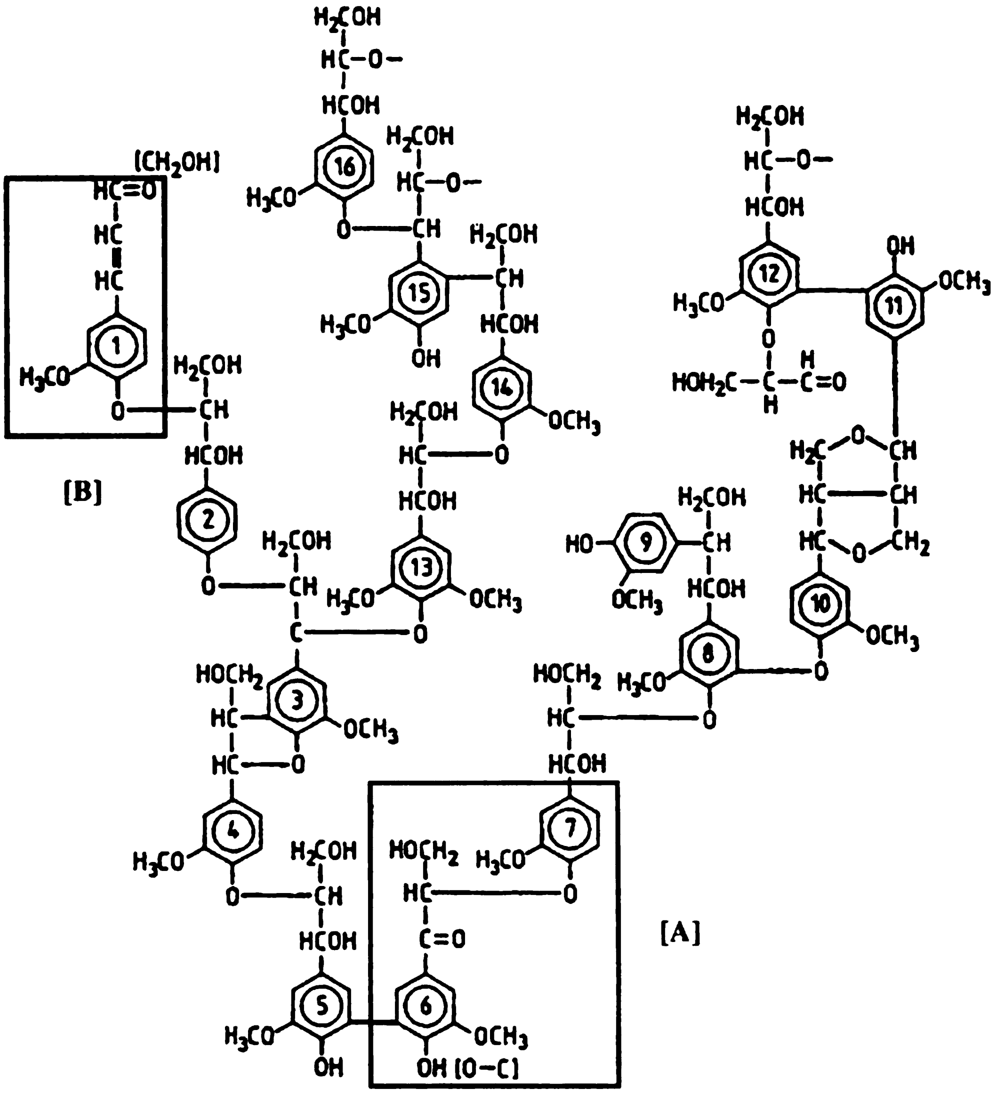

Figure 2.10. The structure of lignin in the soft wood [28].

Extractives and ash

Extractives, accounting for 1-2% of wood substance, consists of a wide range of organic compounds mainly including fats, waxes, terpene, phenolic compounds, and certain carbohydrates [27]. The quantities and qualities of extractives assist in determining the wood's permeability to liquids and influence other wood properties such as density, hardness, and compressive strength. Extractives provide resistance to insect or fungal attack in certain woods. Additionally, extractives generate the odors and colors attributed to most woods [27]. The extractives are often classified by the solvent used for their extraction. The di-chloromethane extractable content of wood refers to the measure of components such as waxes, fats, resins, photosterols, and non-volatile hydrocarbons [27]. The ethanol-benzene extractable content of the wood contains components such as low molecular weight carbohydrates, salts, and other water-soluble substances. The amount of extractives substantially depends on the seasoning or drying of wood [27].

Ash accounts for less than 1% of wood substance. Inorganic minerals, primarily calcium, potassium, and magnesium, form ash.

2.2.2 Anatomic structure of wood

There are two domains in most cells of wood: the cell wall and the cell lumen [27]. The cell lumen is a void space. The cell wall is layer which surrounds the cell lumen. The cell walls of wood are multilayer. They consist of the primary wall (P), and the layers of the outer (S1), middle (S2), and inner (S3) secondary walls [26, 27]. The adjacent cells are glued together by the middle lamella (m.l.). The layered cell wall structure of softwood is shown in Figure 2.11. Difference between these layers lies in their structures, orientations and number of fibrils or fibers, and chemical composition. Cellulose is primarily located in the secondary wall. Lignin is distributed throughout the cell wall but more in the middle lamella region. In contrast, hemicellulose is distributed in both the cell wall and middle lamella.

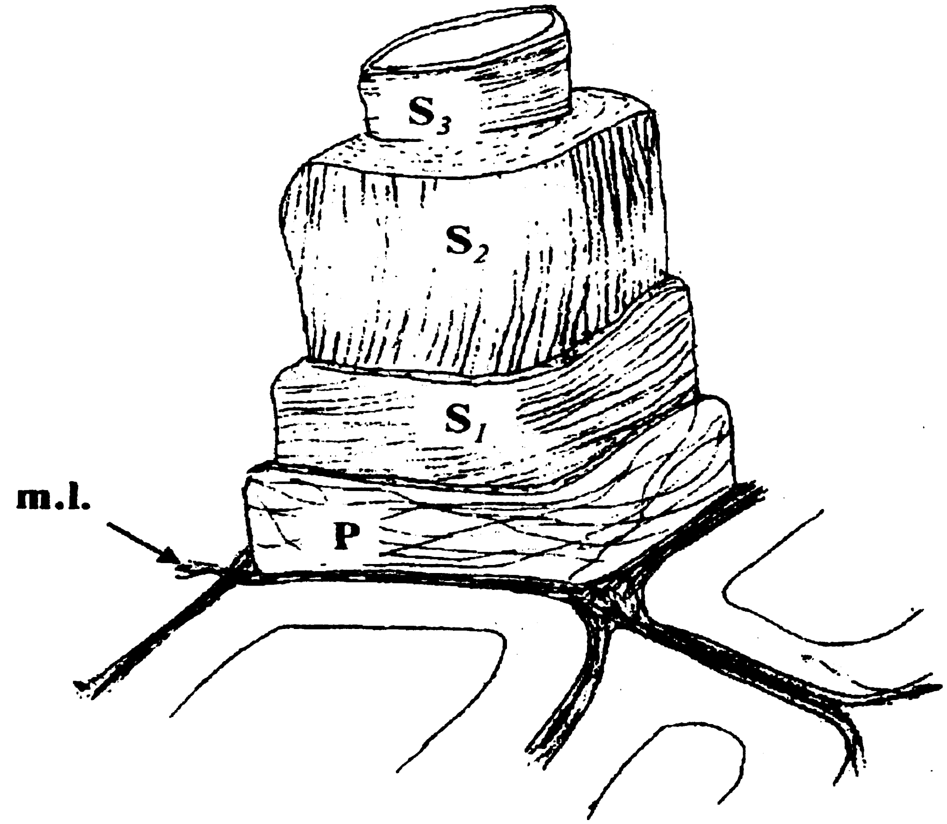

Figure 2.11. The layered cell wall structure of softwood [27].

2.2.3 Moisture absorption of wood

Since holocellulose (cellulose and hemicelluloses) is rich in hydroxyl group, wood absorb water easily and quickly. The moisture content (MC) of wood is calculated by Equation 2.2:

$$MC = \frac{\text{initial weight} - \text{oven dry weight}}{\text{oven dry weight}} \qquad \text{(Equation 2.2)}$$

Water in wood can be categorized into free water (liquid water or water vapor in cell lumens), and bound water (water held chemically within cell walls) [1]. The Fiber saturation point (FSP) refers to the point at which all liquid water in the lumens has been removed but the cell wall is still saturated. When moisture content is below the FSP, physical and mechanical properties of wood change as moisture content changes. In contrast, when moisture content is above the FSP, these properties of wood remain constant as moisture content changes. The moisture content of wood depends on the relative humidity (RH) and temperature of the environment. Equilibrium moisture content (EMC) arises when the wood neither gains nor loses moisture at a given temperature and RH. A strong relationship exists between EMC, relative humidity, and temperature, as shown in Table 2.1 [26]. For most practical purposes, the values in Table 2.1 may be applied to wood of any species [26]. At given temperature, the relationship between the equilibrium moisture content of a material and relative humidity can be displayed graphically by a curve (Figure 2.12.), which is called moisture sorption isotherm. Generally, there are six types of sorption isotherms according to the International Union of Pure and Applied Chemistry (IUPAC) classification [29]. The moisture sorption isotherm of wood best fits type II isotherm as shown in Figure 2.13, which indicates strong adsorbate-adsorbent interactions [29]. In other words, interactions between moisture and wood are strong. This is attributed to the formation of hydrogen bonding between moisture and hydroxyl groups in the wood.

Table 2.1. Equilibrium moisture content of wood at various temperature and relative humidity [26].

Temperature (^oF)	Moisture content (%) at various relative humidity				
	10%	30%	50%	70%	95%
30	2.6	6.3	9.5	13.5	24.3
50	2.6	6.3	9.5	13.4	24.3
70	2.5	6.2	9.2	13.1	23.9
90	2.3	5.9	8.9	12.6	23.3
120	2.1	5.4	8.2	11.7	22.0
150	1.8	4.8	7.4	10.6	20.4

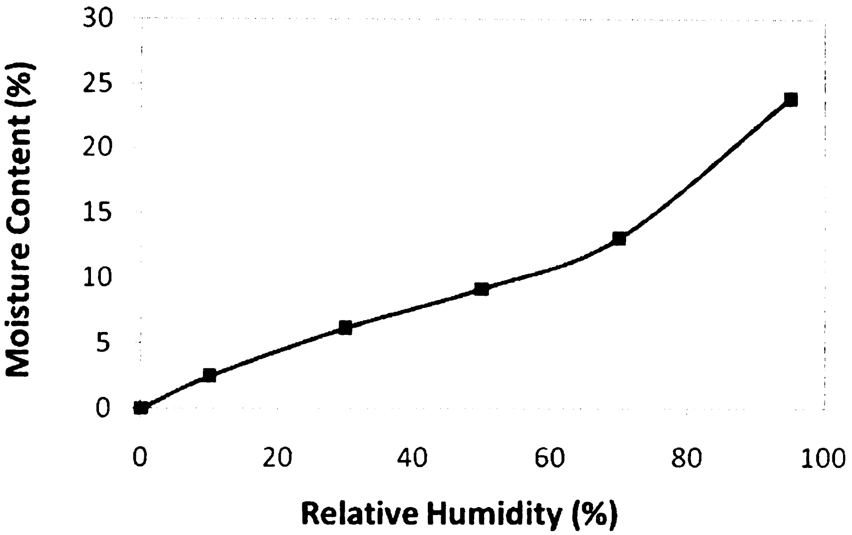

Figure.2.12. Moisture sorption isotherms of wood at 70 °F. Data adapted from Table 2.1 [26].

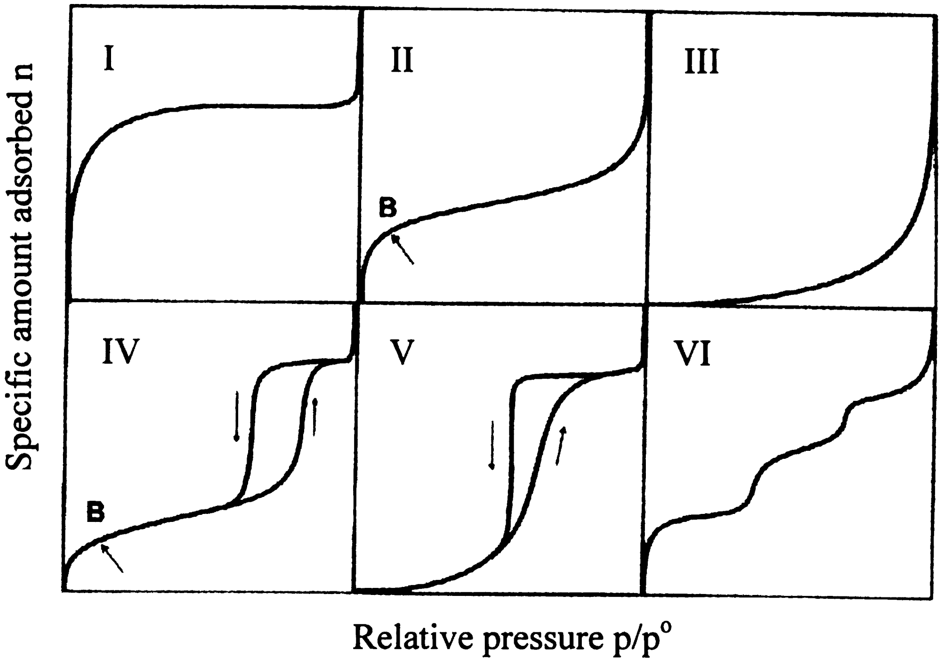

Figure.2.13. The IUPAC classification for adsorption isotherms [29].

2.2.4 Photodegradation of wood

As mentioned in the section of photodegradation of polymer, photodegradation cannot occur without chromophores which absorb photo-energy [14]. Moreover, a reaction occurs only once a molecule obtains the necessary activation energy [30-32]. The bond dissociation energies of several functional groups in wood and corresponding wavelengths are listed in Table 2.2 [27]. Because visible light in the range of 400-700 nm carries energy less than 70 kcal/mol, it fails to provide sufficient energy to break chemical bonds in most of the wood components [30]. Therefore, the ultraviolet part of sunlight (295-400 nm) predominantly accounts for the photodegradation of wood. The general mechanism of photooxidation of wood is similar to that of polymer, including the three same steps: initiation, propagation, and termination, shown in Figure 2.14 [31].

The breakdown of chemical bond by absorption of UV photons generates free radicals. Free radicals react with oxygen and water, forming hydroperoxides. Carbon radicals in a vacuum tend to stabilize themselves by recombination and hydrogen abstraction. In contrast, in the presence of oxygen they are transformed rapidly into hydroperoxide radicals [30]. Both free radicals and hydroperoxides can initiate chain scission reactions.

Table 2.2. Bond dissociation energies and radiation wavelength [27].

Bond	Bond Dissociation Energy (Kcal/mol)	Wavelength (nm)
C-C (Aromatic)	124	231
C-H (Aromatic)	103	278
C-H (Methane)	102	280
O-H (Methanol)	100	286
C-O (Ethanol)	92	311
C-O (Methanol)	89	321
CH_3COO-C (Methyl ester)	86	333
C-C (Ethane)	84	340
C-Cl (Methyl ether)	82	349
C-$COCH_3$ (Acetone)	79	362
C-O (Methyl ether)	76	376

Initiation: $RH \xrightarrow{h\nu} R^{\bullet} + H^{\bullet}$

Propagation: $R^{\bullet} + O_2 \rightarrow RO_2^{\bullet}$

$RO_2^{\bullet} + RH \rightarrow ROOH + R^{\bullet}$

Termination: $RO_2^{\bullet} + RO_2^{\bullet} \rightarrow$ nonradical product

$R^{\bullet} + RO_2^{\bullet} \rightarrow$ nonradical product

$R^{\bullet} + R^{\bullet} \rightarrow$ nonradical product

Figure 2.14. Sequence of photooxidation reactions in wood (RH: cellulose, hemicelluloses, and lignin) [31].

The degrees of photodegradation of wood components largely depend on their ability to absorb UV light. The reflection spectra of wood, cellulose, and lignin are shown in Figure 2.15. Wood absorbs both UV and the shorter wavelengths of visible light. Lignin absorbs light in the both UV and visible regions more efficiently than cellulose [33], due to the chromophoric groups in lignin (Figure 2.10). As a result, lignin experiences more severe photodegradation than cellulose. The chemical component analysis showed an increase in cellulose content and a decrease in lignin content at the wood surface after weathering [30].

Absorption of UV light by wood initiates the photochemical reactions at surface. When cellulose is exposed to sunlight, depolymerzatoin at the glycosidic linkanges, dehydrogenation at the C1 and C5 positions, and dehydroxymethylation at the C5-C6 side chain take place [30]. When liginin is exposed to sunlight, guaiacyl and phenoxy radicals are generated. The following demethylation of guaiacyl and phenoxy radicals yields quinoid chromophores [34]. Quinones can cause an intense color change (yellowing or darkening) even at very low concentration [35]. The photodegradation of lignin leads to the decay of aromatic structures and the formation of quinone and conjugated carbonyl groups [34]. Since the decrease of aromatic skeletal vibrations in the 1600 or 1510 cm^{-1} region and the increase of carbonyl group in the 1730 cm^{-1} region are more pronounced than conjugated carbonyl bonds, the former is often used to evaluate the decay of lignin instead of the latter [34-38].

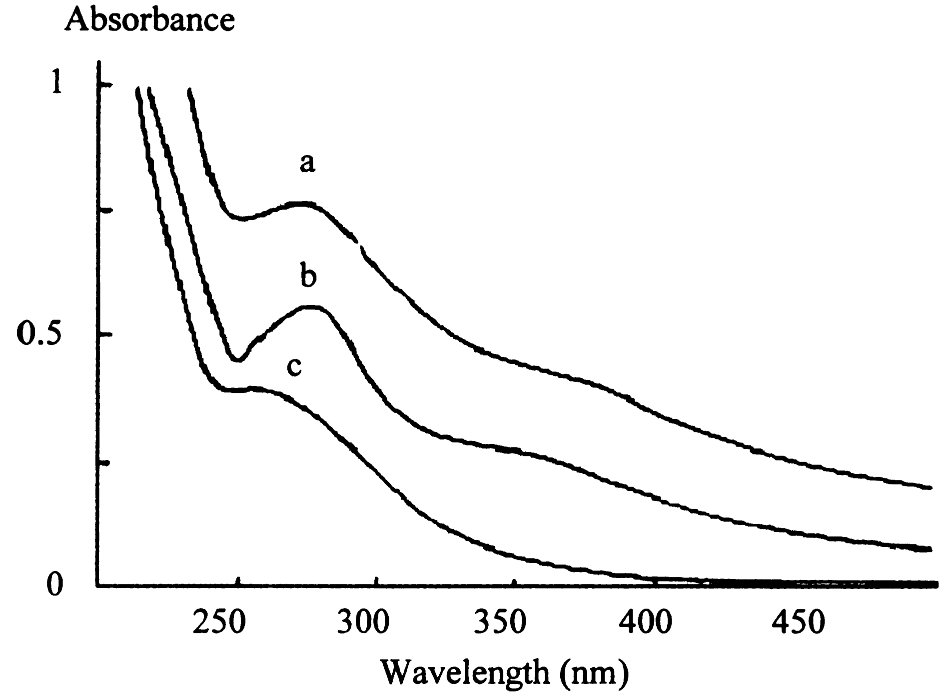

Figure 2.15. Reflection spectra of (a) wood, (b) lignin, and (c) cellulose [33].

Study showed that removal of water/ethanol/toluene extractable compounds from wood can significantly change the color, especially the lightness [38]. However, after exposure to long-term weathering (2400h accelerate artificial weathering), both extractive free and unextracted wood showed similar color in terms of lightness, redness, and yellowness [39]. This can be attributed to the removal of degraded color compound from surface by water spray. Since most of the extractive components are considered phenolic in nature, their photodegradation may be similar to that of lignin, which is also phenolic in nature. Investigation have shown that the FTIR spectra of extractive free wood exposed to xenon arc irradiation experienced less reduction at 1510 cm^{-1} peak compared to unextracted wood [38], implying that extractives like lignin also experienced the decay of benzyl ring.

The degraded products of weathered woods, are mainly organic acids, vanillin, syringaldehyde, and higher molecular weight compounds, which are all leachable [30]. Usually, wood in the outdoor environment initially become yellow and brown due to the photooxidation of lignin, and when the colored degraded products leach out, a silver-gray layer composed of leach-resistant parts of the partially degraded cellulose remains on the wood surface [30].

The intensity of UV/vis light decreases after penetrating wood deeper than 75-200 µm, making photodegradation of wood a surface phenomenon. However, the degradation layer of wood can become deeper with the weathering. Kataoka et al. reported that the degradation layer of sugi sapwood increased to 500 µm after 1500 h of xenon arc radiation [40].

Besides the intensity of UV/vis light, the rate of a photochemical process depends on the moisture content at the wood's surface, the oxygen concentration, the temperature and the type of wood species [41, 42]. Water has various chemical and physical effects on photodegradation. Liquid water can result in the erosion of oxidized layers, swelling of matrix, and extraction of additives soluble in water [31]. Liquid or gaseous water also may induce the hydrolysis of oxidation intermediates or of final products [31]. Especially for wood, water penetrates and swells the wood fiber, opening up non-accessible regions for light penetration [30]. Oxygen is involved in the propagation and termination. Since oxidation needs energy, there is temperature dependence for photodegradation. Wood species dependence can be attributed to variety in chemical constituents of wood species.

Chemical changes also bring about physical changes. Weathering leads to cracking and splitting of the wood, both on a microscopic level inside the cell walls and as visible cracks on the surface [27, 30]. Consequently, weathered wood loses weight and strength [30, 43-45].

2.2.5 Protection against photodegradation

There are two common methods to protect wood against photodegradation. One is wood surface treatment and another is coating [43-46].

Wood surface treatment primarily refers to modification of chemical composition of wood surface by reaction. Grafting of UV absorber (UVA) to wood reduced both weight loss and tensile strength loss since UV absorber can reduce the UV light absorbed by wood [44]. High temperature or microwave irradiation is often needed to bond UVA to wood. Esterification of wood with benzoyl choride also can decrease both the weight loss and color change since benzoyl group can act as a UV screen protecting cellulose and lignin [45, 46].

Coating also can provide protection against environmental damage such as photodegradation, biodegradation, and mechanical abrasion [43, 47-49]. For protection against photodegradation, opaque pigmented coatings block the UV/visible light but cover the aesthetics of wood. Conversely, semi-transparent and clear coatings maintain the natural appearance of wood, but the UV/visible light transparency of the coating results in the photodegradation of wood substrate and the resultant failure of the coating adhesion due to the photodegraded substrate [47]. The addition of photo stabilizers such as UVA into coating reduces the discoloration of coating and wood substrate [48, 49].

2.3 Wood-Plastic Composites

2.3.1 Introduction

The properties of WPCs combine those of wood fiber and polymer matrix. The wood content in the WPCs, the characteristics of the wood and polymer, the interface between the wood and polymer matrix, additives used in the WPC's formulation, as well as processing procedures are factors affecting end-use properties of WPCs. In addition, moisture absorption and weathering of WPCs are important issues for WPC application.

2.3.2 Effect of wood content

Wood fiber content in WPCs significantly influences both processing and end-use properties. In the melting state, the viscosity of composites increases with fiber loading since fiber hinders the movement of polymer chain [50-52]. Generally, the mechanical properties of composites follow the law of mixture. Due to higher strength but lower modulus of thermoplastic compared to wood, generally increasing the wood content up to 40% decreases tensile and flexural strength but increases tensile and flexural modulus [51-53]. Moreover, because of hydrophilic nature of wood component and hydrophobic nature of thermoplastic, moisture sorption increases with the wood component ratio in the WPCs [54, 55].

2.3.3 Effect of the characteristics of the wood fiber

The wood used in WPCs is generally in the form of flour or fiber. The typical length-to-diameter (L/D) ratio of wood flour ranges from about 3:1 to 5:1. The wood flour is graded by mesh size. For example, wood flour with 40 and 80 mesh corresponds to 0.35 and 0.18 mm, respectively. Wood fiber typically has higher L/D ratio than wood flour from 10:1 to 25:1. Fiber length varies from 1 to 10 mm.

The size and geometry of wood fiber have significant effect on moisture absorption and mechanical properties [56-58]. Moisture absorption increases with length-to-diameter (L/D) ratio of wood fiber [56]. Longer fibers may increase the probability of voids within the composite. More voids would contain more water content when composites are exposed to a humid environment. In contrast, large L/D ratio of fiber favors the mechanical properties such as tensile and flexural properties, since increasing the fiber L/D ratio can increase the transfer efficiency of loading from polymer matrix to fiber [56-58].

2.3.4 Effect of the characteristics of the polymer matrix

Characteristics of polymers, including molecular weight and its distribution, rheology properties (MFI and melting point, etc.), mechanical properties, and degradation temperature, influence the properties and/or manufacturing of WPCs.

Melt flow index (MFI) of a polymer, an assessment of average molecular mass and inverse measure of the melt viscosity, is critical to control the processing. Injection molding encompasses higher MFI polymers while extrusion processes use lower MFI polymers. The MFI of a polymer has a complicated effect on the mechanical properties of WPCs. Because polymers with a low MFI often have a high molecular weight, WPCs with a low MFI polymer matrix have better strength and modulus than WPCs with a high MFI polymer matrix [59]. Conversely, at a high wood fiber loading, high MFI polymer matrix improves the wood fiber distribution and wetting, thus results in better mechanical properties [51].

2.3.5 Effect of surface modification of wood and addition of coupling agents

Because of wood's hydrophilic nature and plastic's hydrophobic nature, WPCs often require surface modification of wood or the addition of coupling agents to decrease the hydrophilicity of wood and increase the compatibility between wood fiber and plastics [60-64]. Coupling agents or surface modifiers contain two domains. One domain is a chemical function group, which can form covalent bonds by reacting with hydroxyl group on the wood; the other domain is a long chain, which can form entanglements with polymer matrix. In this way, the hydrophilicity of wood is decreased, as well as the dispersion of wood in the polymer matrix and the adhesion between wood and polymer are improved. As a result, moisture sorption is reduced and mechanical properties sensitive to the interfacial adhesion such as flexural and tensile strength are enhanced. For example, silane or stearic acid surface modified natural fiber-filled PP (50% fiber loading) decreased approximately 40% moisture absorption compared to unmodified fiber -filled PP [60, 61]. Addition of maleated PP significantly increased over 20% the flexural and tensile strength of natural fiber filled-PP composites in the fiber loading range between 20-50% [61, 62].

2.3.6 Effect of manufacturing methods

Manufacturing process can greatly influence surface quality. Study showed that while injection molding led to WPCs with a thicker polymer-rich surface layer, the surface of extruded WPCs, on the other hand, contained many wood particles not encapsulated by polymer [65]. As a result, the water resistance of injection molded WPCs was greater than that of extruded WPCs [65].

2.3.7 Moisture absorption of WPCs

Moisture absorption of WPCs would influence their dimension, mechanical properties, and appearance. Moisture absorption reduces the adhesion between the filler and polymer matrix, a change that results in the loss of mechanical properties [54]. A typical HDPE-based WPCs formulation containing 40% wood flour exposed to 100% relative humidity resulted in loss of 15% in tensile and 30% in flexural properties [54]. Also, upon moisture absorption WPCs swell and thus alter in dimension. Study showed that after water immersion, HDPE-based and PP-based WPCs experienced approximately 5% and 10% thickness swelling respectively [66]. Furthermore, in a high humid environment, water absorption could initiate fungi growth, which causes the discoloration [67]. Therefore, it is necessary to reduce or delay the moisture uptake of WPCs to prolong the long-term performance of the products.

2.3.8 Photodegradation/weathering of WPCs

Because both wood and plastic suffer photodegradation, WPCs also undergo photodegradation. The presence of wood accelerates the photodegradation of a polymer matrix since wood is a good light absorber [68, 69]. Photodegradation of WPCs produces changes in color, surface composition, and mechanical properties. Stark and Matuana reported that after exposure to accelerated weathering, HDPE-based WPCs experienced color fading, surface oxidation, and modulus loss [70-72]. Fabiyi et al. investigated the effects of natural and accelerated weathering on the appearance and chemical changes of HDPE and PP-based WPCs [73]. They observed that the degree of color change/lightness, carbonyl concentrations and lignin content increased with exposure time. PP-based WPCs underwent quicker photodegradation in terms of lightness, carbonyl concentrations and wood loss. The study established strong relationships between lightness and lignin degradation, lightness and carboxylic acid concentration, as well as lightness and esterification.

The presence of moisture/water in the photodegradation accelerates the weathering process. Water functions as a catalyst of an oxidative degradation. Moisture absorption swells the wood fiber, facilitating light penetration. Consequentially, reports noted increased lightening and flexural properties loss in WPCs [74].

2.3.9 Protection against photodegradation

Current approaches to improve the UV resistance of WPCs focus on the bulk of WPCs, i.e., incorporation of photostabilizers into the entire product [74-76]. Stark and Matuana investigated the performance of a low molecular weight diester HALS, a high molecular weight secondary amine triazine HALS, a benzotriazole UVA, and a colorant as photostabilizers of HDPE-based WPCs containing 50% wood flour [75]. The results indicated that both UVA and colorant were more effective photostabilizers than HALS with respect to preventing discoloration and flexural properties loss. The low efficiency of HALS was attributed to the possible reaction between the basic HALS and acidic wood flour. Muasher and Sain compared the performance of diester HALS with different molecular weight, tertiary and secondary amine trizaine HALS as photostabilizers of HDPE-based WPCs containing 40% wood flour. Their findings position high molecular weight diester HALS as most effective in terms of controlling long term fading and yellowing distortions [76].

2.4 Testing and property evaluation

2.4.1 Weathering testing

Natural weathering is a combination of effects of sunlight (UV, visible, and IR), water (dew, rain, snow, and humidity), temperature, oxygen, and biological contamination or competition [30]. For WPCs, the damaging effect of sunlight is most important. The spectral power distribution of noon midsummer sunlight (measured in Cleveland Ohio, 1986) is shown in Figure 2.16. The duration and intensity of sunshine, precipitation, and temperature and its fluctuation are location and season dependent. Because natural weathering is very time consuming, accelerated artificial weathering, which reduces exposure time by increasing the effects of radiation and water, is often used to test the durability of materials. Accelerated artificial weathering is made up of cycles, which simulate damaging effects of sunlight, rain, and dew by artificial light radiation, water spray, and condensation. Xenon arc, UVA-340, and UVB-313 lamps are primary radiation sources used in the accelerated artificial weathering. While Xenon arc lamps mimic both UV and VIS parts of the solar spectra, UVA-340 and UVB-313 lamps only simulate UV-A and UV-B regions of the sunlight [77]. Since photodegradation of WPCs is mainly attributed to the UV-A region of the sunlight, UVA-340 lamps often serve as a light source.

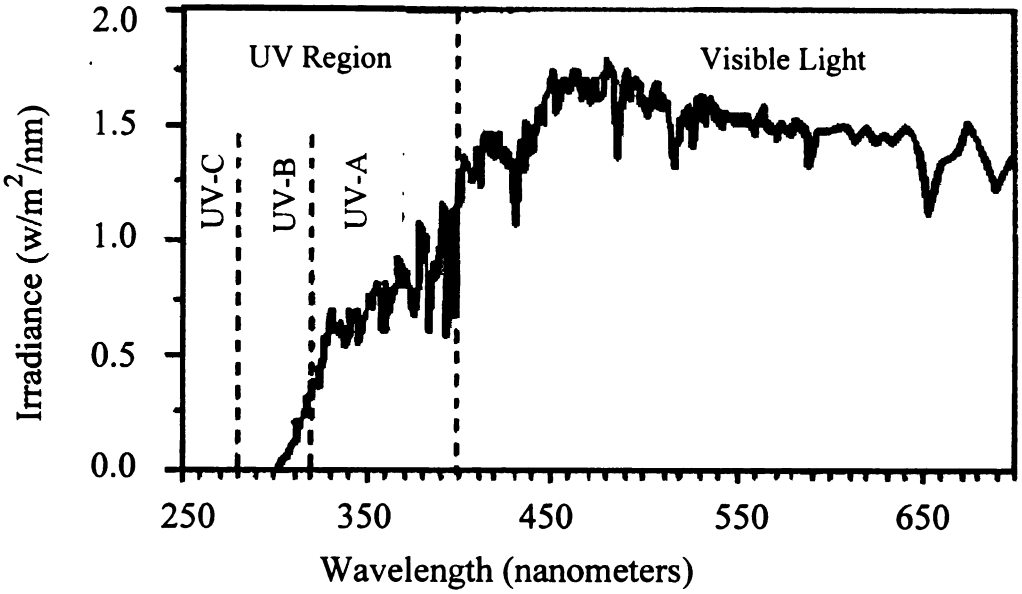

Figure 2.16. The sunlight spectrum [77].

2.4.2 X-ray photoelectron spectroscopy

X-ray photoelectron spectroscopy (XPS), a quantitative spectroscopic technique, measures the elemental composition, empirical formula, chemical state and electronic state of the elements that exist at the surface of the material. XPS spectra is obtained by irradiating a material with a beam of aluminum or magnesium X-rays and measuring the kinetic energy (KE) and number of electrons that escape from the top 1 to 10 nm of the material.

A plot of the number of electrons detected (Y-axis) versus the binding energy of the electrons detected (X-axis) charts a typical XPS spectrum. The already established binding energies of the electron orbitals in atoms allows for identifying the atomic composition of the sample surface. Measurement of the relative areas of the photoelectron peaks allows for the quantitative determination of the sample's composition.

Each element produces a characteristic set of XPS peaks at characteristic binding energy values that can be calculated by the following equation [78].

$$E_{binding} = E_{photon} - E_{kinetic} - \Phi \qquad \text{(Equation 2.3)}$$

where $E_{binding}$ represents the energy of the electron emitted from one electron configuration within the atom, E_{photon} the energy of the X-ray photons, $E_{kinetic}$ the kinetic energy of the emitted electron as measured by the instrument and Φ the work function of the spectrometer. Thus, a survey spectrum can be generated and sample's composition can be determined. A survey spectrum of wood-plastic composites is shown in Figure 2.17.

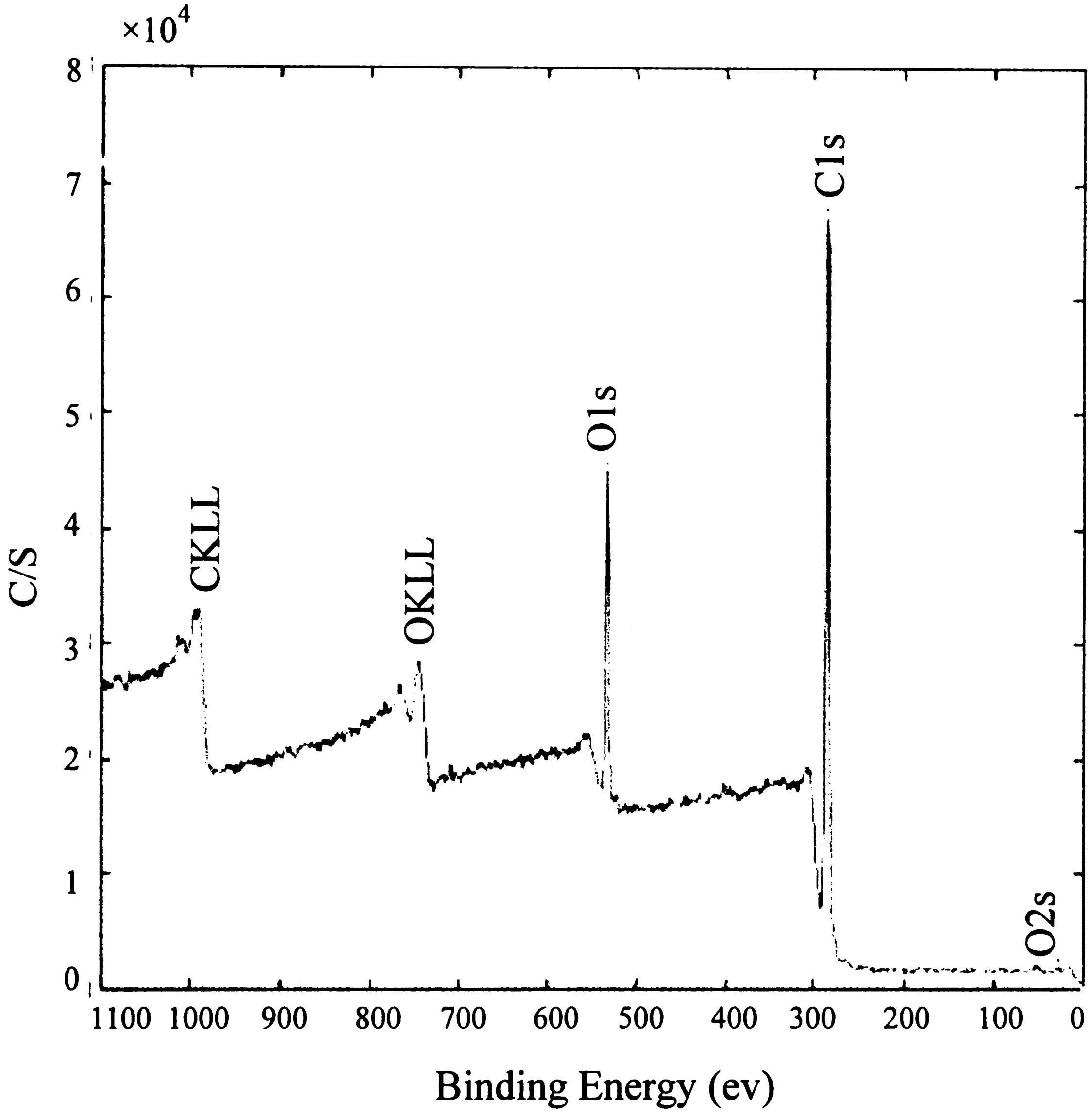

Figure 2.17. A survey spectrum of HDPE-based WPCs (WPCs formulation: 50% maple flour, 44% HDPE, and 6% TPW104).

These characteristic peaks correspond to the electron configuration within the atoms, e.g., 1s, 2s, 2p, 3s, etc. The number of detected electrons in each of the characteristic peaks directly relates to the amount of the element within the indicated area [78].

Chemical bonding frequently affects the binding energy of the electron orbital and results in chemical shift in the kinetic energy of the photoelectron. These binding energy shifts provide information of a chemical nature (such as atomic oxidation state) from the sample surface. A high resolution spectrum of C_{1S} region of WPCs is shown in Figure 2.18. C_{1S} peak consists of four subpeaks, corresponding to carbon in different oxidation states. C1 class of carbon atoms correspond to carbon atoms bonded only by carbon or hydrogen bonds (C-C and C-H); C2 class of carbon atoms are carbon atoms bonded to a single noncarbonyl oxygen (C-OH); C3 class of carbon atoms are carbon atoms bonded to a carbonyl or two noncarbonyl oxygen (C=O or O-C-O); and C4 class of carbon atoms are carbon atoms bonded to a carbonyl and a noncarbonyl oxygen (O-C=O) [68, 70, 72, 79].

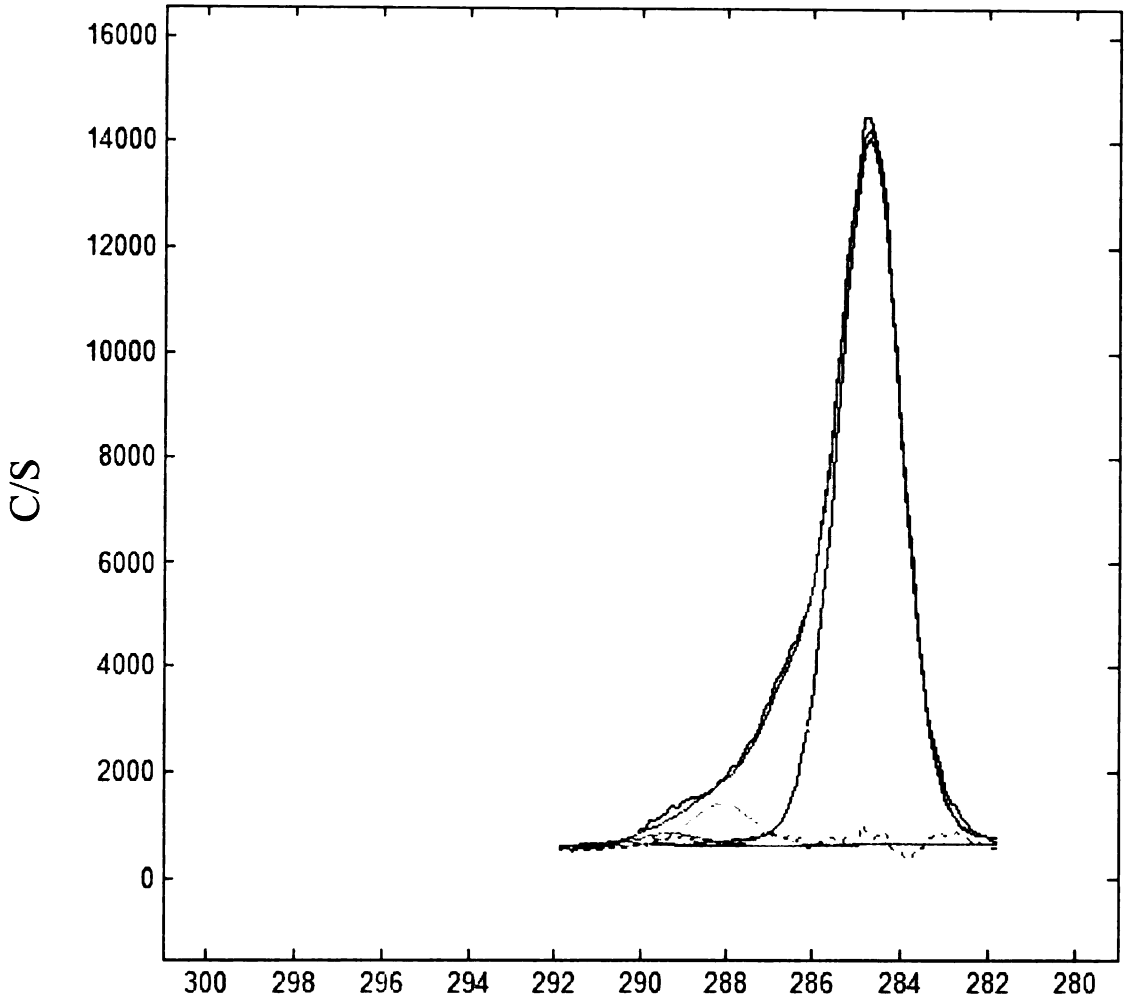

Figure 2.18. A high resolution spectrum of HDPE-based WPCs in C_{1S} region (WPCs formulation: 50% maple flour, 44% HDPE, and 6% TPW104).

2.4

ide

vib

abs

wa

diff

abs

me

The

is tr

loss

mor

2.4.3 Fourier transform infrared spectroscopy

Fourier Transform Infrared Spectroscopy (FTIR) is the powerful tool for identifying the functional groups. This technique works on the fact that chemical bonds vibrate at characteristic frequencies. When a material is irradiated with infrared radiation, absorbed IR radiation usually excites molecules into a higher vibrational state. The wavelength of light absorbed by a particular molecule is a function of the energy difference between the rest and excited vibrational states. The wavelengths that are absorbed by the sample are characteristic of its molecular structure [80]. This technique measures the absorption of infrared radiation by the sample material versus wavelength. The specimen's transmittance and reflectance of the infrared rays at different frequencies is translated into an IR absorption plot consisting of reverse peaks.

The photodegradation of the WPCs results in decay of benzyl ring in the lignin, loss of cellulose component, and increase in carbonyl groups, all of which can be monitored by FTIR.

2.4.4 Color measurement

CIE L*a*b* (CIELAB) is color space, which describes all the colors visible to the human eye (Figure 2.19). Color space has three coordinates, L*, a*, and b*. L* represents the lightness of the color (L* = 0 indicates black and L* = 100 indicates white); a* (negative values indicate green while positive values indicate red) and b* (negative values indicate blue and positive values indicate yellow) are the chromaticity coordinates.

The difference between colors is determined by Equation 2.4. Normally, ΔE of 1.0 is the smallest color difference noticeable for the human eye [81].

$$\Delta E = \sqrt{\Delta L^{*2} + \Delta a^{*2} + \Delta b^{*2}} \qquad \text{(Equation 2.4)}$$

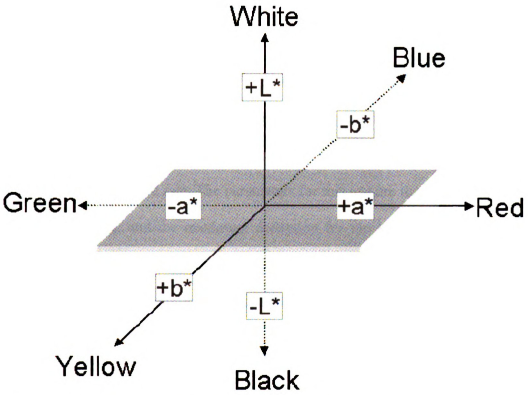

Figure 2.19. CIE L*a*b* (CIELAB) color space [82].

2.

fle

ben

ten

are

be

mo

be

fle

sup

po

spe

par

Fle

whe

defl

2.4.5 Flexural properties

Flexural properties are the ability of the material to withstand bending force. The flexural stress is a combination of tensile and compressive stresses. When composites are bent, one side suffers maximum compressive stress, and the other side suffers maximum tensile stress. Since one of the major applications of WPCs is decking, flexural properties are of a prime concern. Flexural strength, also known as modulus of rupture (MOR) or bending strength, represents the highest stress experienced within the material at its moment of rupture. The flexural modulus, also called modulus of elasticity (MOE) or bending stiffness, is the ratio of stress to strain in flexural deformation. A three point flexural test is often used to determine the flexural properties. The specimen lies on a support span and the load is applied to the center by the loading nose producing three point bending at a specified rate. The parameters for this test are the support span and the speed of the loading, and the maximum deflection for the test. The selection of these parameters is based on the test specimen thickness and is defined by ASTM standard. Flexural strength and modulus are determined by the following equations [4].

$$\text{Flexural strength} = \frac{3PL}{2bd^2} \qquad \text{(Equation 2.5)}$$

$$\text{Flexural modulus} = \frac{PL^2}{4bd^2y} \qquad \text{(Equation 2.6)}$$

where P is applied load, L is support span, b is sample width, d is sample depth, and y is deflection at load point.

2.5 Reference

1. C.M. Clemons, Wood-plastic composites in the United States: the interfacing of two industries, *Forest Products Journal*, **52**(6): 10-18 (2002).
2. A.K. Bledzki, J. Gassan, and S. Theis, Wood-filled thermoplastic composites, *Mechanics of Composite Materials*, **34**(6): 563-568 (1998).
3. D.N. Saheb and J.P. Jog, Natural fiber polymer composites: a review, *Advances in Polymer Technology*, **18**(4): 351-363 (1999).
4. A.A. Klyosov, *Wood-plastic composites*, John Wiley & Sons, Hoboken, (2007).
5. R.O. Ebewele, *Polymer science and technology*, CRC Press, London, (2000).
6. A.J. Peacock, *Handbook of Polyethylene: Structures, Properties, and Applications*, CRC Press, London, (2000).
7. http://en.wikipedia.org/wiki/Polyethylene
8. H.J. Giles Jr., J.R. Wagner Jr., and E.M. Mount III, *Extrusion: The Definitive Processing Guide and Handbook*, William Andrew Publishing, New York, (2004).
9. W.V. Titow, *PVC Technology*, Elsevier Applied Science Publishers, New York (1984).
10. G. Butters, *Particulate Nature of PVC*, Applied Science Publishers LTD, London, (1982).
11. C.H. Chen, C.F. Mao, and Y.W. Lo, Study of fusion percolation thresholds of rigid PVC compounds, *Journal of Applied Polymer Science*, **81**(12): 3022-3029 (2001).
12. L.M. Matuana and J.W. Kim, Fusion characteristics of wood-flour filled rigid PVC by torque rheometry, *Journal of Vinyl & Additive Technology*, **13**(1): 7-13 (2007).
13. J.F. Rabek, Polymer Photodegradation: Mechanisms and Experimental Methods, Chapman & Hall USA, New York (1995).
14. N.S. Allen, *Degradation and Stabilisation of Polyolefines*, Applied Science Publishers, New York (1983).
15. P. Gijsman, G. Meijers, and G. Vitarelli, Comparison of the UV-degradation chemistry of polypropylene, polyethylene, polyamide 6 and polybutylene terephthalate, *Polymer Degradation and Stability*, **65**(3): 433-441 (2006).
16. S. H. Hamid, *Handbook of polymer degradation*, Marcel Dekker, New York, (2000).

17. J.R. White and A.V. Shyichuk, Macromolecular scission and crosslinking rate changes during polyolefin photo-oxidation, *Polymer Degradation and Stability*, **92**(7): 1161-1168 (2007).

18. L.C. Mendes, E.S. Rufino, O.C. Paula and A.C. Torres. Mechanical, thermal and microstructure evaluation of HDPE after weathering in Rio de Janeiro City, *Polymer Degradation and Stability*, **79**(3): 371-383 (2003).

19. J. Attwood, M. Philip, A. Hulme, G. Williams, and P. Shipton, The effects of ageing by ultraviolet degradation of recycled polyolefin blends, *Polymer Degradation and Stability*, **91**(12): 3407-3415 (2006).

20. I. Yakimets, D. Lai, and M. Guigon, Effect of photo-oxidation cracks on behaviour of thick polypropylene samples, *Polymer Degradation and Stability*, **86**(1): 59-67 (2004).

21. C.A. Harper, E.M. Petrie, *Plastics materials and processes: a concise encyclopedia*, John Wiley and Sons, Hoboken, (2003).

22. F. Gugumus, Possibilities and limits of synergism with light stabilizers in polyolefins 2. UV absorbers in polyolefins, *Polymer Degradation and Stability*, **75**(5): 309-320 (2002).

23. C. Schaller, D. Rogez, A. Braig, Hydroxyphenyl-s-triazines: advanced multipurpose UV-absorbers for coatings, *Journal of Coatings Technology and Research*, **5**(1), 25-31(2008).

24. F. Gugumus, Possibilities and limits of synergism with light stabilizers in polyolefins 1. HALS in polyolefins, *Polymer Degradation and Stability*, **75**(2): 295-308 (2002).

25. C. Schaller, D. Rogez, A. Braig, Hindered amine light stabilizers in pigmented coatings, *Journal of Coatings Technology and Research*, **6**(1), 81-88 (2008).

26. Forest Products Laboratory, *Wood handbook—wood as an engineering material*, U.S. Department of Agriculture, Madison, (1999).

27. R.M. Rowell, *Handbook of wood chemistry and wood composites*, CRC Press, New York, (2005).

28. http://en.wikipedia.org/wiki/Lignin

29. M.D. Donohue and G.L. Aranovich. Classification of Gibbs adsorption isotherms, *Advances in Colloid and Interface Science*, **76-77**: 137-152 (1998).

30. W.C. Feist and D.N.-S. Hon, *Chemistry of weathering and protection*, U.S. Department of Agriculture, Madison, (1984).

31. D.N.-S. Hon and N. Shiraishi, *Wood and cellulosic chemistry*, Marcel Dekker INC, New York, (2000).

32. http://en.wikipedia.org/wiki/Photochemistry

33. B. George, E. Suttie, A. Merlin, and X. Deglise, Photodegradation and photostabilisation of wood–the state of the art, *Polymer Degradation and Stability*, **88**(2): 268-274 (2005).

34. U. Müller, M. Ratzsch, M. Schwanninger, M. Steiner, and H. Zöbl, Yellowing and IR-changes of spruce wood as result of UV-irradiation, *Journal of Photochemistry and Photobiology B Biology*, **69**(2): 97-105 (2003).

35. L. Tolvaj and O. Faix. Artificial aging of wood monitored by DRIFT spectroscopy and CIE L*a*b* color measurements I: effect of UV light. *Holzforschung*, **49**(5): 397-404 (1995).

36. K.K. Pandey, Study of the effect of photo-irradiation on the surface chemistry of wood, *Polymer Degradation and Stability*, **90**(1):9-20 (2005).

37. X. Colom, F. Carrillo, F. Nogues, and P. Garriga, Structural analysis of photodegraded wood by means of FTIR spectroscopy, *Polymer Degradation and Stability*, **80**(3):543-549 (2003).

38. K.K. Pandey, A note on the influence of extractives on the photo-discoloration and photo-degradation of wood, *Polymer Degradation and Stability*, **87**(2):375-379 (2005).

39. P. Nzokou and D. P. Kamdem, Influence of wood extractives on the photo-discoloration of wood surfaces exposed to artificial weathering, *Color Research & Application*, **31**(5): 425-434 (2006).

40. Y. Kataoka and M. Kiguchi, Depth profiling of photo-induced degradation in wood by FT-IR, *Journal of Wood Science*, **47**(4): 325-327 (2001).

41. K. Mitsui and S. Tsuchikawa, Low atmospheric temperature dependence on degradation of wood, *Journal of Photochemistry and Photobiology B Biology*, **81**(1): 84-88 (2005).

42. D.N. -S. Hon, S.T. Chang, and W.C. Feist, Participation of singlet oxygen in the photodegradation of wood surfaces, *Wood Science and Technology*, **16**(3) : 193-201 (1982)

43. M.D. Meijer, Review on the durability of exterior wood coatings with reduced VOC-content, *Progress in Organic Coatings*, **43**(4): 217-225 (2001).

44. Y. Xie, A. Krause, C. Mai, H. Militz, K. Richter, K. Urban, and P.D. Evans, Weathering of wood modified with the N-methylol compound 1,3-dimethylol-4,5-dihydroxyethyleneurea, *Polymer Degradation and Stability*, **89**(1): 189-199 (2005).

45. M. Kiguchi and P.D. Evans, Photostabilisation of wood surfaces using a grafted benzophenone UV absorber, *Polymer Degradation and Stability*, **61**(1) 33–45 (1998).

46. P.D. Evans, N.L. Owen, S. Schmid, and R.D. Webster. Weathering and photostability of benzoylated wood, *Polymer Degradation and Stability*, **76**(1) 291–303 (2002).

47. S.T. Chang and P.L. Chou, Photodiscoloration of UV-curable acrylic coatings and the underlying wood, *Polymer Degradation and Stability*, **63**(3): 435-439 (1999).

48. S.T. Chang and P.L. Chou, Photodiscoloration inhibition of wood coated with UV-curable acrylic clear coatings and its elucidation, *Polymer Degradation and Stability*, **69**(3): 355-360 (2000).

49. P.L. Chou, H.T. Chang, T.F. Yeh, and S.T. Chang, Characterizing the conservation effect of clear coatings on photodegradation of wood, *Bioresource Technology*, **99**(5): 1073-1079 (2008).

50. P.Y. Kuo, S.Y. Wang, J.H. Chen, H.C. Hsueh, M.J. Tsai, Effects of material compositions on the mechanical properties of wood-plastic composites manufactured by injection molding, *Materials and Design*, **30**(9): 3489-3496 (2009).

51. P. W. Balasuriya, L. Ye, and Y.W. Mai, Mechanical properties of wood flake–polyethylene composites. Part I: effects of processing methods and matrix melt flow behaviour, *Composites Part A: Applied Science and Manufacturing*, **32**(5): 619-629 (2001).

52. S. Narongrit, C. Kantima, P. Chakarin, and T Sirinthorn, Effect of wood sawdust content on rheological and structural changes, and thermo-mechanical properties of PVC/sawdust composites, *Polymer International*, **52**(12): 1847-1855 (2003).

53. A. J. Nuñez, P. C. Sturm, J.M. Kenny , M. I. Aranguren , N. E. Marcovich , M. M. Reboredo, Mechanical characterization of polypropylene-wood flour composites, *Journal of Applied Polymer Science*, **88**(6): 1420-1428 (2003).

54. N.M. Stark, Influence of moisture absorption on mechanical properties of wood flour-polypropylene composites, *Journal of Thermoplastic Composite Materials*, **14**(5): 421-432 (2001).

55. N.E. Marcovich, M.M. Reboredo, and M.I. Aranguren, Moisture diffusion in polyester–wood flour composites, *Polymer*, **40**(26): 7313-7320 (1999).

56. S. Migneault, A. Kouba, F. Erchiqui, A. Chaala, K. Englund, and M.P. Wolcott, Effects of processing method and fiber size on the structure and properties of wood–plastic composites, *Composites Part A: Applied Science and Manufacturing*, **40**(1): 80-85 (2009).

57. H.C. Chen, T.Y. Chen, and C.H. Hsu, Effects of wood particle size and mixing ratios of HDPE on the properties of the composites, *Holz als Roh- und Werkstoff*, **64**(4): 172-177 (2006).

58. M. C. N. Yemele, A. Koubaa, A. Cloutiera, P. Soulounganga, and M. Wolcott, Effect of bark fiber content and size on the mechanical properties of bark/HDPE composites, *Composites Part A: Applied Science and Manufacturing*, **41**(1): 131-137 (2010).

59. H. Huang and J. Zhang, Effects of filler–filler and polymer–filler interactions on rheological and mechanical properties of HDPE-wood composites, *Journal of Applied Polymer Science*, **111**(6): 2806-2812 (2009).

60. S. Lee, S. Chun, G. Doh, and I. Kang, Influence of chemical modification and filler loading on fundamental properties of bamboo fibers reinforced polypropylene composites, *Journal of Composite Materials*, **43**(15): 1639-1657 (2009).

61. L. Dányádi, J. Móczó, and B. Pukánszky, Effect of various surface modifications of wood flour on the properties of PP/wood composites, *Composites Part A: Applied Science and Manufacturing*, **41**(2): 199-206 (2010).

62. T.J. Keener, R.K. Stuart, and T.K. Brown, Maleated coupling agents for natural fibre composites, *Composites Part A: Applied Science and Manufacturing*, **35**(3): 357-362 (2004).

63. B.L. Shah, L.M. Matuana, Novel coupling agents for PVC/wood-flour composites, *Journal of Vinyl & Additive Technology*, **11**(4): 160-165 (2005).

64. J.Y. Kim, J.H. Peck, S.H. Hwang, J. Hong, S. C. Hong, W. Huh, S.W.Lee, Preparation and mechanical poperties of Poly(vinyl chloride)/bamboo flour composites with a novel block copolymer as a coupling agent, *Journal of Applied Polymer Scienc*e, **108**(2): 2654–2659 (2008).

65. N.M. Stark, L.M. Matuana, and C.M. Clemons, Effect of processing method on surface and weathering characteristics of wood–flour/HDPE composites, *Journal of Applied Polymer Science*, **93**(3): 1021-1030 (2004).

66. K.B. Adhikary, S. Pang, and M.P. Staiger, Long-term moisture absorption and thickness swelling behaviour of recycled thermoplastics reinforced with Pinus radiata sawdust, *Chemical Engineering Journal*, **142**(2) 190-198 (2008).

67. B. Dawson-Andoh and L.M. Matuana, High density polyethylene-wood flour composite lumber: efficacy of two commercial biocides in the control of fungal colonization and discoloration, *Holz als Roh-und Werskstoff*, **65**(5): 331-335 (2007).

68. L.M. Matuana and D.P. Kamdem, Accelerated ultraviolet weathering of PVC/wood-flour composites, *Polymer Engineering and Science*, **42**(8): 1657-1666 (2002).

69. L.M. Matuana, D.P. Kamdem, and J. Zhang, Photoaging and Stabilization of rigid PVC/wood-fiber composites, *Journal of Applied Polymer Science*, **80**(11): 1943-1950 (2001).

70. N.M. Stark and L.M. Matuana, Characterization of weathered wood–plastic composite surfaces using FTIR spectroscopy, contact angle, and XPS, *Polymer Degradation and Stability*, **92**(10): 1883-1890 (2007).

71. N.M. Stark and L.M. Matuana, Surface chemistry and mechanical property changes of wood-flour/high-density-polyethylene composites after accelerated weathering, *Journal of Applied Polymer Science*, **94**(6): 2263-2273 (2004).

72. N.M. Stark and L.M. Matuana, Surface chemistry changes of weathered HDPE/wood-flour composites studied by XPS and FTIR spectroscopy, *Polymer Degradation and Stability*, **86**(1): 1-9 (2004).

73. J.S. Fabiyi, A.G. McDonald, M. P. Wolcott, and P. R. Griffiths, Wood plastic composites weathering: visual appearance and chemical changes, *Polymer Degradation and Stability*, **93**(8): 1405-1414 (2008).

74. N.M. Stark and L.M. Matuana, Influence of photostabilizers on wood flour-HDPE composites exposed to xenon-arc radiation with and without water spray, *Polymer Degradation and Stability*, **91**(12): 3048-3056 (2006).

75. N.M. Stark and L.M. Matuana, Ultraviolet weathering of photostabilized wood-flour-filled high density polyethylene composites, *Journal of Applied Polymer Science*, **90**(10): 2609-2617 (2003).

76. M. Muasher and M. Sain, The efficacy of photostabilizers on the color change of wood filled plastic composites, *Polymer Degradation and Stability*, **91**(5): 1156-1165 (2006).

77. P. Brennan and C. Fedor, *Sunlight, UV and accelerated weathering*, Technical Bulletin, The Q-Panel Company, (1987).

78. M.Stamm, *Polymer surfaces and interfaces: characterization, modification and applications*, Springer, Dresden, (2008).

79. G. Sinn, A. Reiterer and S. E. Stanz-Tschegg, Surface analysis of different wood species using X-ray photoelectron spectroscopy (XPS), *Journal of Materials Science*, **36**(19): 4673-4680 (2001).

80. J.E. Mark, *Physical properties of polymers handbook*, Springer, New York, (2006).

81. American Society for Testing and Materials, *E308-08 Standard practice for computing the colors of objects by using the CIE system*, in Annual Book of ASTM Standards, 06.01, (2008).

82. N.M. Stark, *Photodegradation and photostabilization of weathered wood flour filled polyethylene composites*, PHD Dissertation, Michigan Technological University, (2003).

CHAPTER 3

Coextruded PVC/Wood-Flour Composites with WPC Cap Layers

This chapter is slightly modified from a research paper that was published in the Journal of Vinyl & Additive Technology, 14 (4): 197-203 (2008). It is co-authored by Shan Jin and L.M. Matuana.

3.1 Abstract

Wood-plastic composites (WPCs) can absorb moisture in a humid environment owing to the hydrophilic nature of the wood, thereby making the products susceptible to microbial growth and loss of mechanical properties. In this study, rigid poly(vinyl chloride) (PVC)/wood-flour composites (core layer) were coextruded with either unfilled rigid PVC (cap layer) or rigid PVC filled with a small amount (5–27.5%) of wood flour (composite cap layers) in order to decrease or delay the moisture uptake. The thickness of the cap layer and its composition in terms of wood flour content were the variables examined during coextrusion. Surface color, moisture absorption, and flexural properties of both coextruded and noncoextruded (control) composite samples were characterized. The experimental results indicated that both unfilled PVC and composite cap layers can be encapsulated over rigid PVC/wood-flour composites in a coextrusion process. The moisture uptake rate was lower when a cap layer was applied in the composites, and the extent of the decrease was a strong function of the amount of wood flour in the cap layer but insensitive to cap layer thickness. Overall, coextruding PVC surface-rich cap layers on WPCs significantly increased the flexural strength but decreased the flexural modulus as compared with those of control samples. The changes in bending properties were sensitive to both cap layer thickness and wood flour content.

3.2 Introduction

Wood-plastic composites (WPCs) have experienced significant market expansion in recent years as a replacement for solid wood, mainly in outdoor applications such as railings, decking, fences, window and door frames etc. These products are marketed as low-maintenance and weather-resistant compared with solid wood, because the wood can be encapsulated in a hydrophobic polymer matrix [1, 2]. However, as WPCs are exposed to an outdoor environment of moisture and ultraviolet light in sunlight, the expectation that the products would maintain their new appearance without maintenance has not been realized [1-3].

Indeed, studies have shown that WPCs can absorb moisture in a humid environment because of the highly hydrophilic nature of wood flours in the composites, especially at high loading levels, thereby making the products more prone to microbial growth and biological decay, and thus affecting their appearance [4, 5]. Moisture absorption also reduces the adhesion between the filler and polymer matrix, a change that results in the loss of mechanical properties [3]. Therefore, it is necessary to reduce or delay the moisture uptake of WPCs to prolong the long term performance of the products.

Many researchers have investigated the moisture/(water absorption) behaviors of natural fiber–plastic composites. Marcovich et al. investigated moisture diffusion in polyester-(wood flour) composites and found that the equilibrium moisture content of the composites was dependent on the size and shape of the wood flour [6]. Stark studied the influence of moisture absorption on the mechanical properties of (wood flour)-polypropylene composites [3]. She reported that incomplete encapsulation of wood flour by the polypropylene matrix occurs in both 20% and 40% wood flour composites. In addition, she demonstrated that more moisture was absorbed by the composites with higher wood flour loading, a situation that resulted in a significant decrease of both flexural and tensile properties [3]. Similar results were reported by Bledzki and Faruk, who found that the impact properties of (wood fiber)–polypropylene composites were affected by moisture content [7]. Hygrothermal aging behavior of injection-molded (rice husk)-filled polypropylene composites also has been examined by immersing the specimens in distilled water at 30°C and 90°C [8]. It was found that both the tensile strength and the modulus deteriorated after immersion in water, the extent of the deterioration being dependent on the immersion temperature. This reduction in tensile properties was attributed to the interfacial degradation in the composites [8].

Although several authors have investigated the moisture/(water absorption) behaviors of (natural fiber)-plastic composites, only a few provided the methods to alleviate this problem. The use of additives, such as maleated polyolefins and other compatibilizers, encapsulation of exposed wood during compounding, or the use of protective coating have been reported as methods to improve the moisture uptake of WPCs [9]. These suggested approaches are employed by current WPC manufacturers with limited success. Stark and Matuana have recently demonstrated that covering the WPCs with hydrophobic layers decreases the moisture absorption of WPCs. Their results showed that a cap layer of polyolefin coextruded over (wood flour)-polyolefin composites provides improved moisture resistance compared with that of the control WPC [10].

Coextrusion technology can produce a multilayered product with different properties at outer and inner layers, thus offering different properties between surface and bulk [11-13]. The benefit of coextrusion is that each layer of coextruded material offers a particular property, including impermeability or resistance to moisture uptake and improved mechanical properties, such as stiffness, depending on the compositions of the outer and inner layers. For example, when composites are bent, one side suffers maximum compressive stress, and the other side suffers maximum tensile stress [13]. Therefore, the composition of the outer layer will influence not only the moisture uptake, but also the flexural properties of the overall composite.

The main goal of this study was to coextrude rigid PVC/wood-flour composites with various cap layers in order to decrease or delay the moisture uptake of the composites and thus increase the service life of the WPCs. Particular emphasis was placed on examining the effects of cap layer composition (unfilled PVC vs. WPC) on moisture uptake and flexural properties.

3.3 Experimental

3.3.1 Materials

The PVC matrix and other additives used in the manufacture of the coextruded composites are listed in Table 3.1. Rutile titanium dioxide supplied by Kemira was used as a pigment in the cap layer formulations to differentiate the cap layer from the core. A 0.425 mm (40 mesh) maple wood flour was utilized as filler. The wood flour was oven-dried at 105°C for 48 h to remove moisture before processing. Formulations of core layer (rigid PVC/wood-flour composites) and cap layers [unfilled rigid PVC and rigid PVC filled with a small amount of wood flour (5–27.5 wt%)] are also listed in Table 3.1.

3.3.2 Compounding and coextrusion of composites

A 20-L high-intensity mixer [Papenmeier, Type TGAHK20] was used for dry blending of the TiO_2-pigmented pigmented rigid PVC as well as unpigmented PVC, dried maple wood flour, and other additives at the concentration levels listed in Table 3.1. Six different formulations were compounded in order to produce control and coextruded samples with different types of cap layers. These formulations consisted of:

- 100 phr of nonpigmented rigid PVC and 100 phr of wood flour as control (no cap layer) and core layer,
- unfilled rigid PVC pigmented with 5 phr of TiO_2 for cap layer, and
- pigmented rigid PVC filled with four different amounts of wood flour (5, 12.5, 20, and 27.5 wt%) for cap layers.

Table 3.1. Formulations used in core and cap layers of coextruded rigid PVC/wood-flour composites.

Ingredients	Content (phr)	
	Core Layer and control	Cap layers
PVC (K-value = 66.4) (Shintech)	100	100
Tin stabilizer (PlastiStab 2808-Halstab)	2	2
Calcium stearate (Synpro)	1.5	1.5
Paraffin wax (Gulf Wax)	2	2
Processing aid (Paraloid K-120)[1]	2	2
Processing aid (Paraloid K-175)[1]	2	2
Impact modifier (K-334)[1]	10	10
40 mesh maple (American Wood Fibers)	100	(0-27.5 wt%)
Titanium dioxide (Kemira 460)	-	5

[1] Supplied by Rohm & Haas Co.

Each composition (Table 3.1) was dry blended for 10 min, and the shear heat generated during compounding increased the temperature of the blend from 24°C to 35°C. The compounded materials were discharged to a container at room temperature. The coextrusion system consisted of a coextrusion die connecting a twin-screw extruder for the core layer and a single-screw extruder for the cap layer. Core layer was formed by using a 32-mm conical counter rotating twin screw extruder (C.W. Brabender Instruments, South Hackensack, NJ) with a length-to-diameter ratio of 13:1. Cap layers were produced by using a 19-mm single-screw extruder (C.W. Brabender Instruments, South Hackensack, NJ) with a length-to-diameter ratio of 30:1. The die used in our experiments was specifically designed to ensure that the cap layers covered the entire core layer of the WPCs, i.e., to ensure complete encapsulation of the core layer. The schematic of the coextrusion system used in this study is shown in Figure 3.1.

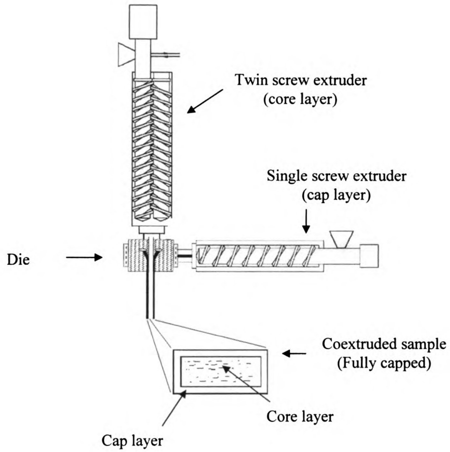

Figure 3.1. Schematic of the coextrusion system used in this study.

Core layers consisted of unpigmented rigid PVC/wood-flour composites made with 100 phr of PVC and 100 phr of wood flour (Table 3.1). It was observed in our previous work that the surface quality of rigid PVC/wood-flour composites was largely dependent on the processing conditions, particularly the barrel temperature profile and screw rotational speed of the extruder as well as on the amount of wood flour used [1]. For example, samples of excellent quality (i.e., smooth without torn edges) were produced for rigid PVC filled with maple flour up to 100 phr by using a decreased temperature profile from the hopper to the die. Consequently, the processing temperature profile of the twin-screw extruder for the core layer was set at 190/180/175/170°C from hopper to coextrusion die. The rotational speed of the screws was maintained at 30 rpm during processing. These processing conditions for the core layer were used in the manufacture of all coextruded composites.

By contrast, various formulations and processing conditions were utilized during the coextrusion process for the cap layers. When unfilled rigid PVC was used as the cap layer, the processing temperature profile of the single screw extruder was set at 155/165/165/170°C from hopper to coextrusion die. However, three different rotational screw speeds (5, 10, and 15 rpm) were employed to vary the thickness of the cap layers. On the other hand, the processing temperature profile of the single-screw extruder for rigid PVC/wood-flour composites cap layers (or composite cap layers) was set at 185/180/175/170°C from hopper to coextrusion die, regardless of the formulations. Similarly, the rotational screw speed was maintained constant at 15 rpm throughout the experiments when cap layers of composites were coextruded over WPCs. Nevertheless, the concentrations of wood flour in the cap layers varied from 5 to 27.5% based on the total weight of the cap layers of the composite. The control samples (rigid PVC/wood-flour composites without cap layer) were also produced by using the coextrusion die. The processing conditions were same as those utilized for core layers.

3.3.3 Property evaluation

Cap layer thickness evaluation

Pictures of the cross sections of coextruded samples were taken by using a digital camera, and samples were visually examined to evaluate the thickness of the cap layer (Table 3.2). Figure 3.2 shows the cross section of unfilled rigid PVC coextruded on WPCs.

Color measurements

Color measurements on the surfaces of control and coextruded samples were made according to the procedure outlined in ASTM D2244. A Minolta CR-420 Chroma Meter (Minolta Corp., Ramsey, NJ) was used to measure the color in L*a*b* coordinates at three locations on each sample by using the Commission International d'Eclairage (CIELAB 1976 color space) three-dimensional color space system. In this system, L*axis (+L* for light, −L* for dark) represents the lightness, and a* (+a* for red, −a* for green), and b* (+b* for yellow, −b* for blue) are the chromaticity coordinates.

Table 3.2. Effects of the composition and processing speed of cap layer on its thickness, surface color, and moisture absorption of coextruded rigid PVC/wood-flour composites and control samples.

Wood flour content in cap layers	Average cap layer thickness[1]		Color parameters			Sorption parameters	
	mm	mil	L*	a*	b*	MC (%)[2]	MUR (10^{-3} %/hr)
None (Control)	-	-	56.8	7.49	15.72	3.92	4.6
27.5% wood flour	1.0	39	74.2	2.40	8.82	-	3.1
20% wood flour	1.0	39	75.5	1.80	8.22	3.17	2.8
12.5% wood flour	0.9	35	79.8	1.51	9.44	2.85	2.6
5% wood flour	0.9	35	85.2	0.50	6.82	1.92	1.8
Processing speeds							
PVC cap layer (5 rpm)	0.6	24	90.5	-1.88	4.97	1.66	1.2
PVC cap layer (10 rpm)	0.8	31	94.0	-0.81	6.30	1.48	1.2
PVC cap layer (15 rpm)	1.0	39	94.2	-0.53	6.02	-	-

[1] The standard deviation for cap layer thickness was 0.1 mm (0.4 mil) for all samples.

[2] The moisture content was calculated after approximately 8124 h (338.5 days) of exposure in the chamber.

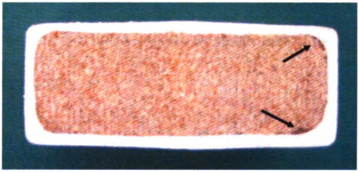

Figure 3.2. Cross section of unfilled rigid PVC cap layer coextruded on WPCs. The arrows show the areas of poor interfacial adhesion between cap and core layers.

Moisture absorption tests

The moisture absorption tests were carried out by following the method described by Kim et al. [14]. In these tests, a saturated ammonium chloride solution was placed in a sealed chamber to provide a constant relative humidity of 79% at 20°C, which yielded an equilibrium moisture content of approximately 16%. The nominal width, depth and length of the samples were 2.54 cm (1 inch), 0.95 cm (3/8 inch), and 7.62 cm (3 inch), respectively. Both dried control and coextruded composite samples with unsealed edges were weighed and placed in this sealed chamber. Samples were removed from the chamber and weighed again at various intervals to record mass gained. The percentage of moisture absorbed by the sample or moisture content (MC) was calculated from the recorded mass of the sample at time t (M_t) and the initial mass of the dry sample (M_o) by using the following equation:

$$\mathrm{MC} = \left[\left(\frac{M_t - M_o}{M_o}\right)\right] \times 100 \qquad \text{(Equation 3.1)}$$

The mass of specimens was measured to a precision of 0.0001 g. At least 3 replicates were used to obtain an average value for each formulation.

Moisture uptake curves as a function of exposure time (*MC* versus time) were derived from the data obtained with Equation 3.1. From these curves, a moisture uptake rate (*MUR*) was defined to estimate how fast the moisture absorption occurred in the samples:

$$\mathrm{MUR} = \frac{\Delta \mathrm{MC}}{\Delta t} \qquad \text{(Equation 3.2)}$$

where ΔMC is the change in moisture content (%) and Δt is change in time (hours). Values for MUR (%/h) were calculated from the initial slope of a plot of MC versus time. Only the straight-line region below the maximum moisture content was used for this calculation.

Flexural property evaluation

Three-point flexural tests were carried out in a walk-in conditioning room at (23 ± 2)°C and (50 ± 4)% relative humidity on an Instron 5585H (with Bluehill 2 software) testing machine. Samples were stored in this conditioning room for at least 48 h before property testing. The testing was performed with a crosshead rate of 4.3 mm/min in conformance with ASTM standard D7031-2004, the standard test method for evaluating the mechanical and physical properties of WPC products. At least six replicates were tested to obtain an average value for each formulation. Data were collected on modulus of rupture (MOR or flexural strength) and modulus of elasticity (MOE or flexural stiffness).

Statistical analysis

A two-way analysis of variance (ANOVA) was performed on the MOR and MOE data to distinguish statistical differences ($p < 0.05$) between coextruded and control samples. All statistical analyses were performed by using Design Expert software (v. 7) from Stat-Ease (Minneapolis, MN). The superscript letters in Tables 3.3 and 3.4 represent the ANOVA results. The same letter denotes that the difference between two treatments is not statistically significant. Otherwise, the difference is statistically significant ($p < 0.05$).

3.4 Results and Discussion

3.4.1 Color measurements

As illustrated in Figure 3.1, the goal of coextrusion was to encapsulate rigid PVC/wood-flour composites completely with both unfilled rigid PVC and rigid PVC filled with a small amount of wood flour (or composite cap layers). An image of the cross section of a coextruded sample is shown in Figure 3.2, and the average thicknesses of the cap layers are listed in Table 3.2. The thickness of the cap layer was affected by different rotational screw speeds of the extruder feeding the die for cap layers. Increasing the rotational screw speed tended to increase the thickness of the cap layer, mainly owing to the increased output during coextrusion processing. However, the amount of wood flour in the cap layers appeared to have no significant effect on their thicknesses, probably because all coextruded samples with composite cap layers were produced at a constant rotational screw speed.

Color measurements were performed to monitor the change in surface color of coextruded and control samples. The surfaces of WPC coextruded with unfilled and wood-flour-filled PVC cap layers are shown in Figure 3.3 and Table 3.2 summarizes the color parameters obtained on the surfaces of coextruded and control samples.

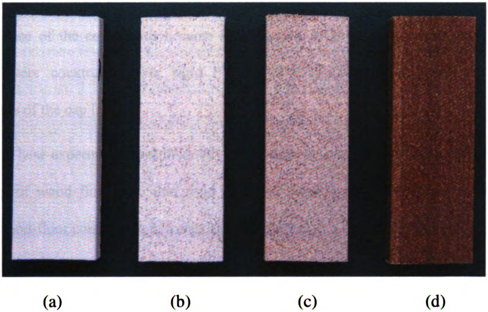

Figure 3.3. WPC samples coextruded with (a) unfilled PVC cap layer, (b) 5% wood flour filled PVC cap layer, (c) 20% wood flour filled PVC cap layer, and (d) control WPC (no cap layer).

Coextruded samples with composite cap layers had higher L* but lower a* and b* values than the composites without a cap layer (control or nonencapsulated sample), irrespective of the wood flour content in the cap layers. This result was expected, because more wood flour was exposed on the surface of the control sample, which darkened its surface because of improper encapsulation of wood by the matrix. The extent of darkening was dependent on the amount of wood flour in the cap layer, as can be seen in Figure 3.3. Increasing the wood flour content in the cap layers tended to darken the surface of coextruded composites owing to the darker color of wood flour. As expected, the surface of the composites became lighter when TiO_2-pigmented unfilled PVC cap layers were coextruded over rigid PVC/wood-flour composites, regardless of the thickness of the cap layer.

These experimental results imply that composite cap layers which contain a small amount of wood flour or a thin rigid PVC cap layer can be encapsulated over rigid PVC/wood-flour composites in a coextrusion process.

3.4.2 Moisture absorption

Moisture absorption curves as a function of exposure times of various cap layers (unfilled PVC and composites) coextruded over rigid PVC/wood-flour composites (WPCs) are shown in Figure 3.4. The sorption parameters estimated from these curves, i.e., maximum moisture content and the rate of moisture uptake determined from Equation 3.2, are summarized in Table 3.2.

It should be mentioned that the samples did not reach the equilibrium moisture content even after approximately 8124 h (338.5 days) of exposure in the chamber, probably because of their larger dimensions. However, the absence of distinct plateau regions in Figure 3.4 does not affect the initial slope of the curves used to calculate the rate of moisture uptake. In addition, the linear region is not clearly seen in the moisture absorption curves of coextruded samples with unfilled rigid PVC cap layers of various thicknesses (Figure 3.4b), mainly because of the magnitude of the moisture content absorbed by nonencapsulated WPCs (control sample). Instead, a clear linear region could be seen for these samples by discarding the curve of the control sample in this figure.

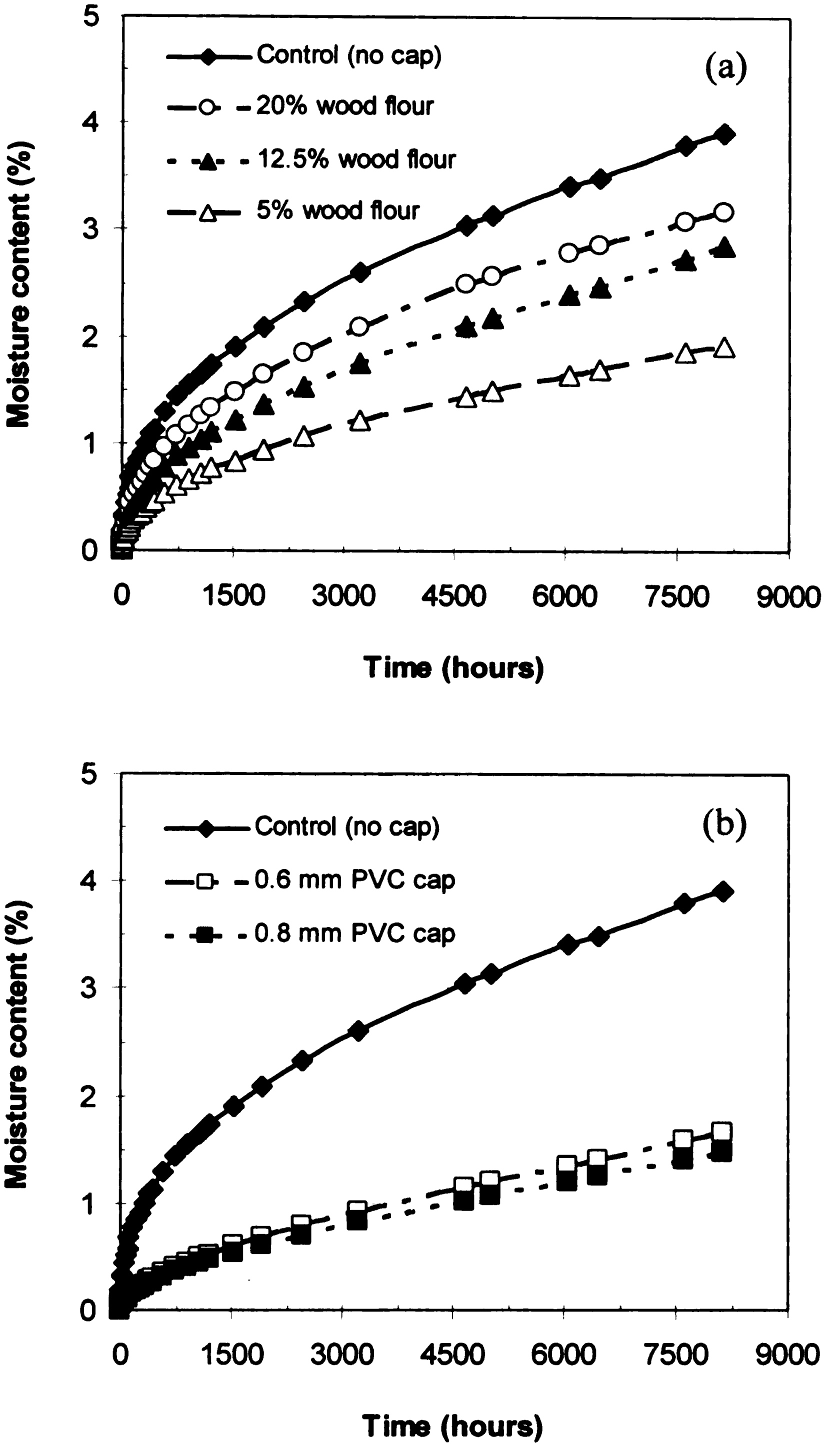

Figure 3.4: Moisture absorption curves of control samples and coextruded rigid PVC/wood-flour composites with various types of cap layers: (a) wood-flour (5-20 wt%) filled rigid PVC cap layers and (b) unfilled rigid PVC cap layers of various thicknesses.

Nonencapsulated WPCs (control) not only absorbed more moisture than the coextruded counterparts after 338.5 days, but also experienced a quicker moisture uptake than the coextruded samples, regardless of the type of cap layer. This great affinity for moisture can be attributed to the presence of hygroscopic wood on the surface of noncoextruded WPC samples. By contrast, cap layers of both composites with a small wood flour content (Figure 3.4a) and unfilled rigid PVC (Figure 3.4b) significantly slowed the moisture uptake of WPCs, probably because of the hydrophobic layer of PVC on the surface of the WPCs. A similar trend was reported by Stark and Matuana, who found that the plastic-rich polymer film that forms on the surface of coextruded WPCs increases their moisture resistance over that of noncoextruded WPCs [10].

The extent of MUR was a strong function of the amount of wood flour in the cap layer. As shown in Figure 3.4a and Table 3.2, the MUR was lower when a cap layer was applied in the composites. Increasing wood flour content in the cap layer tended to increase the moisture absorption rate in the WPCs. This deleterious effect can clearly be seen in Figure 3.4a by comparing the magnitude of the slope of the curves (or the rate of moisture uptake in Table 3.2) as well as the exposure time needed by the samples to absorb a certain amount of moisture. As shown by the slopes in Figure 3.4a, the rate of moisture absorption (Table 3.2) in coextruded samples decreased as the wood flour content decreased in the cap layer. It is also noted that by drawing a horizontal line parallel to the x-axis at an arbitrary moisture content (e.g., 1% in Figure 3.4a), four intersection points with the data can be obtained. The first intersection point is detected at lower exposure time (control), and the next three are seen at higher exposure time (coextruded samples), thus clearly indicating the advantage of coextruding WPCs in delaying the rate of moisture uptake.

Conversely, the extent of MUR for coextruded WPCs was not sensitive to the thickness of the cap layer. As illustrated in Figure 3.4b and Table 3.2, the thickness of unfilled PVC cap layers coextruded on WPCs did not affect the rate of moisture uptake of the samples. Nevertheless, coextruded samples with a rigid PVC cap layer still absorbed moisture, despite the presence of the hydrophobic layer of PVC on the surface of the WPCs. As the surface of coextruded samples was covered by a PVC layer, the only means by which they could absorb moisture was through their unprotected edges [15]. A lack of a good interfacial adhesion between the PVC cap layer and the WPC core also may have provided channels through which moisture diffused into the samples. As seen at the areas close to the sample edges in Figure 3.2, the adhesion between cap and core layers deteriorated more as the amount of wood flour increased in the cap layers. As a result, the moisture content absorbed after 8124 h by coextruded samples with only 5% of wood flour in the cap layer (Figure 3.4a) was almost 30% greater than that absorbed by their counterparts with unfilled PVC cap layers.

3.4.3 Flexural properties

The effect of cap layer thickness on the flexural properties of coextruded WPC is summarized in Table 3.3. Significant improvement in bending strength (MOR) occurred in WPCs coextruded with unfilled rigid PVC cap layers. Increasing the cap layer thickness did not affect the strength of coextruded WPCs. By contrast, the stiffness (MOE) of WPCs was significantly reduced when they were encapsulated with unfilled PVC cap layers. Generally, the stiffness of coextruded WPCs decreased as the cap layer thickness increased (Table 3.3).

The distinct trends described earlier were expected, because the mechanical properties of coextruded samples depend on the properties of the materials in both outer and inner layers. Generally, stronger and stiffer materials on the outer layer would enhance the overall performance of the coextruded samples compared with that of the product made by the inner material alone. Therefore, the increased bending strength and decreased bending modulus induced by coextruding unfilled PVC cap layers over WPCs can be attributed to greater strength but lower stiffness of unfilled PVC compared with WPCs.

The effect of composite cap layer composition in terms of wood flour content is listed in Table 3.4. Composites used as cap layers contained less wood flour (up to 27.5 wt%) than the one used in the core, which contained 50 wt%, thus implying that the formulation used for the outer layer was rich in PVC. Consequently, the bending strength of WPCs increased while their modulus decreased significantly on encapsulating with composite cap layers.

Table 3.3. Effect of the thickness of cap layer on the flexural properties of coextruded WPCs.

Thickness of unfilled PVC cap layers	Flexural properties	
	MOR (MPa)	MOE (GPa)
None (Control or not coextruded)	44.2 ± 2.3^{A}	4.52 ± 0.22^{A}
0.6 mm (24 mil)	54.9 ± 1.3^{B}	4.29 ± 0.06^{B}
0.8 mm (31 mil)	54.8 ± 3.0^{B}	3.84 ± 0.24^{C}
1 mm (39 mil)	53.6 ± 0.7^{B}	3.43 ± 0.05^{D}

The superscript letters indicate ANOVA results.

Table 3.4. Effects of wood flour content in cap layers on the flexural properties of coextruded WPCs.

Wood flour content (%) in cap layers	Flexural properties	
	MOR (MPa)	MOE (GPa)
None (Control or not coextruded)	44.24 ± 2.31^{A}	4.52 ± 0.22^{A}
5% wood flour	52.65 ± 3.57^{B}	3.29 ± 0.34^{B}
12.5% wood flour	52.46 ± 0.80^{B}	3.56 ±0.15^{C}
20% wood flour	52.40 ± 3.08^{B}	4.01 ± 0.22^{D}
27.5% wood flour	55.23 ± 2.88^{B}	4.46 ± 0.23^{A}

The superscript letters indicate ANOVA results.

The extent of strength improvement was not a function of the wood flour content in the composite cap layer. Interestingly, the bending strengths of coextruded WPCs with composite cap layers (Table 3.4) were similar to those produced with unfilled PVC cap layers (Table 3.3). These results imply that the surface of WPCs became more hydrophobic or PVC surface-rich after coextrusion. By contrast, the amount of wood flour in the composite cap layers affected the stiffness of coextruded WPC in two distinct ways. The stiffness of coextruded WPCs significantly decreased when a small amount of wood flour (5%) was used in the composite cap layer, a result which was expected owing to the large concentration of unfilled PVC on the surface of the coextruded samples. An opposite trend was observed upon increasing the wood flour content, a finding which also was expected from the rule of mixtures, i.e., the stiffness of composites increases with increases in filler content.

3.5 Conclusions

Rigid PVC/wood-flour composites (core layer) were coextruded with either unfilled PVC (cap layer) or PVC filled with a small amount (5-27.5 wt%) of wood flour (composite cap layers) in order to decrease or delay the moisture uptake of the composites. The thickness of the cap layer and its composition in terms of wood flour content were the variables examined during the coextrusion process. The surface color, moisture absorption, and flexural properties of both coextruded and noncoextruded (control) composite samples were characterized as functions of cap layer thickness and amount of wood flour in the cap layer. The following conclusions were drawn from the experimental results.

Both unfilled PVC and composite cap layers can be encapsulated over rigid PVC/wood-flour composites in a coextrusion process.

Nonencapsulated WPCs (control) not only absorbed more moisture than the coextruded counterparts after 338.5 days, but also experienced a quicker moisture uptake than the coextruded samples, regardless of the type of cap layer. The MUR was lower when a cap layer was applied in the composites, and the extent of the decrease was a strong function of the amount of wood flour in the cap layer but insensitive to the cap layer thickness.

Overall, coextruding PVC surface-rich cap layers on WPCs has significantly increased their flexural strength but decreased their flexural modulus compared with those of control samples. The changes in flexural properties were sensitive to both the thickness of the cap layer and its wood flour content.

3.6 Acknowledgements

The authors are grateful for the generous donation of materials provided by the manufacturers listed in the Experimental section and Table 3.1. The authors also are grateful for the financial support of USDA-CSREES Grant-Advanced Technology Applications to Eastern Hardwood Utilization (contact grant number: 2006-34158-17581).

3.7 References

1. J.M. Pilarski and L.M. Matuana, Durability of wood flour-plastic composites exposed to accelerated freeze-thaw cycling. Part I. Rigid PVC matrix, *Journal of Vinyl & Additive Technology*, **11**(1): 1-8 (2005).

2. J.M. Pilarski and L.M. Matuana, Durability of wood flour-plastic composites exposed to accelerated freeze-thaw cycling. II. High density polyethylene matrix, *Journal of Applied Polymer Science,* **100**(1): 35-39 (2006).

3. N.M. Stark, Influence of moisture absorption on mechanical properties of wood flour- polypropylene composites, *Journal of Thermoplastic Composite Materials*, **14**(5): 421-432 (2001).

4. B. Dawson-Andoh, L.M. Matuana, and J. Harrison, Susceptibility of high density Polyethylene/wood-flour composite to mold discoloration, *Journal of the Institute of Wood Science,* **17**(2): 114-119 (2005).

5. B. Dawson-Andoh, L.M. Matuana, and J. Harrison, Mold susceptibility of rigid PVC/wood-flour composites, *Journal of Vinyl & Additive Technology*, **10**(4): 179-186 (2004).

6. N.E. Marcovich, M.M. Reboredo, and M.I. Aranguren, Moisture diffusion in polyester–woodflour composites, *Polymer*, **40**(26): 7313–7320 (1999).

7. A.K. Bledzki and O. Faruk, Creep and impact properties of wood fibre–polypropylene composites: Influence of temperature and moisture content, *Composites Science and Technology,* **64**(5): 693-700 (2004).

8. Z.A. Mohd Ishak, B.N. Yow, B.L. Ng, H.P.S.A. Khalil, and H.D. Rozman, Hygrothermal aging and tensile behavior of injection-molded rice husk-filled polypropylene composites, *Journal of Applied Polymer Science,* **81**(3): 742-753 (2001).

9. J. Markarian, Wood-plastic composites need protection, *Plastics Engineering,* **63**(7): 54-56 (2007).

10. N.M. Stark and L.M. Matuana, Coating WPCs using coextrusion to improve durability. *Proceedings: Coating Wood and Wood Composites: Designing for Durability,* July 23–25, 2007, Seattle, WA.

11. C. Rauwendaal, *Understanding Extrusion*, Hanser/Gardner, Cincinnati, (1998).

12. H.J. Giles Jr., J.R. Wagner Jr., and E.M. Mount III, *Extrusion: The Definitive Processing Guide and Handbook,* William Andrew Publishing, New York, (2004).

13. Z. Gürdal, R.T. Haftka, and P. Hajela, *Design and Optimization of Laminated Composite Materials*, John Wiley & Sons, New York, (1999).

14. J.W. Kim, K. Carlborn, L.M. Matuana, and P.A. Heiden, Thermoplastic modification of urea-formaldehyde wood adhesives for increased moisture Resistance, *Journal of Applied Polymer Science*, **101**(6): 4222-4229 (2006).

15. S. Jin and L.M. Matuana, Improving water resistance of wood-plastic composites through coextrusion, *SPE ANTEC Papers*, **66**: 19-23 (2008).

CHAPTER 4

Wood Plastic Composites Coextruded with Multi-Walled Carbon Nanotube Filled Rigid PVC Cap Layer

This chapter is slightly modified from a research paper that was published in the Polymer International, 59 (5): 648-657 (2010). It is co-authored by Shan Jin and L.M. Matuana.

4.1 Abstract

Wood-plastic composites (WPCs) can absorb moisture in a humid environment due to the hydrophilic nature of the wood in the composites, making products susceptible to microbial growth and loss of mechanical properties. Coextruding a poly(vinyl chloride) (PVC)-rich cap layer on a WPC significantly reduces the moisture uptake rate, increases the flexural strength but, most importantly, decreases the flexural modulus compared to uncapped WPCs. A two-level factorial design was used to develop regression models evaluating the statistical effects of material compositions and a processing condition on the flexural properties of coextruded rigid PVC-wood flour composites with the ultimate goal of producing coextruded composites with better flexural properties than uncapped WPCs. Material composition variables included wood flour content in the core layer and carbon nanotube (CNT) content in the cap layer of the coextruded composites, with the processing temperature profile for the core layer as the only processing condition variable. Fusion tests were carried out to understand the effects of the material compositions and processing condition on the flexural properties. Regression models indicated all main effects and two powerful interaction effects (processing temperature/wood flour content and wood flour content/CNT content interactions) as statistically significant. Factors leading to a fast fusion of the PVC-wood flour composites in the core layer, i.e. low wood flour content and high processing temperature, were effective material composition and processing condition parameters for improving the flexural properties of coextruded composites. Reinforcing the cap layer with CNTs also produced a significant improvement in the flexural properties of the coextruded composites, insensitive to the core layer composition and the processing temperature condition.

4.2 Introduction

Wood-plastic composites (WPCs) have experienced significant market expansion in recent years as a replacement for solid wood, mainly in outdoor applications such as railings, decking, landscaping timbers, fencing, playground equipment, window and door frames, etc. The acceptance of WPCs into the construction industry to replace solid wood in several outdoor applications contributes to the popularity of WPCs [1].

Originally marketed as weather-resistant products requiring little or no maintenance compared to solid wood, expectations fail in accounting for exposure to outdoor environment of ultraviolet rays and moisture which affects the product retaining its new appearance without maintenance. With many years in outdoor service, customers have complained of surface staining, discoloration, and other maintenance-oriented issues in WPC products [1–3]. Studies have shown that WPCs can absorb moisture in a humid environment due to the highly hydrophilic nature of the wood flour in the composites, especially at high loading level, making products more prone to microbial growth and biological decay, thus affecting the appearance of the products [2–6]. Moisture absorption also reduces the adhesion between the filler and polymer matrix, which results in modest loss of mechanical properties [7]. Aware of these durability issues, the industry continues to take steps to ensure the long-term performance of WPC products. In particular, WPC producers seeking improved products focus on water absorption resistance, color and appearance retention, physicomechanical property retention, as well as mould and mildew resistance over time [1–16].

Several proposed approaches substantially reduce or delay the moisture and water uptake of WPCs. Reports mention the use of performance-enhancing additives such as lubricants, coupling agents and other compatibilizers, encapsulation of exposed wood during compounding or the use of protective coatings as methods to reduce the moisture uptake of WPCs [14]. Although proven to reduce moisture absorption of WPCs, these suggested approaches have not eliminated this factor completely. Unsurprisingly, investigations have recently demonstrated that covering WPCs with hydrophobic layers decreases moisture absorption. A cap layer of polyolefin or poly(vinyl chloride) (PVC) coextruded over a WPC provides improved moisture resistance compared with an uncapped control WPC [7–19].

Although coextruded WPCs have advantages over uncapped (control) WPCs in terms of less moisture absorption and a slower rate of moisture uptake, their performance in terms of flexural properties is very sensitive to the properties of the polymer of the cap layer [18]. It has been shown that coextruding rigid PVC cap layers on WPCs significantly increases their flexural strength but decreases their flexural modulus compared to control samples. The increased bending strength and decreased bending modulus induced by coextruding a PVC layer over a WPC are attributed to the greater strength but lower stiffness of PVC compared to WPCs [18].

In addition to durability, the mechanical properties of WPCs are another important concern. As some surveys indicate, key factors to open new markets for WPCs are good durability and mechanical properties [20]. With flexural properties as critical, determining the maximum load capacity and span ratings for the acceptance of a material in various lumber applications, enhancing the strength and stiffness of coextruded WPCs could not only improve their acceptance in load-bearing structural applications, but also open new applications for these products, thus expanding their market share [1].

The mechanical properties of coextruded samples depend on the properties of the materials in both outer and inner layers. Generally, stronger and stiffer materials in the outer layer enhance the overall performance of the coextruded samples compared to products made with the inner material alone [21, 22]. Therefore, coextruded WPCs with stronger and stiffer PVC outer layers could offset the reduction in flexural modulus observed in previous investigations [18].

Thus far, much effort has been expended on manufacturing PVC products with satisfactory performance. Notably, significant factors include the choice of proper resin, processing additives and processing conditions in order to achieve optimal mechanical properties [23–26]. In general, both the processing and performance of PVC products are intrinsically linked to the resin molecular weight, which is expressed as inherent viscosity (IV) or k-value, the morphology of the particles (e.g. apparent bulk density, porosity, particle size distribution), the additives used and other parameters [24]. All factors being equal, the intrinsic values of many mechanical properties of PVC products increase as the resin molecular weight increases, similar to other thermoplastics [23, 24]. However, reports indicate some confusion in the literature while attempting to correlate mechanical properties to the molecular weight of PVC. It has been shown that increased molecular weight has little effect on increasing the yield stress but a significant effect in decreasing the tensile modulus of PVC [27]. This results partly because of the dependency of the resin's properties on the processing conditions used in the manufacturing of PVC products, which affect the fusion of PVC [23–26]. Since the resin requires proper fusion in order to achieve optimal mechanical properties, the higher the molecular weight, the slower the fusion and the more difficult the processing [23–26, 28]. These findings suggest that processing conditions such as processing temperature play an important role in the mechanical performance of PVC products.

Reinforcement of PVC matrices with inorganic and organic fillers constitutes another approach to improve mechanical properties [29, 30]. Generally, increasing the amount of fillers in PVC significantly enhances its stiffness due to the greater stiffness of the fillers [30]. This approach also leads to a significant reduction in strength due to the weak interfacial adhesion between the filler and the matrix [30, 31]. However, recent investigations have shown that PVC filled with nanoparticles such as nanoclay, carbon nanotubes (CNTs) and nano-$CaCO_3$ possesses both greater flexural strength as well as modulus than the base resin [32–39], suggesting the potential for enhancement of the flexural properties of coextruded WPCs by reinforcing the cap layer with nanoparticles.

Consequently, using a two-level factorial design, the study reported here examined the effects of material compositions in both outer and inner layers as well as a processing condition on the flexural properties of coextruded rigid PVC/wood flour composites. Particular emphasis was placed on understanding the effects of processing temperature for the core layer, reinforcing the outer layer with CNTs and the amount of wood flour in the core layer on the performance of coextruded composite samples.

4.3 Experimental

4.3.1 Materials

Table 4.1 lists the PVC resin and other additives used in the rigid PVC formulation. A 0.425 mm (40 mesh) maple flour from American Wood Fibers was used as wood flour. The wood flour was oven-dried at 105°C for 48 h to remove moisture before processing. Industrial grade 90 wt% multi-walled carbon nanotube (diameter: 10–30 nm, length: 10–30 μm), purchased from Cheap Tubes (Vermont), served as reinforcing material for the outer layer.

Table 4.1. Formulation of rigid PVC.

Ingredients	Content (phr)
PVC resin (K-value = 66.4) (Shintech)	100
Tin stabilizer (PlastiStab 2808-Halstab)	2
Calcium stearate (Synpro)	1.5
Paraffin wax (Gulf Wax)	2
Processing aid (Paraloid K-120)[1]	2
Processing aid (Paraloid K-175)[1]	2
Impact modifier (K-334)[1]	10

[1] Supplied by Rohm & Haas Co.

4.3.2 Rigid PVC formulation

The PVC resin and other additives listed in Table 4.1 were blended in a 20 L high-intensity mixer (Papenmeier, Type TGAHK20) at room temperature for 10 min. This compounded material was used as matrix in inner and outer layers of coextruded PVC-wood flour composites.

4.3.3 Compounds for core layer

The formulations used in core layers consisted of blends of PVC and wood flour. The composites used in the inner layers contained 40 or 60 wt% wood flour based on the total weight of the composites. These blends were also mixed in a high-intensity mixer at room temperature for 10 min.

4.3.4 Compounds for outer layer

Outer layers of coextruded WPCs used both unfilled and CNT-filled rigid PVC. The addition of CNTs into PVC matrix followed the approach described in our previous study [33]. The pre-blended PVC was placed into a 60 ml electrically heated three-piece internal mixer/measuring head (3:2 gear ratios) with roller-style mixing blades (C.W. Brabender Instruments, Inc.) and the mixing process started to follow the fusion curve. CNTs (5% based on the total weight of the blend) were added into the mixer at the onset of the fusion, i.e., the point where the material reached a void-free state and started to melt. At this point, the PVC primary particles were reduced from micrometric in size to submicrometric particles [32], allowing for a much better dispersion of CNTs into the matrix. After CNT addition, the materials remained in the mixer until reaching equilibrium torque. The mixing process ran at a constant mixer temperature of 150 °C for 5 min. The rotor speed was 50 rpm and weight charge set at 65 g. The experiments had a 5 kg dead weight on the top of the ram throughout [32, 33, 40].

4.3.5 Experimental design

With multiple variables to account for, as in this study, difficulty arises in studying the system with the common approach of varying only one factor at a time, while holding the others constant. This approach is not only time-consuming, but it also presents problems in identifying all of the interactions between factors [41, 42]. Developing a mathematical model allows for greater efficiency in investigating these systems by describing the relationship between the response and independent variables, and ultimately determining the significance of individual factors and multifactor interactions [43–47]. Response surface methodologies such as a central composite design (CCD) and a Box-Behnken design (BBD) present versatile methods to statistically model and optimize response variables affected by multiple independent factors [41, 42]. However, the limitation in processing temperature to avoid thermal degradation of PVC/wood flour composites makes the use of CCD and BBD methods difficult in this study to fit the axial points required in these designs. Instead, preference is for a two-level factorial design since it includes only factorial points in the experiments. The value of a two-level factorial design lies in its ability to examine the effects of more than one variable in a system and its ability to reveal the effects of interactions between variables unobtainable from the traditional method of changing one variable at a time [46, 47].

A two-level factorial design was performed using Design Expert® software v.7 (STAT-EASE, Corp., Minneapolis, MN). The three variables studied were the wood flour content in the inner layer, the CNT content in the outer layer and the processing temperature for the inner layer, whereas the responses obtained were the flexural strength and modulus. Table 4.2 lists the experimental design matrix, showing two different methods of displaying the levels of factors, i.e., factor levels in actual scale (or the actual values in the experiments) and in coded scale (as +1 and -1 for high and low levels, respectively). The coded factor levels are defined as follows:

$$\text{Coded factor levels} = \frac{\text{Actual value} - \text{Factor mean}}{(\text{Range of factorial values}/2)} \qquad \text{(Equation 4.1)}$$

Each design point included at least six replicates to determine the statistical significance of the results.

After obtaining all responses, the software generated first-order surface models describing the main effects and interactions on the response in terms of coded variables based on Equation 4.2 [41, 42].

$$Y = \beta_0 + \sum_{i=1}^{3} \beta_i X_i + \sum_{i=1}^{3} \sum_{j=1}^{3} \beta_{ij} X_i X_j \qquad \text{(Equation 4.2)}$$

where Y is the predicted response; X_i the main effect, X_iX_j the interaction, β_0 the intercept, and β_i and β_{ij} the regression coefficients, which are one-half of the corresponding factor effect estimates. The model functioned as a first-order response surface model because the experiment design did not include the center point.

Table 4.2. Factorial design matrix in terms of both actual and coded factor levels.

Factors			Responses	
A: Temperature profile for core	B: Wood flour content in core (%)	C: CNT content in cap (%)	Strength (MPa)	Modulus (MPa)
low (−1)	40 (−1)	0 (−1)	56.5	2887.6
high (+1)	40 (−1)	0 (−1)	62.8	3933.6
low (−1)	60 (+1)	0 (−1)	37.2	2243.3
high (+1)	60 (+1)	0 (−1)	50.9	3707.4
low (−1)	40 (−1)	5 (+1)	59.9	3417.3
high (+1)	40 (−1)	5 (+1)	64.7	4276.8
low (−1)	60 (+1)	5 (+1)	48.6	2968.0
high (+1)	60 (+1)	5 (+1)	57.3	4600.7

4.3.6 Coextrusion of PVC/wood-flour composites

Table 4.2 shows each design point, coextruded in a system consisting of a coextrusion die connecting a twin screw extruder (TSE) for the inner layer and a single screw extruder (SSE) for the outer layer (Figure 4.1). Formation of the core layer used a 32 mm conical counter rotating TSE (C.W. Brabender Instruments, Inc.) with a length-to-diameter ratio of 13:1. Production of cap layers used a 19 mm SSE (C.W. Brabender Instruments, Inc.) with a length-to-diameter ratio of 30:1. The specifically designed die used in coextrusion insured that the cap layers covered the entire core layer of WPCs (complete encapsulation of core layer), which created rectangular samples with a nominal width and depth of 2.54 cm (1 inch) and 0.95 cm (3/8 inch), respectively.

While the temperature profiles of the twin screw extruder varied from the heating zone 1 to zone 3, the temperature profile of the SSE and the die remained constant. The TSE maintained a rotational speed of 30 rpm throughout the experiments. Conversely, various rotational screw speeds were used for the SSE to produce coextruded samples with a cap layer having constant thickness (*ca* 1 mm). Table 4.3 presents the conditions used during coextrusion process.

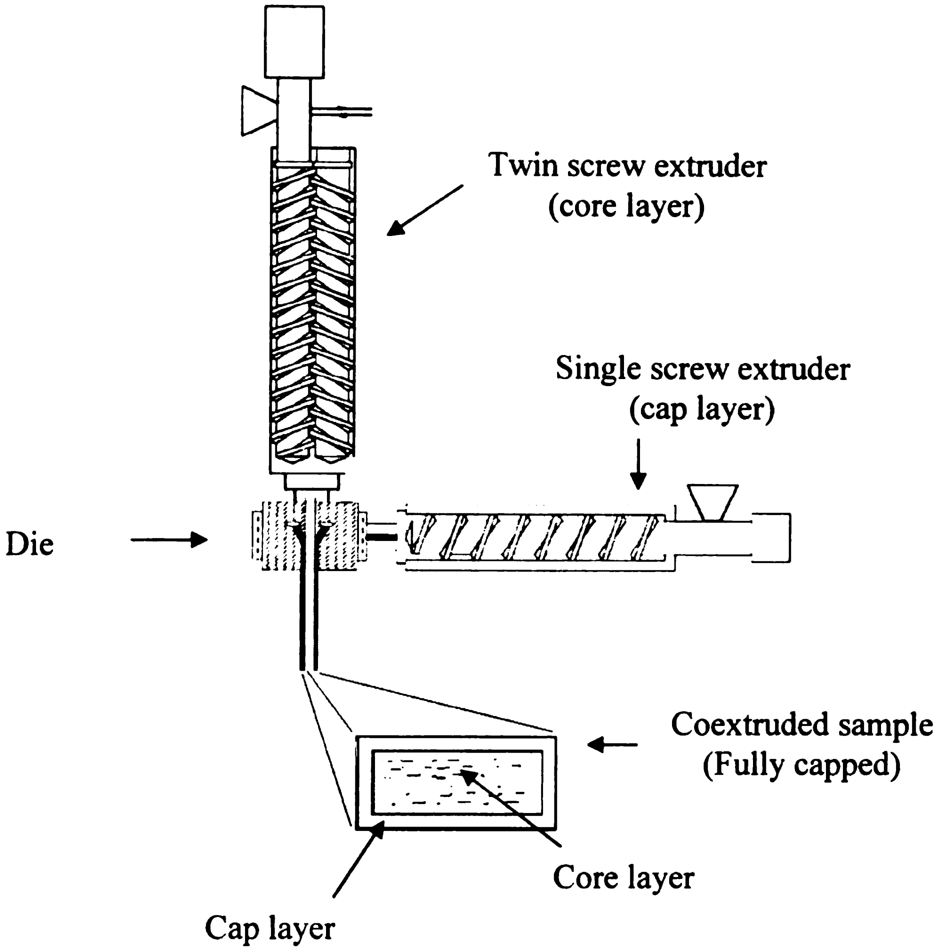

Figure 4.1. Schematic of the coextrusion system used in this study.

Table 4.3. Processing conditions for coextrusion process.

Variables	Processing conditions for extruders		Die temperature (°C)
Core layer processing temperature	Twin screw extruder		
	Temperature profile[1] (°C)	Screw speed (rpm)	
High	190-185-177	30	173
Low	180-175-167	30	173
Cap layer material compositions	Single screw extruder		
	Temperature profile[1] (°C)	Screw speed (rpm)	
Unfilled PVC Cap	155-165-167	9-12	173
5% CNT-filled PVC Cap	155-165-167	5-7	173

[1] The temperature profiles are shown from the hopper to the die.

4.3.7 Flexural property evaluation

Three-point flexural tests were carried out using an Instron 5585H testing machine equipped with Bluehill 2 software. Tests were performed in a walk-in conditioning room at 23±2 °C and 50±4 % relative humidity. Samples were stored in this conditioning room for at least 48 h prior to property testing. The dimensions of samples were about $200\times25.4\times9.5$ mm^3 with the tests performed at a crosshead rate of 4.3 mm/min in accordance with ASTM standard D7031-2004. At least six replicates were tested to obtain an average value for each design point (Table 4.2).

4.3.8 Fusion tests

Performance of fusion tests assisted in understanding the influences of material compositions and temperature processing condition on the flexural properties of coextruded composites. A 7.5 hp Intelli-Torque Plasti-Corder Torque Rheometer® drive (C.W. Brabender Instruments, Inc.) was employed for fusion studies using a 60 ml electrically heated three-piece internal mixer/measuring head (3:2 gear ratio) with roller style mixing blades (C.W. Brabender Instruments, Inc.) [32, 33, 40, 47]. The tests ran at constant mixing temperatures of 180 and 190 °C for 10 min. All compounds used the weight charge set at 60 g with the rotor speed maintained at 50 rpm. A 5 kg dead weight was put on top of the ram throughout the experiments. The Brabender® Mixer Program (WINMIX, version 3.2.11) recorded the fusion time. Each formulation included at least three replicates to obtain average values for the fusion characteristics.

4.3.9 Scanning electron microscopy

SEM images were obtained to qualitatively view the effect of processing temperatures (180 and 190 °C) on the extent of fusion inside the PVC filled with 40 and 60% wood flour (core layer). A JEOL JSM-6400 SEM at 15kv accelerating voltage was used for SEM images. The samples were oven-dried at 105°C to remove the moisture and gold coated before observation.

4.4 Results and Discussion

4.4.1 Statistical significance of effects

A two-level factorial design was employed to evaluate the statistical effects of processing temperature for the core layer (factor A), wood flour content in the core layer (factor B) and CNT content in the cap layer (factor C) on the flexural properties of coextruded rigid PVC/wood flour composites. The analysis of the data assists in identifying the major factors affecting the flexural properties as well as understanding interactions between different variables.

For a two-level factorial design, the normal probability plot, a graphical tool, assesses the importance of the factor effects. Figure 4.2 shows the normal probability plots of the effect estimates for flexural strength and stiffness of coextruded composites. While all negligible and non-significant effects lie along the straight line, all the main effect factors (A, B and C) and the most significant two-factor interaction terms (BC for flexural strength and AB and BC for flexural modulus) affecting the flexural properties fall off to the left (negative effect) or to the right (positive effect) of the line.

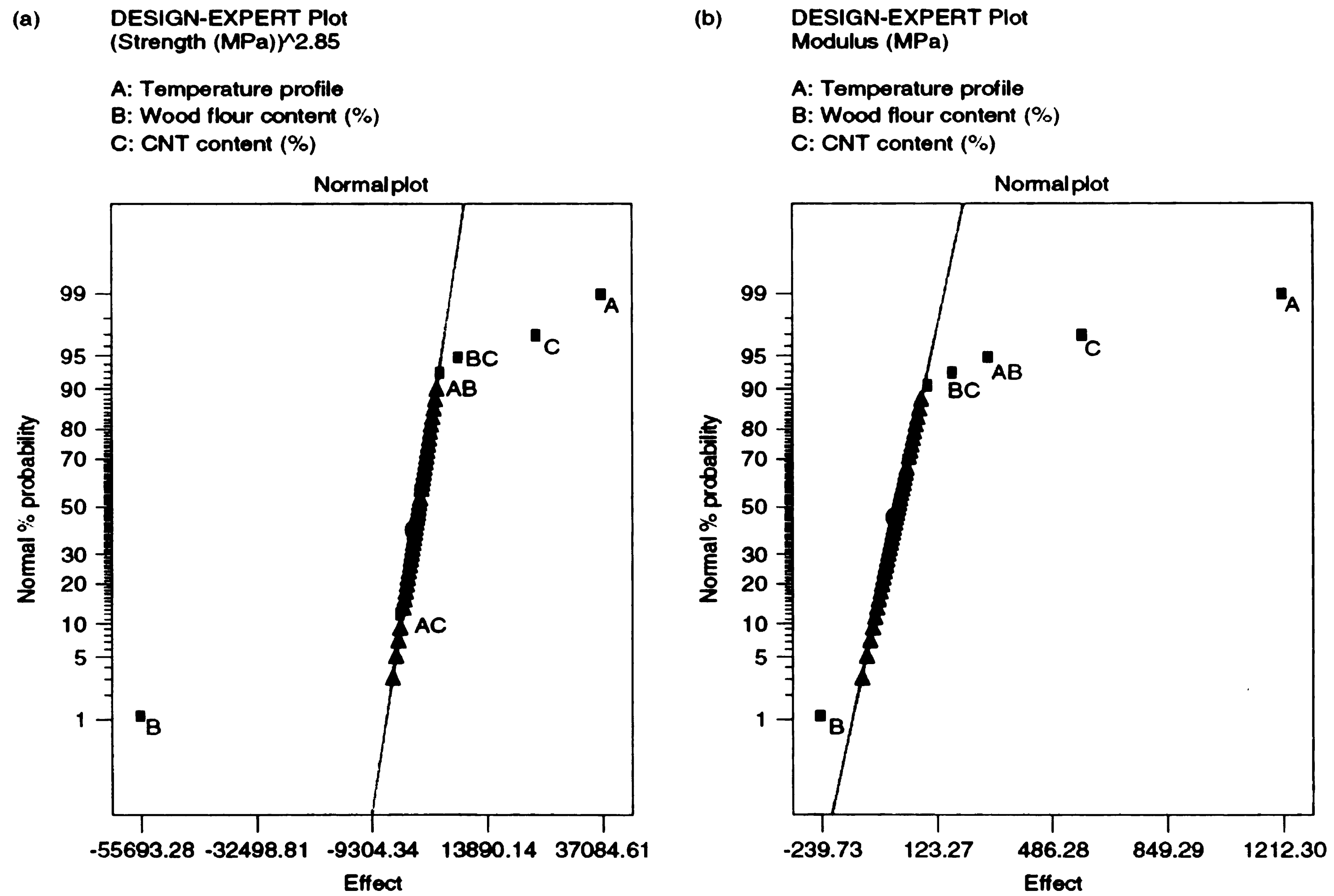

Figure 4.2. Normal probability plots of effects for (a) flexural strength and (b) flexural modulus of coextruded rigid PVC/wood-flour composites.

The perturbation plot, another tool, assists in comparing the relative significance of the main effects on the response. It illustrates the changes in a response as each factor moves from the chosen reference, with all other factors held constant at the middle level of the design space [41, 42]. Because this study used the processing temperature (factor A) as a categorical factor, the perturbation plots for flexural strength and modulus were created at both low and high levels of processing temperature for the core layer (Figures 4.3 and 4.4) while keeping the wood flour content and CNT content at their middle level of the design space. The midpoint acts as the reference point (the coded zero level of each factor). Steep slopes observed for the main factors B and C in Figure 4.3 indicate the sensitivity of the flexural strength to both wood flour content in the core layer (factor B) and CNT content in the cap layer (factor C), regardless of the processing temperature used for the core layer. While the CNT content in the outer layer has a significant impact on the stiffness of coextruded composites independent of the processing temperatures used for the core layer, the amount of wood flour in the core layer largely affects the stiffness of the coextruded composites at low processing temperature (Figure 4.4(a)) and shows only a small effect at high processing temperature (Figure 4.4(b)).

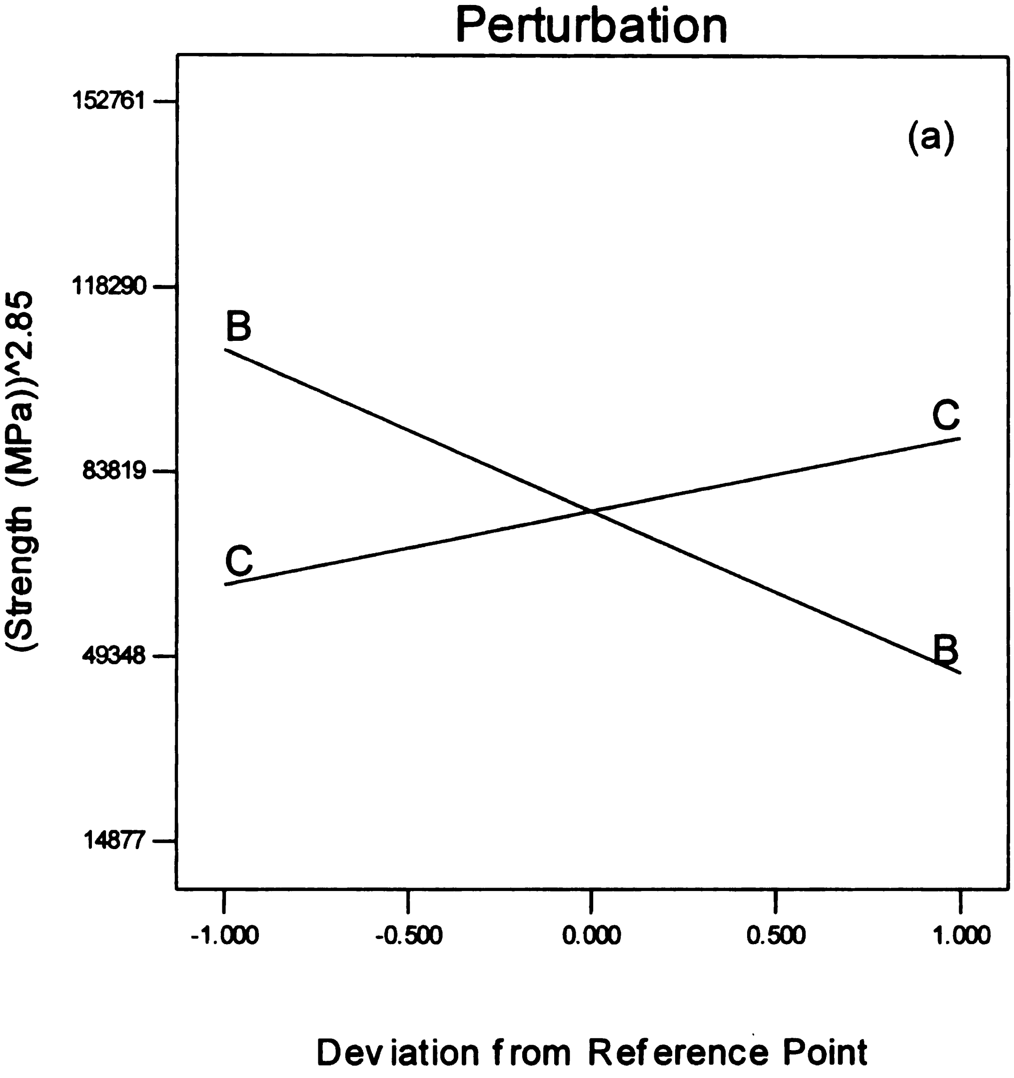

Figure 4.3. Perturbation plots of the flexural strength of coextruded composites against wood flour content in core layer and CNT content in cap layer of coextruded composites processed at (a) low temperature and (b) high temperature profile for the core layer.

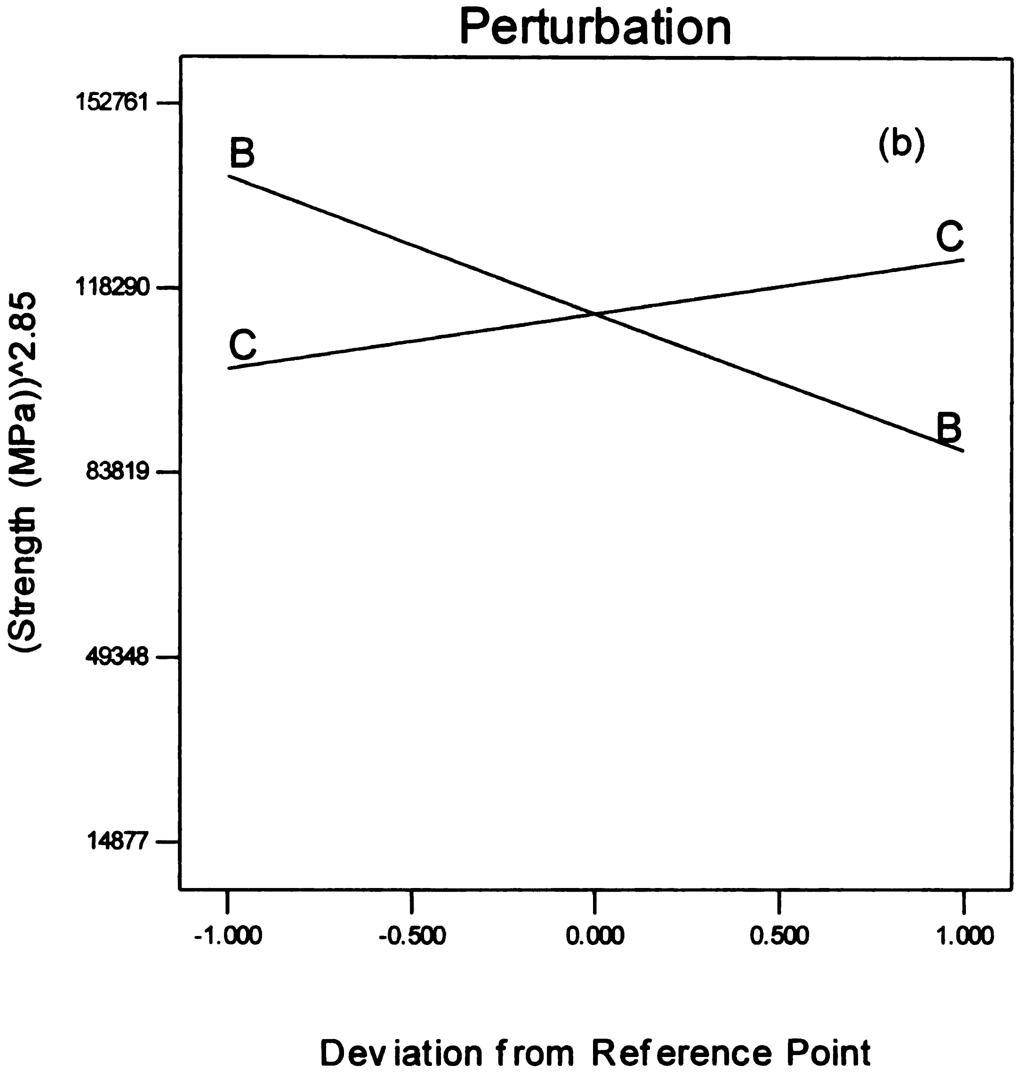

Figure 4.3. Perturbation plots of the flexural strength of coextruded composites against wood flour content in core layer and CNT content in cap layer of coextruded composites processed at (a) low temperature and (b) high temperature profile for the core layer.

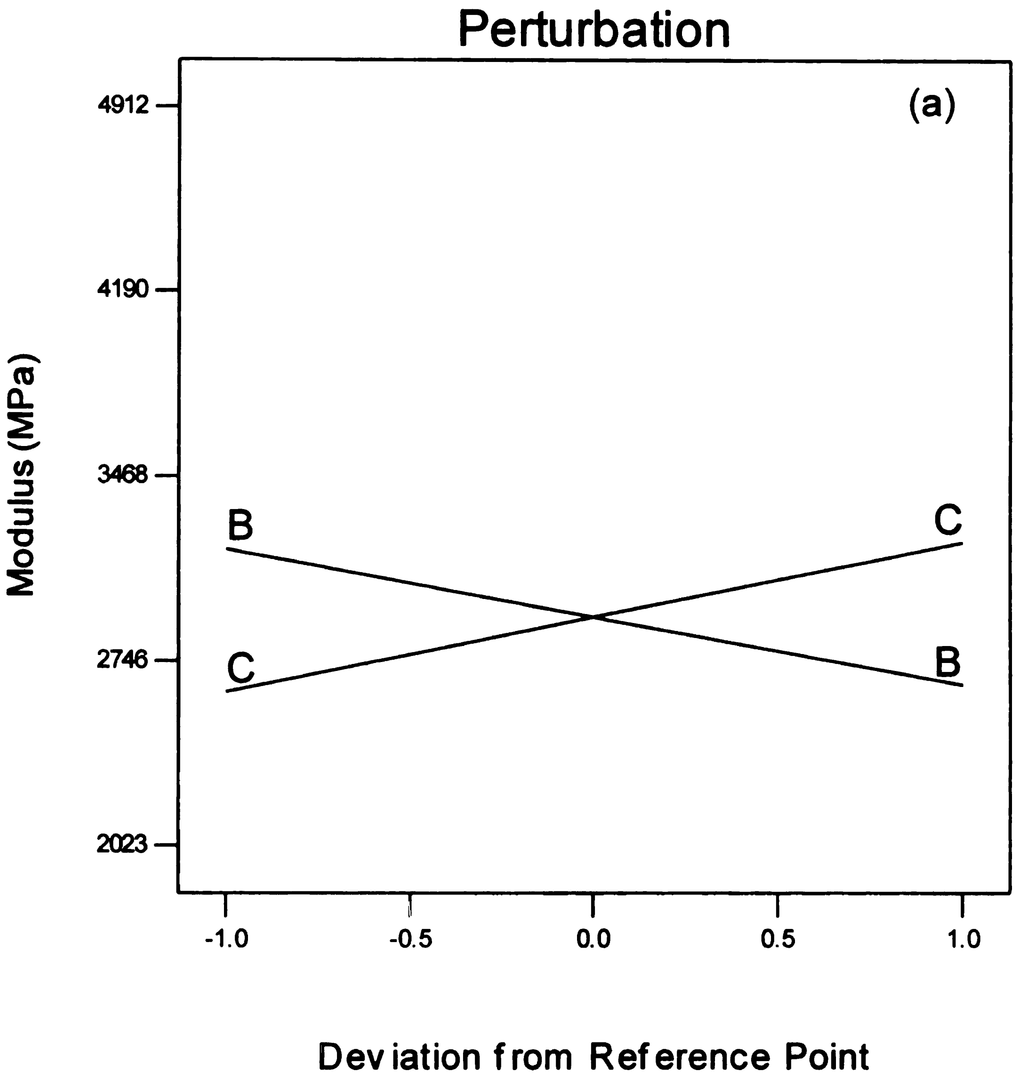

Figure 4.4. Perturbation plots of the flexural modulus of coextruded composites against wood flour content in core layer and CNT content in cap layer of coextruded composites processed at (a) low temperature and (b) high temperature profile for the core layer.

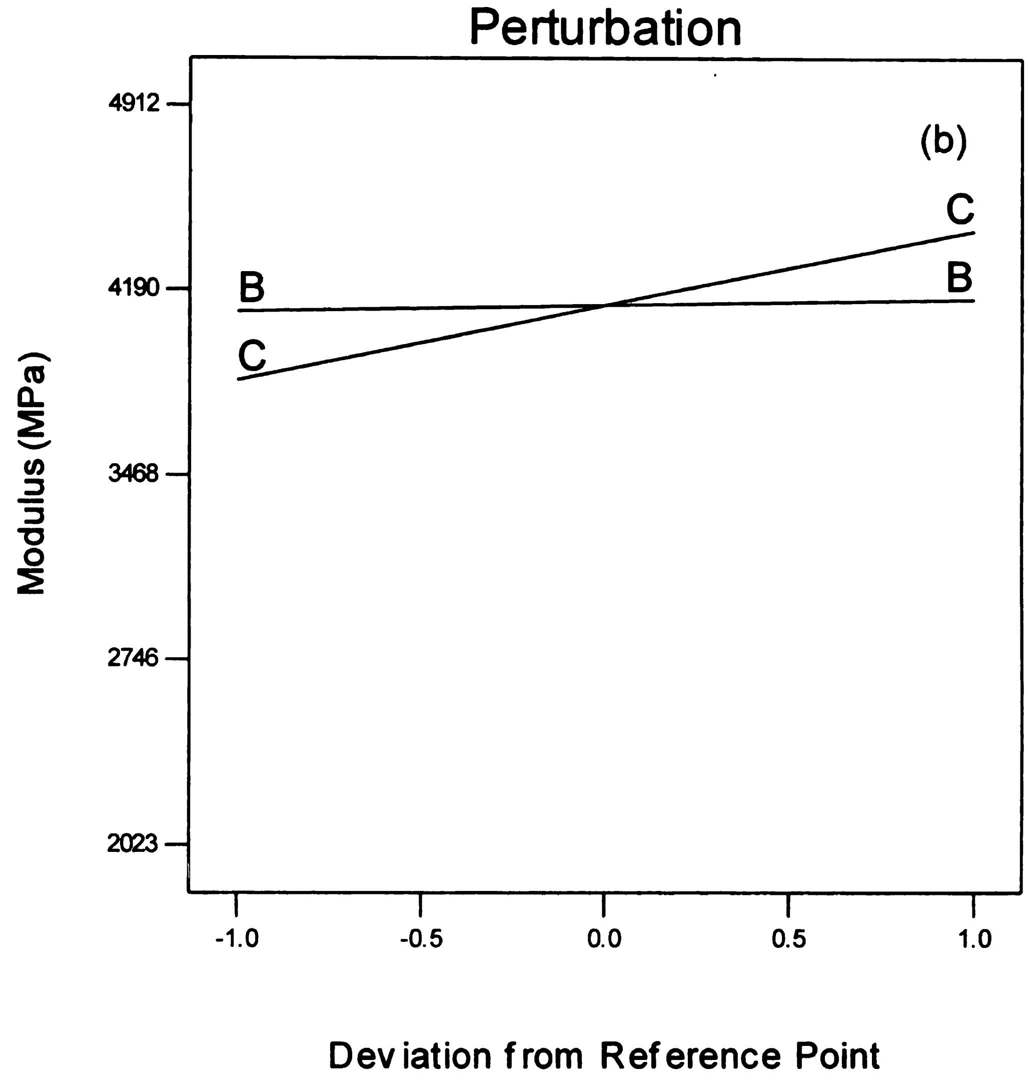

Figure 4.4. Perturbation plots of the flexural modulus of coextruded composites against wood flour content in core layer and CNT content in cap layer of coextruded composites processed at (a) low temperature and (b) high temperature profile for the core layer.

The analysis of variance (ANOVA) confirms the interpretation of the data based on the normal probability plots (Figure 4.2) and perturbation plots (Figures 4.3 and 4.4) according to the p-values (Prob > F) showing the statistically significant factor effects (Tables 4.4 and 4.5).

A regression analysis was carried out to obtain the best-fit model to the experimental data. The analysis suggests that a power model with positive lambda value best fits the relationship between the flexural strength and the three independent variables, whereas a linear model best fits the flexural modulus. The following equations describe the derived regression models predicting the flexural strength and stiffness of coextruded composites in terms of coded factors:

$$(\text{Strength})^{2.85} = +95037.5 + 18542.3A - 27846.6B + 12025.2C + 4179.8BC \quad \text{(Equation 4.3)}$$

$$\text{Modulus} = +3523.5 + 606.2A - 119.9B + 292.2C + 144.3AB + 88.5BC \quad \text{(Equation 4.4)}$$

where A is the processing temperature for the core layer, B the wood flour content in the inner layer and C the CNT content in the outer layer of coextruded composites.

Table 4.4. ANOVA for selected factorial model of flexural strength of coextruded composites.

Source	Sum of squares	Degree of freedom	Mean square	F-Value	Prob > F[a]
Model	6.150×10^{10}	4	1.538×10^{10}	156.51	< 0.0001
A	1.650×10^{10}	1	1.650×10^{10}	167.99	< 0.0001
B	3.722×10^{10}	1	3.722×10^{10}	378.87	< 0.0001
C	6.941×10^{9}	1	6.941×10^{9}	70.65	< 0.0001
BC	8.386×10^{8}	1	8.386×10^{8}	8.54	0.0055
Lack of fit[b]	4.019×10^{8}	1	1.34×10^{8}	1.40	0.2563

[a] Values of Prob > F less than 0.0500 indicate model terms are significant. In this case A, B, C, and BC are the significant model terms.

[b] The "Lack of Fit" F value of 1.4 implies the lack of fit is not significant relative to the pure error. There is a 25.63% chance that a lack of fit F value this large could occur due to noise. Non-significant lack of fit is good.

Table 4.5. ANOVA for selected factorial model of flexural modulus of coextruded composites.

Source	Sum of squares	Degree of freedom	Mean square	F-Value	Prob > F[a]
Model	2.380×10^{7}	5	4.760×10^{6}	103.58	< 0.0001
A	1.764×10^{7}	1	1.764×10^{7}	383.78	< 0.0001
B	6.897×10^{5}	1	6.897×10^{5}	15.01	0.0004
C	4.099×10^{6}	1	4.099×10^{6}	89.20	< 0.0001
AB	9.993×10^{5}	1	9.993×10^{5}	21.75	< 0.0001
BC	3.760×10^{5}	1	3.760×10^{5}	8.18	0.0066
Lack of fit[b]	1.289×10^{5}	2	64434.78	1.43	0.2511

[a] Values of Prob > F less than 0.0500 indicate model terms are significant. In this case A, B, C, and BC are the significant model terms.

[b] The "Lack of Fit" F value of 1.43 implies the lack of fit is not significant relative to the pure error. There is a 25.11% chance that a lack of fit F-value this large could occur due to noise. Non-significant lack of fit is good.

With Equations (4.3) and (4.4) displayed in terms of coded factors, the absolute value of regression coefficients indicates the relative significance of the effect of factors on the response, and the algebraic sign of each factor reflects the positive or negative relation between factors and response. As shown in these equations, all significant main effect factors (A, B and C) and two-factor interaction terms (AB and BC) have the same algebraic signs. These expected results occur because with the flexural strength as the highest stress experienced within the material at its moment of rupture, and the stiffness as the ratio of stress to strain in flexural deformation, the effects would influence both strength and stiffness in a similar way [48]. In other words, the effects with a positive impact on strength will also have a positive impact on stiffness and vice versa.

Because factors A and C have positive algebraic signs, an increase in processing temperature for the core layer (factor A) and CNT content in the cap layer (factor C) improves the flexural properties of coextruded composites. By contrast, the negative effect of wood flour content (factor B) suggests that increasing the wood flour content from the low level (40%) to the high level (60%) worsens the flexural properties of coextruded composites. The amount of wood flour in the core layer of coextruded composites (factor B) has the largest effect on flexural strength (large regression coefficient), followed by the processing temperature (factor A) and CNT content (factor C). A different trend is obtained for flexural modulus: largely affected by the processing temperature for the core layer followed by the amounts of CNT in the outer and wood flour in the inner layers. Equations (3) and (4) also reveal powerful interactions between processing temperature and wood flour content (interaction AB), as well as wood flour content and CNT content (interaction BC). These interactions have positive algebraic signs, indicating a positive effect on flexural properties of the coextruded composites.

With three of the main effect factors (A, B and C) that affect the flexural properties of coextruded composites being part of two significant interactions (AB and BC), the co-dependent behavior of one factor on the level of the other would make investigating these main factors separately inappropriate [43-47]. Consequently, the significant interactions (AB and BC) require simultaneous consideration.

4.4.2 Effect of the interaction factor on the flexural strength

Examining the two-dimensional response surface plots generated according to Equations (3) and (4) would assist in understanding the relationship between the flexural properties of coextruded rigid PVC/wood flour composites and the significant main effect factors as well as their interactions. Figure 4.5 shows the interaction graphs displaying flexural strength dependence as a function of the wood flour content in the inner layer and CNT content in the outer layer interaction (interaction BC). This shows the interaction's effect for the processing temperatures for the core layer set at low (Figure 4.5(a)) and high levels (Figure 4.5(b)).

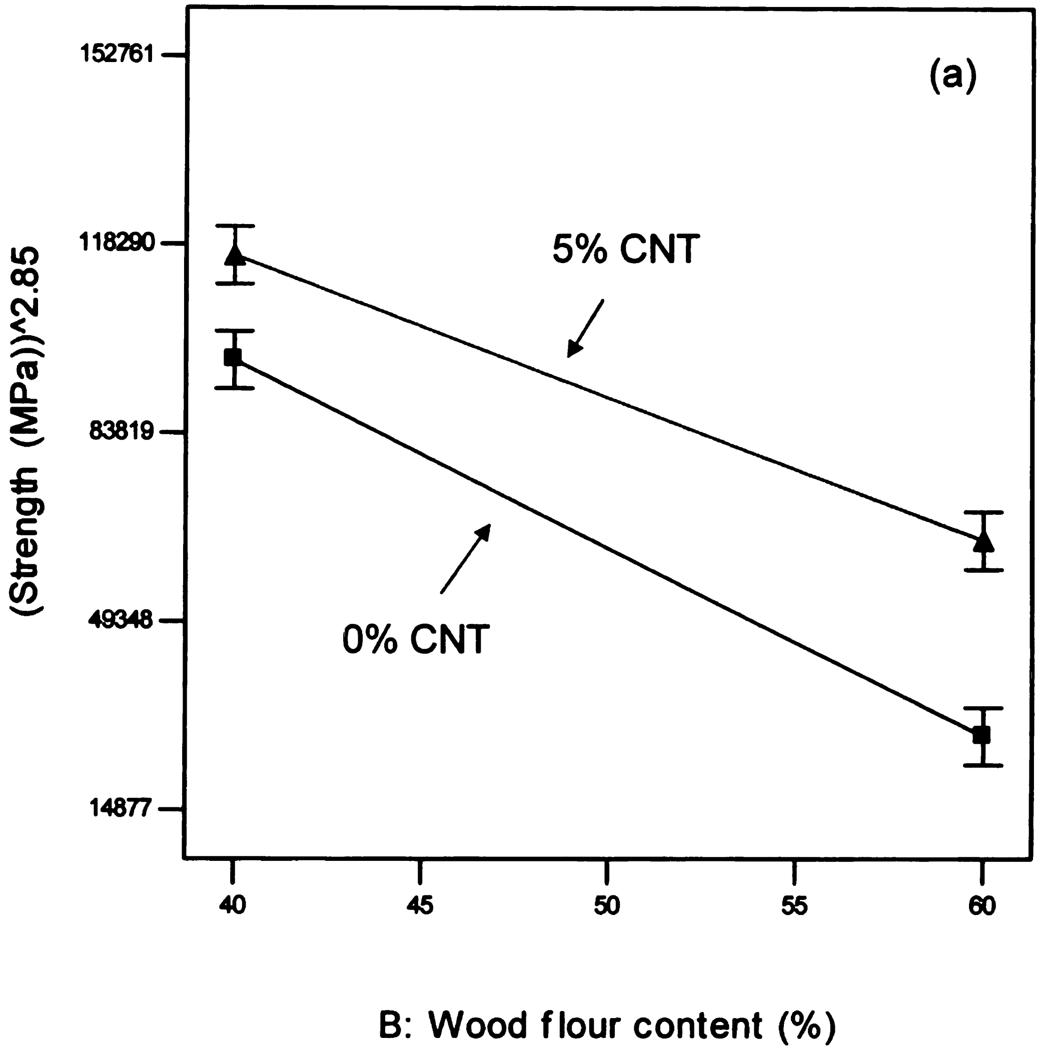

Figure 4.5. Interaction graphs of the variation in flexural strength as a function of the interaction between wood flour content in the core and CNT content in the cap layers of coextruded composites processed at (a) low temperature and (b) high temperature profile for the core layer.

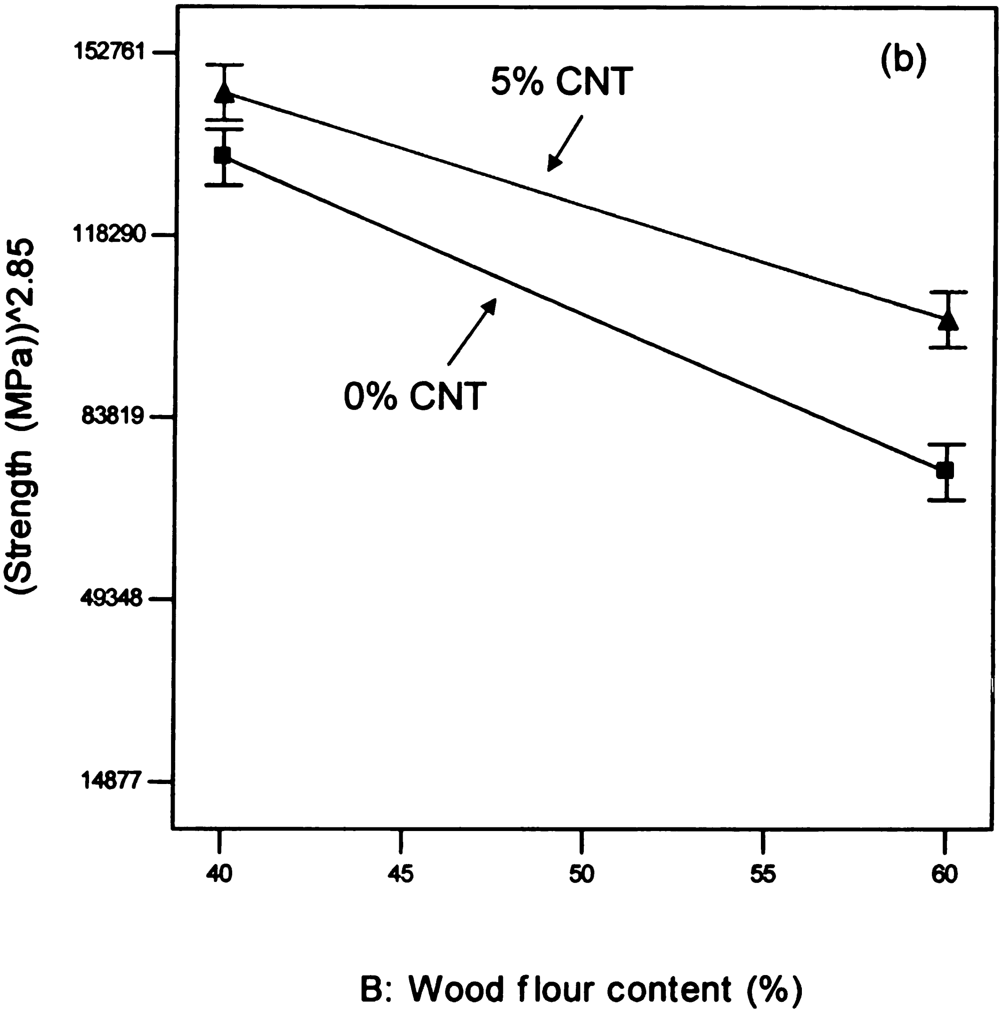

Figure 4.5. Interaction graphs of the variation in flexural strength as a function of the interaction between wood flour content in the core and CNT content in the cap layers of coextruded composites processed at (a) low temperature and (b) high temperature profile for the core layer.

Observations show a dependency of the flexural strength on the wood flour content and CNT content. As previously mentioned, the flexural strength of coextruded composites decreases with increasing wood flour content, but increases with increasing CNT content. The addition of CNT in the outer layer produces more notable changes in the flexural strength; uninfluenced by the core layer composition and the processing temperature condition (Figure 4.5). This expected trend is attributed to the reinforcing effect of CNTs [33]. However, the amount of CNTs in the outer layer has a minimal effect on the flexural strength of coextruded composites at low wood flour content (40%) but its effect intensifies with increased wood flour content (60%) in the core of coextruded composites. Comparing the difference in magnitude between the lines for unfilled (0% CNT) and filled (5% CNT) cap layers in Figure 4.5 verifies this effect. Additionally, non-parallel lines in Figure 4.5 reflect the interaction effect on the flexural strength. Since the strength of WPCs decreases as the amount of wood flour increases in the composites [30], reinforcing the cap layer with CNTs has a greater effect on the strength of coextruded composites with a greater amount of wood flour in the core layer. The shallow slope of C+ (5% CNT) and the steep slope of C− (0% CNT) imply that CNT-reinforced cap layer offsets part of the negative effect that high wood flour content in the inner layer has on the strength of coextruded composites.

Evidence indicates that increasing the processing temperature for the core layer significantly increases the flexural strength of the coextruded composites, insensitive to the material composition (Figure 4.5). Generally, strength and stiffness of individual components (rule of mixtures), as well as the interface's ability to transfer stresses between the filler and matrix, determine the strength and stiffness of polymer composites [30, 31, 49-52]. The advantage of processing at a high temperature lies in its effect on the fusion behavior of PVC matrix [23-26]. The degree of fusion in PVC affects not only the interfacial adhesion, but also the stress-transferring ability between components in the composites [2, 40].

Table 4.6. Effects of wood flour content and test temperature on the fusion time of rigid PVC/wood-flour composites.

Wood flour content in composites (%)	Fusion time (s)	
	180°C	190°C
40	48	34
60	311	217

As shown in Table 4.6, the fusion time of PVC/wood flour composites remains highly sensitive not only to the processing temperature for the core layer, but also to the amount of wood flour in the inner layer. A slight increase in processing temperature (10°C) reduces the fusion time significantly (about 30%), which promotes a high fusion level in the WPC used in the core layer. Increasing the processing temperature reduces the fusion time, mainly because the interdiffusion between PVC microparticles forming a three-dimensional network among polymer chains proceeds at a much faster rate [53]. The formation of this three dimensional network would proceed at a slower rate with a lower processing temperature. PVC particles well fused at elevated processing temperature indicate an enhancement in the wood flour's encapsulation by the matrix, as well as the adhesion between the WPC in the core layer and the PVC in the cap layer, leading to improved flexural strength of coextruded composite samples. The SEM images shown in Figure 4.6 support this contention. While the surfaces of PVC/wood flour composites processed at a high temperature are relatively smooth, those processed at a reduced temperature have relatively coarse surfaces.

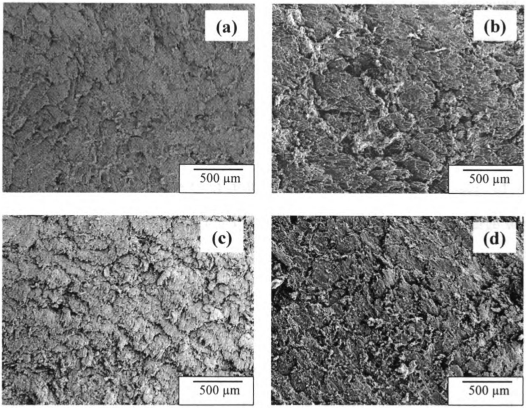

Figure 4.6. SEM micrographs of the rigid PVC/wood-flour composites core layer containing various amounts of wood flour and processed with different temperature profiles: (a) 40% wood flour/high temperature; (b) 40% wood flour/low temperature; (c) 60% wood flour/high temperature; (d) 60% wood flour/low temperature.

Similarly, increasing wood flour content in the composites generates a prolonged fusion time (Table 4.6). The poor thermal conductivity of wood may attribute to the delayed fusion time in the composites, which decreases the transfer of heat and shear throughout the PVC grains [40]. Considering the corresponding increase in the fusion time with increasing wood flour content, the composites with high wood content (60%) would require additional thermal energy to be absorbed by the composite in order for the PVC particles to fuse together. The lower bulk density of the composites could also explain the delayed fusion process in the composites with high wood content. Fusion begins once a sufficient amount of heat has been put into the resin grains [23-26]. A high bulk density creates ample compaction, additional shear and accelerated heat build-up [54]. Because the mass fraction of the resin in the composites decreases as the wood flour content increases, the bulk density of neat resin will decrease as the amount of wood increases in the composites [40]. Consequently, for the equivalent mixer charge weight (mass of the material), the build-up of heat will be slow in the composites with high wood flour content, which delays the fusion process. As mentioned, slow fusion results in poor adhesion between wood flour and PVC. Moreover, SEM micrographs of samples containing 40 and 60% wood flour support these findings. As seen in Figures 4.6 (a) and (b), a relatively smooth cross-section surface occurs in PVC/wood flour core with low wood flour content compared to relatively rough surfaces occurring with those of high wood flour content (Figures 4.6 (c) and (d)) at the same processing temperature. Smoother surfaces suggest a well-fused PVC matrix, better encapsulation of wood flour by the PVC matrix in the core layer and good interfacial adhesion between the WPC in the core and the PVC matrix in the cap layers.

4.4.3 Effect of the interaction factors on the flexural modulus

Unlike the flexural strength (Equation (4.3)), the two-level factorial design reveals two powerful interactions (interactions AB and BC) positively affecting the flexural modulus of coextruded composites (Equation (4.4)). However, examining the relationship between the flexural modulus and these interactions involves considering only the interaction between processing temperature and wood flour (interaction AB), due to its predominant effect on the flexural modulus compared to the wood flour content/CNT content interaction (interaction BC).

Figure 4.7 shows the interaction graphs of the variation of the flexural modulus as a function of the processing temperature for the core layer and wood flour content in the inner layer (interaction AB). The figure incorporates the effect of this interaction for coextruded composites with unfilled (0% CNT) (Figure 4.7(a)) and 5% CNT-filled (Figure 4.5(b)) rigid PVC cap layers. The data demonstrate two distinct trends.

First, the flexural modulus of coextruded composites does not conform to the rule of mixtures with the core layer processed at low temperature (Figure 4.7). Although the modulus of PVC/wood flour composites increases with increasing wood flour content (rule of mixtures) [29-31], contrarily, this study found the opposite trend (Figure 4.7). Coextruded composites with a large amount of wood flour (60%) have lower flexural modulus than their counterparts with lower wood flour content (40%), regardless of the cap layer composition. Prolonged fusion time and inadequate interfacial adhesion induced by the low processing temperature profile may account for the decreased stiffness. However, the CNT-reinforced cap layer significantly improves flexural stiffness, regardless of core layer composition.

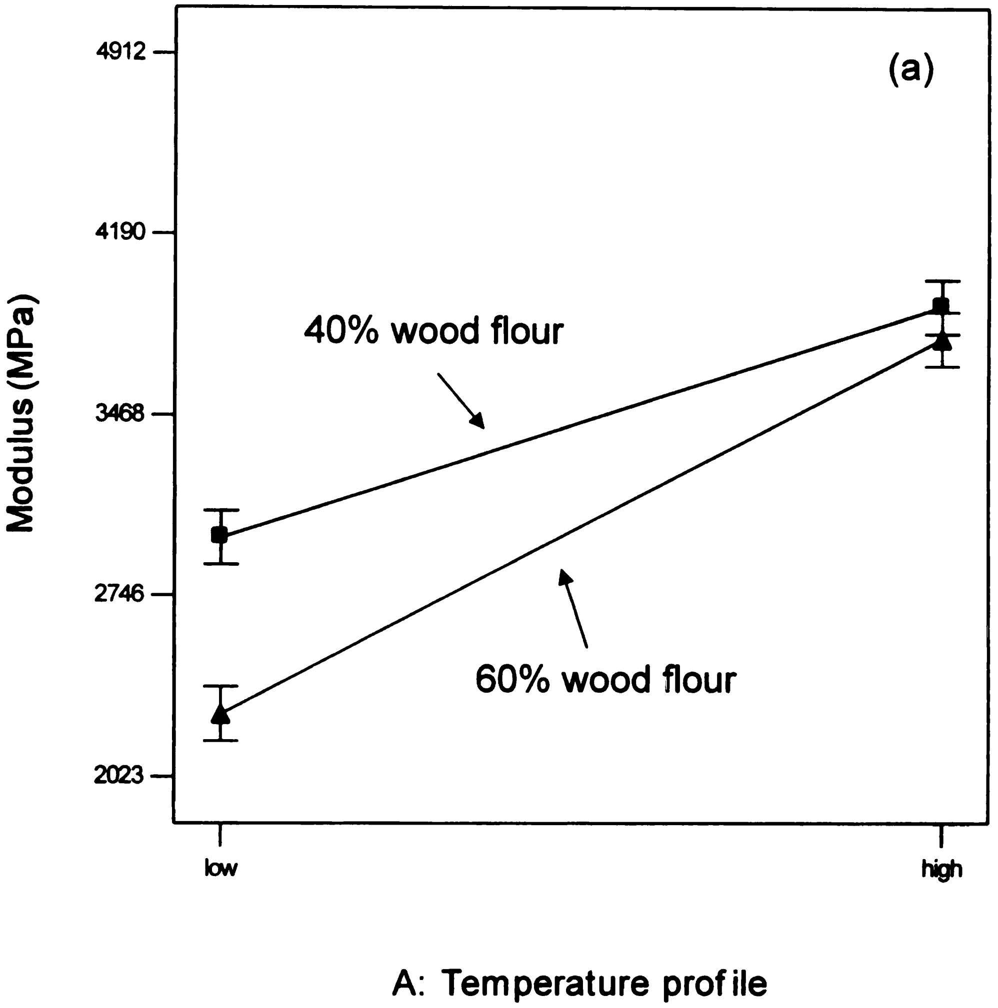

Figure 4.7. Interaction graphs of the variation in flexural modulus of coextruded composites as a function of the processing temperature for core layer-wood flour content in inner layer interaction: (a) no CNT in cap layer and (b) cap layer reinforced with 5% CNT.

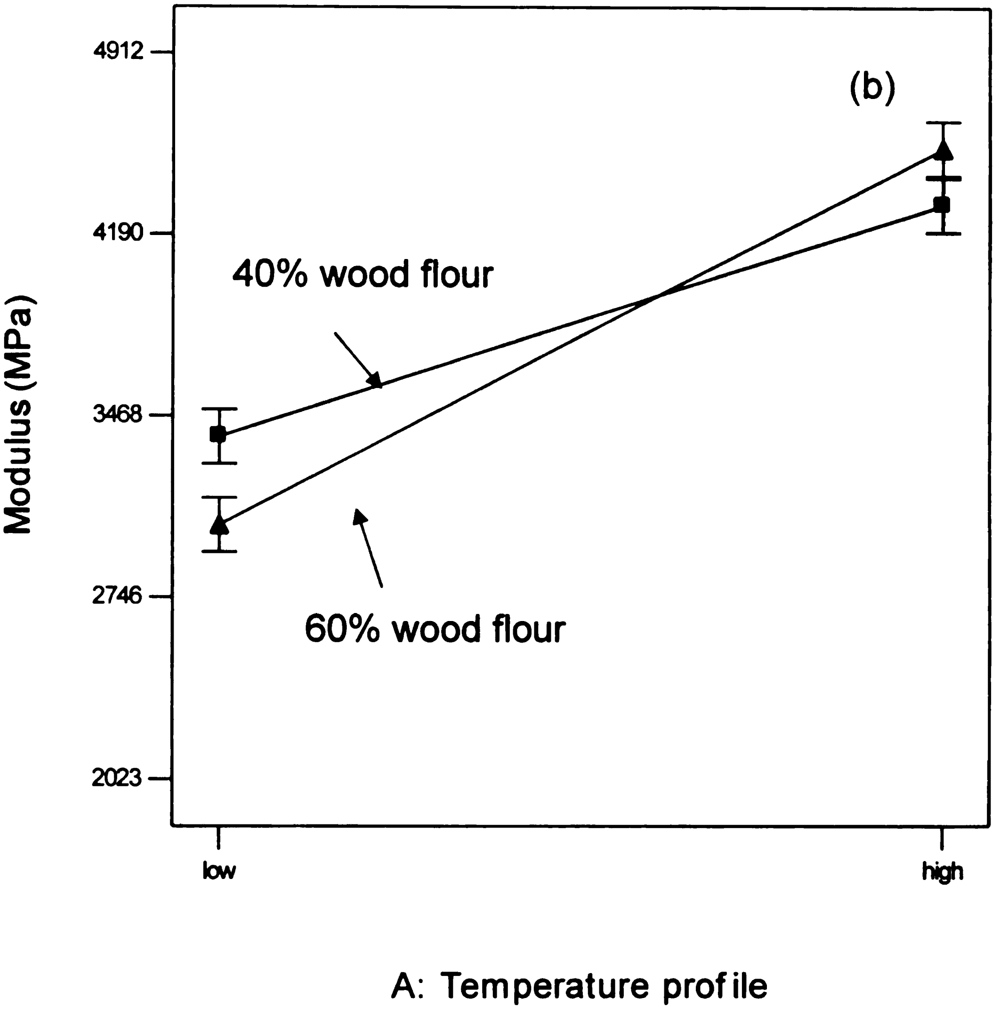

Figure 4.7. Interaction graphs of the variation in flexural modulus of coextruded composites as a function of the processing temperature for core layer-wood flour content in inner layer interaction: (a) no CNT in cap layer and (b) cap layer reinforced with 5% CNT.

Second, processing at an elevated temperature has a noticeable effect on the flexural modulus of the coextruded composites. As seen in Figure 4.7, its actions in shortening PVC fusion time and enhancing the interfacial adhesion between wood flour and PVC matrix in the core layer result in the flexural modulus of coextruded composites increasing with processing temperature. Nevertheless, the composites with unfilled cap layer do not conform to the rule of mixtures. By contrast, the reinforcing effect of CNTs results considering their addition in the outer layer produces notable changes in the flexural strength of coextruded composites, as well as the coextruded composites with high wood flour content (60%) outperforming the counterparts with 40%wood flour in the inner layer (Figure 4.7(b)).

Because the flexural properties of coextruded composites depend on the properties of the components in cap and core layers, the results of this study indicate that the production of coextruded composites with greater flexural strength and modulus requires the use of CNT-reinforced PVC in the outer layer combined with a high processing temperature for the WPC core layer. A low level of wood flour (40%) in the core layer is beneficial in enhancing the flexural strength of coextruded composites. Conversely, greater flexural modulus occurs in coextruded composites with high wood flour content (60%) in the core layer.

As discussed, coextruding the rigid PVC cap layer on WPCs significantly increases their flexural strength but decreases their flexural modulus owing to the greater strength but lower stiffness of PVC compared to WPCs. The results summarized in Table 4.7 clearly support these findings. Significant improvement in bending strength occurs in WPCs coextruded with an unfilled rigid PVC cap layer. By contrast, the flexural modulus of WPCs is significantly reduced when encapsulated with an unfilled PVC cap layer. The greater strength but lower stiffness of unfilled PVC compared to WPCs justifies these foreseeable results. The reinforcing effect of CNTs is evident since their addition into the outer layer increases the flexural modulus of coextruded composites.

Table 4.7. Comparison of flexural properties between uncapped (control) and coextruded rigid PVC/wood-flour composites. Composites contained 50% wood flour.

Types of cap layer	Flexural properties	
	Strength (MPa)	Modulus (MPa)
None (control)	44.24 ± 2.31	4518 ± 224
Unfilled rigid PVC	54.75 ± 3.03	3842 ± 236
5% CNT-filled rigid PVC	65.04 ± 0.89	4915 ± 237

4.4 Conclusions

Coextruding a rigid PVC cap layer on WPCs significantly increases their flexural strength yet decreases their flexural modulus as a result of the greater strength but lower stiffness of PVC compared to WPCs. An implemented two-level factorial design developed regression models evaluating the statistical effects of material compositions and processing conditions on the flexural properties of coextruded rigid PVC/wood flour composites, with the intention to produce coextruded composites with better flexural properties than uncapped WPCs. Material composition variables were wood flour content (40 and 60 %) in the core layer and CNT content (0 and 5 %) in the cap layer of coextruded composites with the processing temperature profile (low and high) for the core layer as the only processing condition variable. Fusion tests assisted in understanding the effects of material compositions and processing condition on the flexural properties. The conclusions drawn are as stated below.

Regression models indicated all main effects and several powerful interaction effects (processing temperature/wood flour content and wood flour content/CNT content interactions) as statistically significant.

The fusion behavior of PVC/wood flour composites used in the core layer of coextruded composites, which depends on both processing temperature and wood flour content, plays a key role in the performance of the coextruded composites. While high processing temperature accelerated the fusion, increasing the wood flour content in the composites prolonged fusion time. Rapid fusion resulted in an improved interface between the PVC matrix and wood flour in the core layer while simultaneously promoting desirable adhesion between the WPC inner and rigid PVC outer layers of coextruded composites, resulting in better overall flexural properties. These results imply that factors leading to a fast fusion of PVC/wood flour composites in the core layer are effective processing and material composition parameters for improving the flexural properties of coextruded composites. The noticeable reinforcing effect of CNTs included in the outer layer produced drastic changes in the flexural strength and modulus of coextruded composites, insensitive to the core layer composition and the processing temperature condition.

Because the flexural properties of coextruded composites depend on the properties of the components in cap and core layers, the results of this study indicate that production of coextruded composites with enhanced flexural strength and modulus requires the use of CNT-reinforced PVC in the outer layer combined with a WPC core layer processed at high temperature. A low level of wood flour in the core layer is beneficial in enhancing the flexural strength, while greater flexural modulus occurs in coextruded composites with high wood flour content in the core layer.

4.5 Acknowledgements

The authors gratefully acknowledge the USDA-CSREES Grant-Advanced Technology Applications to Eastern Hardwood Utilization (Grant No. 2008-34158-19510) for the financial support for this research work. The authors are grateful for the generous donation of materials provided by the manufacturers listed in the Table 4.1. The authors gratefully acknowledge Ms. Valerie Edge, an undergraduate student at Michigan State University, for her thoughtful and constructive comments on the paper.

4.6 References

1. L.M. Matuana, Recent research developments in wood plastic composites, *Journal of Vinyl & Additive Technology*, **15**(3): 136-138 (2009).
2. J.M. Pilarski and L.M. Matuana, Durability of wood flour-plastic composites exposed to accelerated freeze-thaw cycling. Part I. Rigid PVC matrix, *Journal of Vinyl & Additive Technology*, **11**(1): 1-8 (2005).
3. J.M. Pilarski and L.M. Matuana, Durability of wood flour-plastic composites exposed to accelerated freeze-thaw cycling. II. High density polyethylene matrix, *Journal of Applied Polymer Science*, **100**(1): 35-39 (2006).
4. B. Dawson-Andoh, L.M. Matuana, and J. Harrison, Susceptibility of high density Polyethylene/wood-flour composite to mold discoloration, *Journal of the Institute of Wood Science*, **17**(2): 114-119 (2005).
5. B. Dawson-Andoh, L.M. Matuana, and J. Harrison, Mold susceptibility of rigid PVC/wood-flour composites, *Journal of Vinyl & Additive Technology*, **10**(4): 179-186 (2004).
6. B. Dawson-Andoh and L.M. Matuana, High density polyethylene-wood flour composite lumber: Efficacy of two proprietary biocides in the control of fungal colonization and discoloration, *Holz als Roh-und Werskstoff*, **65**(5): 331-335 (2007).
7. N.M. Stark, Influence of moisture absorption on mechanical properties of wood flour-polypropylene composites, *Journal of Thermoplastic Composite Materials*, **14**(5): 421-432 (2001).
8. J.S. Fabiyi, A.G. McDonald, M.P. Wolcott, and P.R. Griffiths, Wood plastic composites weathering: visual appearance and chemical changes, *Polymer Degradation and Stability*, **93**(8): 1405-1414 (2008).
9. N.M. Stark and L.M. Matuna. Characterization of weathered wood-plastic composite surfaces using FTIR spectroscopy, contact angle, and XPS, *Polymer Degradation and Stability*, **92**(10): 1883-1890 (2007).
10. N.M. Stark and L.M. Matuana, Influence of Photostabilizers on Wood Flour-HDPE Composites Exposed to Xenon-Arc Radiation with and without Water Spray, *Polymer Degradation and Stability*, **91**(12): 3048-3056 (2006).
11. N.M. Stark, L.M. Matuana, and C.M. Clemons, Effects of processing method on surface and weathering characteristics of wood-flour/HDPE composites, *Journal of Applied Polymer Science*, **93**(3): 1021-1030 (2004).
12. N.M. Stark and L.M. Matuana, Surface chemistry and mechanical property changes of wood-flour/high density polyethylene composites after accelerated weathering, *Journal of Applied Polymer Science*, **94**(6): 2263-2273 (2004).

13. N.M. Stark and L.M. Matuana, Surface chemistry changes of weathered HDPE/wood-flour composites studied by XPS and FTIR spectroscopy, *Polymer Degradation and Stability,* **86**(1): 1-9 (2004).

14. N.M. Stark and L.M. Matuana, Ultraviolet weathering of photostabilized wood-flour-filled high density polyethylene composites, *Journal of Applied Polymer Science,* **90**(10): 2609-2617 (2003).

15. L.M. Matuana and D.P. Kamdem, Accelerated ultraviolet weathering of PVC/wood-flour composites, *Polymer Engineering and Science,* **42**(8): 1657-1666 (2002).

16. L.M. Matuana, D.P. Kamdem, and J. Zhang, Photoageing and stabilization of rigid PVC/wood-fiber composites, *Journal of Applied Polymer Science,* **80**(11): 1943-1950 (2001).

17. N.M. Stark and L.M. Matuana, Coating WPCs using co-extrusion to improve durability, *Proceedings: Coating Wood and Wood Composites: Designing for Durability,* July 23-25, 2007, Seattle, WA.

18. S. Jin and L.M. Matuana, Coextruded PVC/wood-flour composites with WPC cap layers, *Journal of Vinyl & Additive Technology,* **14**(4): 197-203 (2008).

19. S. Jin and L.M. Matuana, Improving water resistance of wood plastic composites Through coextrusion, *SPE ANTEC Papers*, **66**: 19-23 (2008).

20. G. Pritchard, Second-generation wood composites: the US shows Europe the way, *Reinforced Plastics,* **49**(6): 34-35 (2005).

21. C. Rauwendaal, *Understanding Extrusion*, Gardner Publications, Inc., Cincinnati, (1998).

22. Z. Gürdal, R.T. Haftka and P. Hajela, *Design and Optimization of Laminated Composite Materials*, John Wiley & Sons, Inc., New York, (1999).

23. W.V. Titow, Elementary Principles of PVC Formulation, in *PVC Technology,*. Elsevier Applied Science Publishers, New York, (1984).

24. P. Kroushl, *Handbook of Vinyl Formulating,* 2nd Edition, John Wiley & Sons, Inc., Hoboken (2008).

25. J.W. Summers, *PVC Handbook*, Hanser Gardner Publications, Cincinnati, pp 3-4 (2005).

26. G. Matthews, Properties of Vinyl Chloride Polymers and Copolymers, in *PVC: Production, Properties and Uses,* The Institute of Materials, London, pp 55-56 (1996).

27. J.C. Garcia and A. Marcilla, A influence of the type of resin in the gelation and fusion processes of PVC plastisols. *Polymer,* **39**(2): 431-435 (1998).

28. M. Moghri, H. Garmabi and M. Akbarian, Effect of processing parameters on fusion and mechanical properties of a twin-screw extruded rigid PVC pipe, *J Vinyl Addit Technol*, **9**(2): 81-89 (2003).

29. L.M. Matuana, C.B. Park, and J.J. Balatinecz, The effect of low levels of plasticizer on the rheological and mechanical properties of polyvinyl chloride/newsprint-fiber composites, *Journal of Vinyl and Additive Technology,* **3**(4): 265-273 (1997).

30. B.L. Shah and L.M. Matuana, Novel coupling agents for PVC/wood-flour composites, *Journal of Vinyl & Additive Technology,* **11**(4): 160-165 (2005).

31. L.M. Matuana, R.T. Woodhams, J.J. Balatinecz, and C.B. Park, Influence of interfacial interactions on the properties of PVC/cellulosic-fiber composites, *Polymer Composites,* **19**(4) 446-455 (1998).

32. L.M. Matuana, Rigid PVC/(Layered Silicate) nanocomposites produced through a novel melt-blending approach, *Journal of Vinyl & Additive Technology,* **15**(2): 77-86 (2009).

33. O. Faruk and L.M. Matuana, Reinforcement of rigid PVC/wood-flour composites with multi-walled carbon nanotubes, *Journal of Vinyl & Additive Technology,* **14**(2): 60-64 (2008).

34. D. Wang and C.A. Wilkie, Preparation of PVC-clay nanocomposites by solution blending, *Journal of Vinyl & Additive Technology,* **8**(2): 238-245 (2002).

35. C. Wan, X. Qiao, Y. Zhang and Y. Zhang, Effect of different clay treatment on morphology and mechanical properties of PVC-clay nanocomposites, *Polymer Testing,* **22**(4): 453-461 (2003).

36. C.H. Chen, C.C. Teng, M.S. Tsai and F.S. Yen, Preparation and characterization of rigid poly(vinyl chloride)/MMT nanocomposites. II. XRD, morphological and mechanical characteristics, *Journal Polymer Science Part B Polymer Physics,* **44**(15): 2145-2154 (2006).

37. T. Ren, J. Yang, Y. Huang, J. Ren and Y. Liu, Preparation, characterization, and properties of poly(vinyl chloride)/organophilic-montmorillonite nanocomposites *Polymer Composites,* **27**(1): 55-64 (2006).

38. D. Wang, D. Parlow, Q. Yao and C.A. Wilkie, Melt blending preparation of PVC-sodium clay nanocomposites, *Journal of Vinyl & Additive Technology,* **8**(2): 139-150 (2002).

39. C. Xiong, S. Lu, D. Wang, L. Dong, D.D. Jiang and Q. Wang, Microporous polyvinyl chloride: novel reactor for PVC/$CaCO_3$ nanocomposites, *Nanotechnology,* **16**(9): 1787-1792 (2005).

40. L.M. Matuana and J.W. Kim, Fusion characteristics of wood-flour filled rigid PVC by torque rheometry, *Journal of Vinyl & Additive Technology,* **13**(1): 7-13 (2007).

41. R.H. Myers and D.C. Montgomery, *Response Surface Methodology: Process and Product Optimization Using Designed Experiments*, Wiley, New York, pp 91-102 (1995).

42. D.C. Montgomery, *Design and Analysis of Experiments,* 5th Edition, Wiley, New York, (2001).

43. K. Carlborn and L.M. Matuana, Modeling and optimization of formaldehyde-free wood-based composites using a box-behnken design, *Polymer Composites,* **27**(5): 497-503 (2006).

44. L.M. Matuana and Q. Li, Statistical modeling and response surface optimization of extruded HDPE/wood-flour composite Foams, *Journal of Thermoplastic Composite Materials,* **17**(2): 185-199 (2004).

45. L.M. Matuana and F. Mengeloglu, Manufacture of rigid PVC/wood-flour composite foams using moisture contained in wood as foaming agent, *Journal of Vinyl and Additive Technology,* **8**(4): 264-270 (2002).

46. L.M. Matuana and Q. Li, A factorial design applied to the extrusion foaming of polypropylene/wood-flour composites, *Cellular Polymers,* **20**(2): 115-130 (2001).

47. B.L. Shah and L.M. Matuana, Online measurement of rheological properties of PVC/wood-flour composites, *Journal of Vinyl & Additive Technology,* **10**(3): 121-128 (2004).

48. J.M. Hodgkinson, *Mechanical Testing of Advanced Fibre Composites,* Woodhead Publishing, (2000)

49. D.N. Saheb and J.P. Jog, Natural fiber polymer composites: A review, *Advanced Polymer Technology,* **18**(4): 351-363 (1999).

50. K.B. Adhikary, S. Pang and M.P. Staiger, Dimensional stability and mechanical behaviour of wood–plastic composites based on recycled and virgin high-density polyethylene (HDPE), *Composites Part B: Engineering,* **39**(5): 807-815 (2008).

51. S.T. Georgopoulos, P.A. Tarantili, E. Avgerinos, A.G. Andreopoulos and E.G. Koukios, Thermoplastic polymers reinforced with fibrous agricultural residues, *Polymer Degradation and Stability,* **90**(2): 303-312 (2005).

52. J.E. Crespo, L. Sanchez, F. Parres and J. Lopez, Study of the mechanical and morphological properties of plasticized PVC composites containing rice husk fillers, *Journal of Thermoplastic Composite Materials,* **22**(3): 259-272 (2009).

53. E.J. Comeaux, C.H. Chen, J.R. Collier and R.D. Wesson, Fusion study of polyvinyl chloride (PVC): Relation of Processing time and processing temperature to the degree of fusion, *Polymer Bulletin,* **33**(6): 701-708 (1994).

54. J.D. Bower, The function of lubricants in processing of rigid poly(vinyl chloride), *Journal of Vinyl & Additive Technology,* **8**(4):179-182 (1986).

CHAPTER 5

Ultraviolet Weathering of HDPE/Wood-Flour Composites Coextruded with a Clear HDPE Cap Layer

This chapter was submitted to Polymer Degradation and Stability in June 2010.

5.1 Abstract

This study examined the effect of coextruding a clear HDPE cap layer onto HDPE/wood-flour composites on the discoloration of coextruded composites exposed to accelerated UV tests. Chroma meter, FTIR-ATR, XPS, SEM, and UV vis measurements accounted for the analysis of discoloration, functional group, and degree of oxidation of both uncapped (control) and coextruded composites before and after UV exposures. Two separate discoloration characteristics occurred in the discoloration of composites. For uncapped WPCs (control), chemical changes due to photooxidation resulted in darkening followed by physical changes, including loss of colored wood components from the surface, as well as increased roughness on the surface, which led to lightening of WPCs. By contrast, because a hydrophobic cap layer prevented the loss of colored components from the surface, coextruding a clear hydrophobic HDPE cap layer over WPCs significantly decreased the discoloration during the weathering process. Photooxidation of wood components at the interface accounted for the discoloration of coextruded WPCs before the failure of cap layer. Moreover, as the cap layer absorbed a specified amount of UV light and reduced oxygen available to interface, it decreased the photooxidation rate at the interface compared to that at the WPCs surface.

5.2 Introduction

Wood fiber and polymers such as PVC, HDPE, and PP comprise wood-plastic composites (WPCs). The major applications of WPCs in North America include decking, siding, railings, fences, window and door frames, etc. These outdoor applications expose WPCs to moisture, fungi, freeze-thaw actions, and ultraviolet light in sunlight. The presence of the hydrophobic polymer phase in WPCs improves the durability in terms of resistance to water absorption and biological decay compared to that of solid wood [1-4]. However, since both wood fiber and polymer matrix experience photodegradation upon exposure to ultraviolet light, weathering of WPCs results in severe discoloration and a modest loss of mechanical properties [5-14]. A significant feature of WPCs, aesthetic value, becomes compromised through discoloration, making it a major concern.

Controlling the discoloration of WPCs upon weathering requires a comprehensive understanding of weathering mechanisms. Photodegradation of WPCs, also understood as the weathering of the major components of WPCs (wood and polymer), results from the combined effects of light, water, oxygen, and heat.

All main polymeric components of wood, such as cellulose, hemicellulose, lignin, and extractives, suffer from photodegradation [15]. Because visible light (400-700 nm) carries energy less than 70 kcal/mol, it cannot provide sufficient energy to break the major chemical bonds in the wood components [15]. Thus, the photodegradation of wood results primarily from the ultraviolet aspect of sunlight. The degrees of photodegradation of wood components largely depend on their ability to absorb UV light. Because of the location of most wood chromophores in the lignin, lignin accounts for 80-95% of light absorption of wood, making its photodegradation a significant contribution to wood discoloration [16]. Absorption of UV light initiates the photochemical reactions of wood surfaces leading to the formation of aromatic and other free radicals, which causes the degradation of lignin and photo-oxidation of cellulose and hemicelluloses, effectually causing discoloration [15, 17]. Generally, wood in outdoor environments initially becomes yellow and brown due to the photooxidation of lignin, and then gray due to leaching of the degraded product of lignin [15]. This discoloration and yellowing of wood surfaces result from the loss of methoxyl content of lignin, photo-dissociation of carbon-carbon bonds and formation of carbonyl-based chromophoric groups. Numerous studies report that wood exposed to artificial weathering (only exposure to UV radiation) darkens as the radiation time increases [15-18].

Similar to the photodegradation of wood, the photodegradation of polyolefins is a radical-based oxidative process. The presence of catalyst residues, hydroperoxide groups, and carbonyl groups introduced during polymer manufacturing, processing, and storage accounts for this similarity [19]. All of these species absorb UV light above 290 nm and initiate photochemical reactions. Photodegradation causes changes in all scales of polymer dimension, including the monomer unit (oxidation), the chain (crosslinking or chain scission), the morphology (breakdown of tie molecules and crystal), and on the macroscopic scale [20]. Diffusion of oxygen in the polymer controls polyolefin photodegradation. Density gradients due to oxidation gradients cause the stresses, which combined with chain scission, could initiate and propagate cracks. Cracks on the surface result in light diffusion (a whitening effect in appearance) and also lead to the mechanical properties loss [21].

Photodegradation of WPCs involves several factors including the wood flour content, coupling agents, manufacturing methods, and weathering conditions, among others. Matuana and Kamdem investigated the influence of accelerated artificial weathering on the color changes and tensile properties of PVC/wood-flour composites with various wood flour contents [6]. While the composites retained original tensile properties, they experienced severe discoloration (darkening) after weathering for 2600 hours. PVC/wood-flour composites containing 15 phr wood flour darken more than those containing 30 phr and 45 phr wood flour. Conversely, reports indicate the opposite trend for weathered HDPE/wood-flour composites; the composites containing 50% wood flour lighten more than the counterparts with 25% wood flour [22]. Ndiaye and coworkers studied the effects of wood flour content and compatibilizer on the durability of HDPE-based and PP-based WPCs [23]. Their results indicated that the oxidation rate of the composites increases with wood content and decreases with the presence of compatibilizer due to better dispersion of wood flour in polymer matrix [23].

Examining the effect of weathering conditions (UV radiation with or without water spray) and manufacture methods (injection molding and extrusion) on the changes in lightness and flexural properties of HDPE/wood-flour composites, Stark and Matuana reported that the composites experienced more lightening and flexural properties loss when exposed to UV radiation with water spray cycle compared to UV radiation cycle alone [11-13]. Wood particle bleaching due to UV radiation and removal of water-soluble extractives by water spray caused the color fading of these composites. Not only did water spray accelerate oxidation reactions and facilitate light penetration into the composites, but it also removed water-soluble wood extractives, thus causing faster fading. Weathered injection-molded composites lightened more slowly than extruded ones due to the hydrophobic HDPE-rich surface layer that formed on the surface of injection molded composites [11-13].

Recent investigations studied the effects of natural and accelerated artificial weathering on the appearance and chemical changes of HDPE-based and PP-based WPCs [6-14, 24]. The lightness, total color change, and wood loss increased with exposure time. PP-based WPCs experienced quicker photodegradation in terms of lightness and wood loss. Delignification and oxidation accounted for the increased lightness of weathered composites. Muasher and Sain also investigated the discoloration of HDPE-based WPCs exposed to natural weathering and reported that WPCs underwent two competing redox reactions upon UV exposure: the formation of paraquinone chromophoric structures generated by the oxidation of lignin, resulting in yellowing, as well as the reduction of the paraquinone structures to hydroquinones, leading to photobleaching [24]. The yellowing mechanism dominant during the first 250 hours of exposure preceded the photobleaching mechanism that became dominant with increased exposure time.

Current approaches of improving the weathering resistance of WPCs focus on the bulk of WPCs, i.e., incorporation of additives into the entire product or surface treatment of the wood fiber. For example, adding photostabilizers and pigments provides protection against discoloration caused by UV radiation. Stark and Matuana studied the effects of an ultraviolet light absorber (UVA), a colorant, and two hindered amine light stabilizers (HALS, low molecular weight diester and secondary amine triazine) on the photostabilization of HDPE-based WPCs composites using a factorial design [25]. Because the UVA's ability to absorb some UV radiation and the colorant's ability to block the penetration of UV radiation, as well as masking the bleaching of wood fiber, UVA and colorant significantly lowered the lightness upon weathering. Conversely, the two HALS did not show significant effects on lightness. Investigation of five HALS (low, medium, and high molecular weight diester, and tertiary and secondary amine triazine) and combinations of HALS and UVA on the color changes of HDPE-based WPCs indicated that the molecular weight of diester HALS played an important role in the color changes [24]. Low molecular weight diester HALS shows high effectiveness in the initial stage due to their fast diffusion to the surface but alternatively, low effectiveness with increased exposure time due to their loss by surface evaporation [24]. Assuming the loss of color-imparting extractives from wood flour as responsible for fading, examinations studied the role of fiber pretreatment on the color stability of HDPE/wood-flour composites. As a result, fiber pretreatment methods included removing water-soluble extractives from wood flour and coloring wood flour with a water-based dye or an oil-based stain [22]. Whereas the removal of water-soluble extractives from wood flour and coloring wood flour with a water-based dye did not improve the color stability of the composites upon weathering, coloring wood flour with an oil-base stain significantly improved the color stability [22].

Although adding stabilizer or pigment into the entire composites improves their resistance to photodegradation, weathering primarily occurs at the surface of a material [6-15]. Pursuing a cost-effective means to cope with weathering would not favor adding photo stabilizers into the bulk of a material instead of the surface. The best approach in improving durability would involve adding photo stabilizers protection only on the surface of composite samples.

Several methods can provide a durable surface to withstand weathering. Coating, one of the methods widely used in the wood industry, provides protection against environmental damage such as weathering, biodegradation, and mechanical abrasion. For protection against photodegradation, opaque pigmented coatings block the UV/visible light but cover the aesthetics of wood. Conversely, semi-transparent and clear coatings maintain the natural appearance of wood, but the UV/visible light transparency of the coating results in the photodegradation of wood substrate and the resultant failure of the coating adhesion due to the photodegraded substrate [26-29].

Investigation of the photo-discoloration of UV-curable acrylic coatings and the underlying wood revealed that coating wood specimens with non-photostabilized UV-curable acrylic clear films such as aromatic urethane, aliphatic urethane, epoxy and silicone, fails to protect wood underneath the films against discoloration [27]. Both the coating films and wood specimens underneath these films experienced severe discoloration after exposure to UVA lamps at 60°C for 12 hours. Photodegradation of the interfacial layer led to flaking and peeling of the coating. Poor UV light resistance of the clear films could account for the lower color stability of these coatings, as it reduces the intensity of UV light reaching the interface layer between wood surface and the films [27].

In a subsequent study, investigations examined the effect of photostabilized aliphatic or aromatic urethane-modified acrylic clear coatings on the photo-discoloration of coated wood as a means to reduce the intensity of UV light reaching the interfacial layer without changing the natural color of coatings and wood [29]. The evident screening effect of ultraviolet light absorbers (UVA) such as benzophenone and hydroxyphenyl benzotriazole resulted since their incorporation into coating films inhibited the photodiscoloration of wood coated with both aliphatic and aromatic urethane-modified acrylics (19-24 h exposure). The addition of HALS failed to reduce the discoloration of wood coated with aromatic urethane-modified acrylate containing UVA, attributable to its inability to capture the radicals produced by the photodiscoloration of aromatic urethane films. In contrast, observations focused on a synergitic effect of HALS for wood coated with aliphatic urethane-modified acrylic containing light absorbers. The addition of HALS further reduced the color changes of coated wood due to its actions in scavenging the free radicals produced from the photodegradation process and protecting light absorbers against the attach of free radicals [29]. However, difficulty arises in coating the plastic composite at the surface of WPCs due to the low surface energy of plastic. Coating also involves solvent evaporation, which often causes environmental concerns. Furthermore, the drying stage of coating requires additional time, reducing the efficiency of the assembly line.

Another method for providing a protective surface includes lamination. Melt fusion or an adhesive layer allow for the lamination of a surface layer over substrate. Nevertheless, delamination often occurs with the bending of the laminated composites [30]. Moreover, difficulty arises in the usage of lamination technology to manufacture a fully encapsulated structure in wood plastic composites rather than a planar layered structure.

Coextrusion, another method for providing a protective surface, can produce a multilayered product with different properties at outer and inner layers, thus offering different properties between surface and bulk [31, 32]. Encapsulation of WPCs with an HDPE or PVC surface rich cap layer through coextrusion significantly delays the water absorption and improves flexural strength compared to nonencapsulated WPCs [33-35]. Because of water's significance in weathering of WPCs [11-13], coextruding a hydrophobic clear cap layer onto WPCs may retard their discoloration.

Therefore, the main aim of this study examined the role coextruding a clear HDPE cap layer onto HDPE/wood-flour composites has on the photo-discoloration of coextruded composites exposed to accelerated weathering tests in order to elucidate the discoloration mechanisms involved in WPCs and assist in developing strategies to reduce the weathering-induced discoloration of WPCs. Particular emphasis focused on exposing both uncapped (control) and coextruded WPCs to accelerated weathering tests and monitoring the surface changes by color measurement, FTIR, XPS, SEM, and UV-vis measurement.

5.3 Experimental

5.3.1 Materials

NOVA Chemicals supplied the neat HDPE (SCLAIR® 19G) used as the cap layer. This polymer (termed as $HDPE_{1.2}$), in pellet form, had a melt flow index of 1.2 g/10 min and a density of 0.96 g/cm^3. Another HDPE (FORTIFLEX™ B53–35H-FLK) obtained from B.P. Solvay Polymers was used as the polymeric matrix for uncapped composites (control) and as the core layer for coextruded composites. This polymer (termed as $HDPE_{0.4}$), in flake form, had a melt flow index of 0.49 g/10 min and a density of 0.9 g/cm^3. Materials for wood flour included the 0.425 mm (40 mesh) maple from American Wood Fibers (Schofield, WI). The wood flour was oven-dried at 105 °C for ~48 h before processing to remove moisture. The lubricant TPW104 (a blend of aliphatic carboxylic acid salts and mono and diamides) from Struktol® Company (Stow, OH) was used to ease processing and improve the surface quality of composites.

5.3.2 Compounding and extrusion

A 20-L high intensity mixer (Papenmeier, Type TGAHK20) used for room temperature dry blending of the $HDPE_{0.4}$ matrix, dried wood flour, and lubricant operated for 10 minutes. The formulation of the core layer composites contained 50% maple flour, 44% $HDPE_{0.4}$, and 6% lubricant, based on the total weight of the composites.

The coextrusion system consisted of a coextrusion die connecting a twin screw extruder for the core layer and a single screw extruder for the cap layer, as described in detail in previous studies [33-35].

Manufacturing of coextruded composites used core layers that contained $HDPE_{0.4}$/wood-flour composites formed using a 32-mm conical counter rotating twin-screw extruder (C.W. Brabender Instruments, South Hackensack, NJ) with a length-to-diameter ratio of 13:1. The processing temperature profile of the extruder performed at 130/135/135/135°C from hopper to the coextrusion die and the rotational screw maintained a constant speed at 40 rpm throughout processing. A 19 mm single-screw extruder (C.W. Brabender Instruments, South Hackensack, NJ) with a length-to-diameter ratio of 30:1 produced the neat HDPE with MFI of 1.2 g/10 min ($HDPE_{1.2}$) used as cap layers. The processing temperature profile of this extruder ran at 165/155/145/135°C from hopper to coextrusion die. The rotational screw maintained a speed set at 2 rpm to produce a thin cap layer (0.20 ± 0.03 mm), which encapsulated the core layer completely (Figure 5.1).

Uncapped or noncoextruded $HDPE_{0.4}$/wood-flour composites (control) were also produced using coextrusion die to investigate the effect of a cap layer on the weathering of the WPCs. Manufacturing of the control samples included the twin screw extruder with a coextrusion die using the processing conditions similar to those mentioned above for core layers.

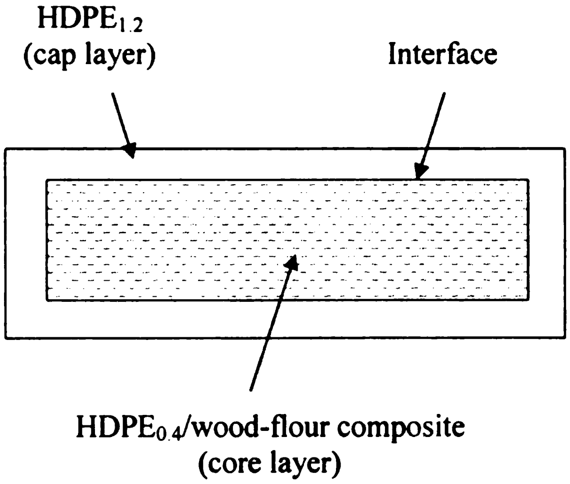

Figure 5.1. Schematic of the cross section of coextruded HDPE/wood-flour composite.

5.3.3 Accelerated weathering tests

An accelerated UV radiation weathering chamber simulates damaging effects of long term outdoor exposure by exposing test samples to ultraviolet radiation, moisture and heat. The QUV weatherometer from Q-Lab Corporation housed both coextruded and noncoextruded control samples. Tests carried out according to the procedures outlined the ASTM G 154 included a 12 h cycle consisting of 8h UVA-340 radiation at 60 °C, 15 min water spray, and 3 h 45 min condensation at 50 °C. The UVA-340 lamps give an excellent simulation of sunlight in the critical short wavelength region from 365 nm down to 295 nm. UVA-340 radiation, water spray, and condensation could simulate sunlight, rain, and dew, respectively. Water spray also could introduce thermal shock and mechanical erosion.

5.3.4 Scanning electron microscopy (SEM)

SEM pictures taken using JEOL JSM-6400 SEM at 12 kv accelerating voltage assisted monitoring the formation of cracks on the cap layer of control and coextruded composites exposed to UV light. Moisture removal consisted of over-drying the weathered samples at 105 °C followed by gold coating prior to observation.

5.3.5 UV-vis reflectance spectroscopy

A Lambda 25 UV-vis spectrophotometer (PerkinElmer) functioned as the means in acquiring measurements of the UV-vis diffuse reflectance spectra of the $HDPE_{1.2}$ (for cap layer) and the $HDPE_{0.4}$ (used as cap layer and polymer matrix in both core layer of coextruded composites and uncapped WPCs). The scans were run from 600 to 250 nm with data interval of 1 nm. The scanning speed was set at 240 nm/min.

5.3.6 Fourier transform infrared spectroscopy

PerkinElmer Spectrum 100 with attenuated total reflectance (ATR) acquired the Fourier transform infrared spectroscopy (FTIR) spectra. The surface of samples in contact with a ZnSe crystal had a 45° angle of incidence. Scans ran at a resolution of 4 cm^{-1} from 4000 to 650 cm^{-1}. Quantifying data used the net peak absorbance obtained after the baseline correction. Following the approach described by Stark and Matuana, the peak intensities of absorption bands at 1030, 1715, and 2915 cm^{-1} were used to calculate both wood and carbonyl indices using the following equations [8-10]:

$$\text{Wood index} = \frac{I_{1030}}{I_{2915}} \times 100 \qquad \text{(Equation 5.1)}$$

$$\text{Carbonyl index} = \frac{I_{1715}}{I_{2915}} \times 100 \qquad \text{(Equation 5.2)}$$

5.3.7 X-ray photoelectron spectroscopy

A PHI 5400 ESCA spectrometer (Physical Electronics, Eden Prairie MN) functioned as the instrument responsible for collecting the X-ray photoelectron spectra. Low-resolution spectra from 0 to 1100 eV binding energy and high-resolution spectra of C_{1s} in the region from 280 to 300 eV were collected with a take-off angle of 45°C. The degree of surface oxidation was calculated by the ratios of oxidized-to-unoxidized carbon atoms (C_{1s} peaks) using the following equation developed in our previous study [6-8]:

$$C_{ox/unox} = \frac{C_{oxidized}}{C_{unoxidized}} = \frac{C2 + C3 + C4}{C1} \qquad \text{(Equation 5.3)}$$

With Carbon component C1 arises from carbon atoms bonded only to carbon and hydrogen atoms (C-C/C-H), C2 from carbon atoms bonded to a single oxygen atom, other than a carbonyl oxygen (C-OH), C3 from carbon atoms bonded to two noncarbonyl oxygen atoms or to a single carbonyl oxygen atom (O-C-O, C=O), and C4 from carbon atoms, which are linked to a carbonyl and a noncarbonyl group (O-C=O) [6].

5.3.8. Color measurements

The procedure outlined in ASTM D2244 served as the means by which to determine the color measurements on the surfaces of coextruded and control samples. A Minolta CR-420 Chroma Meter (Minolta Corp., Ramsey, NJ) measured the color in L*a*b* coordinates at three locations on each sample using the Commission International d'Eclairage (CIELAB 1976 color space) three-dimension color space system. In this system, L* axis (+L* for light, -L* for dark) represents the lightness, a* (+a* is for red, -a* for green), and b* (+b* for yellow, and -b* for blue) the chromaticity coordinates. At least four replicates were measured for each formulation to obtain the average values of color. Calculations incorporated the values of lightness and chromaticity coordinates before and after weathering tests to determine the discoloration (ΔE*) of the weathered samples using the following equation [6]:

$$\Delta E = \sqrt{\Delta L^{*2} + \Delta a^{*2} + \Delta b^{*2}} \qquad \text{(Equation 5.4)}$$

with ΔL*, Δa*, and Δb* as the difference of initial and final values of L*, a*, and b*.

5.4. Results and Discussion

5.4.1 Morphology and surface characteristics of weather composites

Investigations have shown that wood flour filled HDPE composites manufactured by different processes (injection and extrusion) undergo morphological and chemical changes in surface characteristics as they weather due to the accelerated cyclic UV/water spray actions [8,11]. Using SEM, FTIR, and XPS techniques, Stark and Matuana demonstrated that exposure to cyclic UV actions causes surface cracking of the matrix and degradation of the lignin portion of the wood particles. Whereas exposure to water spray causes wood particles to swell, which not only creates microcracks in the matrix, but also wash away loose wood particles, loose cellulose, and degraded lignin at the wood surface [8]. Similar techniques are used in this study to understand the effect of coextruding a cap layer onto WPC surface on the photodegradation of the composites. Figure 5.2 shows the micrographs of the surfaces of both uncapped (control) and coextruded composites before and after weathering.

Prior exposure to UV/water spray cycling, coextruded WPC surface (Figure 5.2(g)) was relatively smoother than the surface of uncapped WPC (Figure 5.2(a)) mainly due to the presence of a thin HDPE layer on the surface of coextruded composites. Improper encapsulation of wood particles by the matrix could also account for the rougher surface of uncapped WPC. As a result, cracks appeared faster (after only 192 h) and more degradation occurred on the surface of uncapped WPC upon accelerated weathering than the coextruded composite surface (Figure 5.2(b) to (e)), owing to the swelling and shrinking of wood particles after absorbing and desorbing moisture during weathering water spray cycle [8].

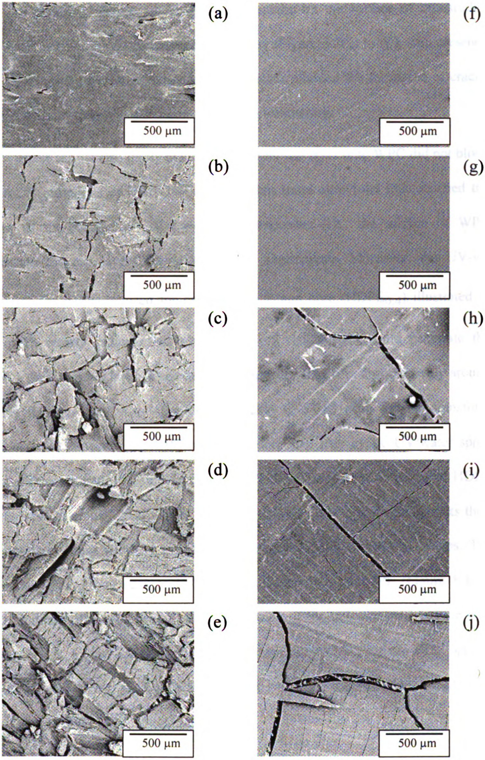

Figure 5.2. SEM (×80k) of surface of noncoextruded WPCs (left column) and coextruded WPCs (right column) as a function of UV radiation exposure times: (a and f) 0 h, (b and g) 432 h, (c and h) 744 h, (d and i) 1392 h, and (e and j) 1952 h.

In contrast, surface cracking did not appear on the surface of coextruded composites until 432 h of accelerated weathering (Figure 5.2(h) to (j)). The presence of an HDPE-rich layer on coextruded WPC surface retarded the formation of cracks in composites by delaying water sorption during weathering.

These results also imply that the transparent cap layer onto WPC did not block all the UV radiations of UVA-340 lamps so that some ultraviolet light reached the surface of the inner layer of coextruded composites (i.e., the surface of WPC underneath the cap layer) during weathering experiments. Moreover, the UV-vis spectra of the polymers used for cap ($HDPE_{1.2}$) and core ($HDPE_{0.4}$) illustrated in Figure 5.3 clearly indicate that almost 85% of visible light could penetrate the $HDPE_{1.2}$ used as outer layer in coextruded composites. The film absorbed only around 15-25% light in the UVA-340 radiation region (295-365 nm). Fourier transform infrared (FTIR) spectra of HDPE matrices before and after cyclic UV/water spray exposures corroborate this finding (Figure 5.4). Distinct absorption peaks of HDPE are observed at around 2915, 2847, 1472, 730, and 718 cm^{-1} and Table 5.1 lists their wavenumbers along with the assignments of corresponding functional groups. The appearance of a strong peak at 1713 cm^{-1} on the surface of HDPE (Figure 5.4(b)) clearly indicates the evidence of photodegradation of the polymer used in both core and cap layers. Figure 5.4(a) also shows important absorption bands in FTIR spectra associated with wood. Peaks associated with wood are clearly seen around 3354 (broad peak), 2903, 1737, 1591, and 1029 cm^{-1}.

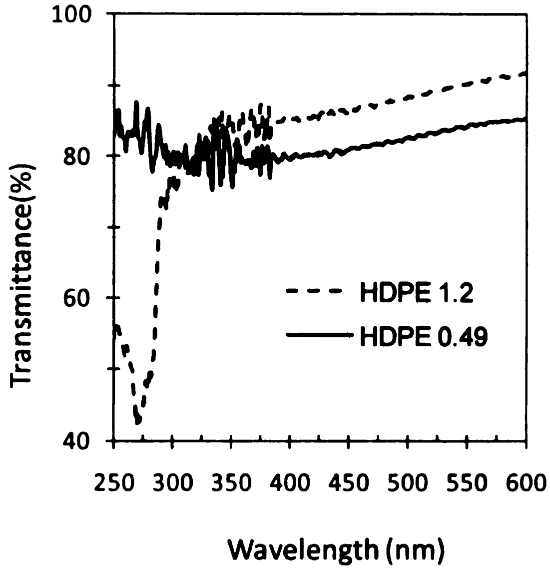

Figure 5.3. UV transmission spectra of films of $HDPE_{1.2}$ (for cap layer) and $HDPE_{0.4}$ (polymer matrix for uncapped WPC and core layer of coextruded WPCs).

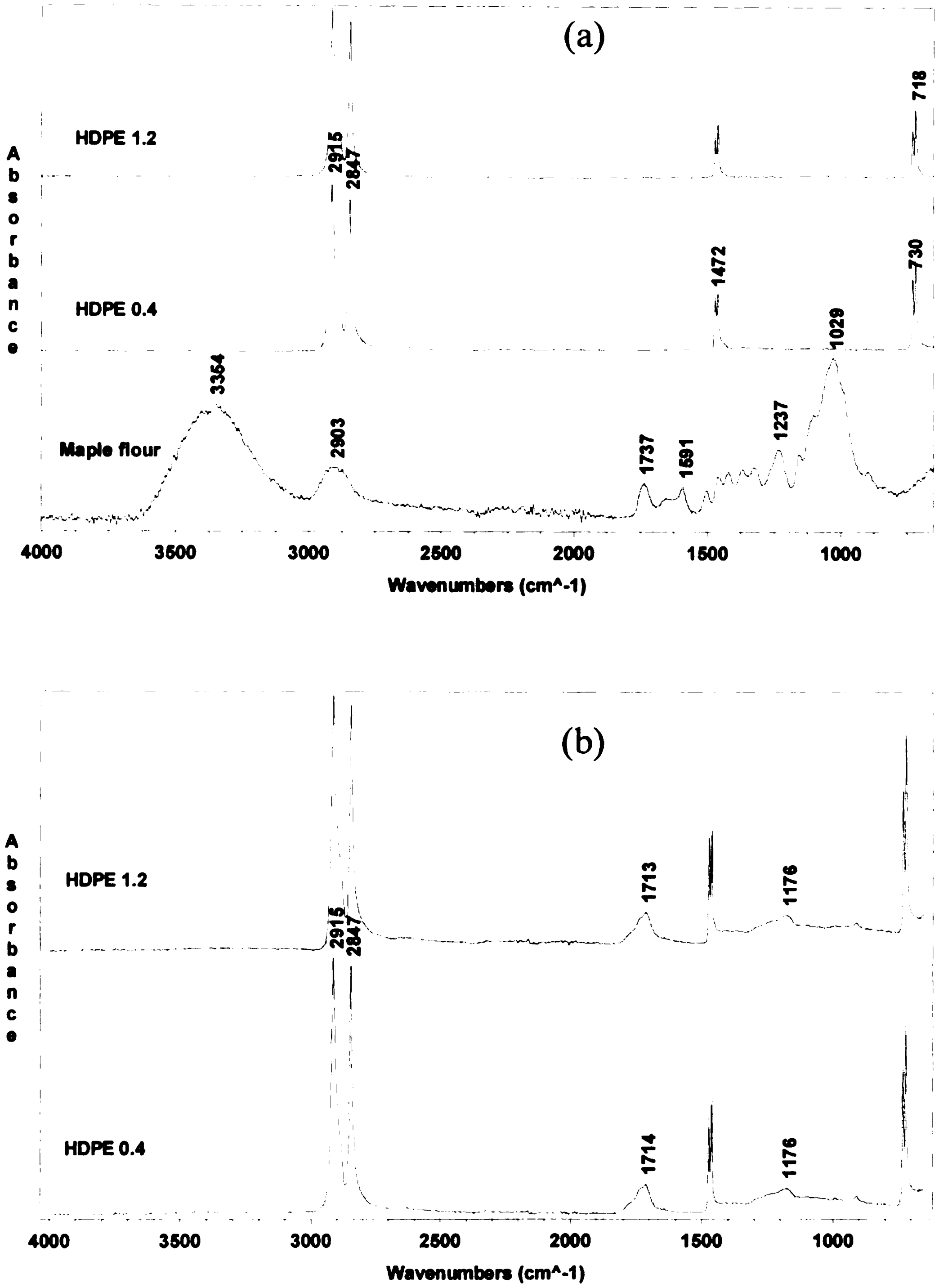

Figure 5.4. FTIR spectra of wood flour (maple) and HDPE (a) before and (b) after exposure to 1952 h UV.

Table 5.1. Assignment of absorption bands of IR spectrum.

Wavenumbers (cm^{-1})	Assignments [6-10, 36-42]
Wood	
3354	–OH stretching in hydroxyl groups originating mainly from cellulose
2903	CH stretching in $-CH_2-$ groups
1729-1737	C=O stretching (ester carbonyl)
1714-1717	C=O stretching (acid carbonyl)
1591	Aromatic ring stretching (lignin)
1029	C-O stretch in cellulose and deformation in the primary alcohols of lignin
HDPE	
2915	CH_2 stretching of CH_2, CH_3 (asym.)
2847	CH_2 stretching (sym.)
1713	C=O stretching (acid carbonyl)
1472	CH_2 deformation (scissor vibration), crystalline
1462	CH_2 deformation (scissor vibration), amorphous
730	CH_2 rocking vibration, crystalline
718	CH_2 rocking vibration, amorphous

The infrared spectra of uncapped and coextruded composites are illustrated in Figures 5.5 and 5.6, respectively. Before exposure, both uncapped (spectrum a in Figure 5.5) and coextruded (spectrum a in Figure 5.6) composite surfaces combined the characteristics of wood particles and HDPE matrices (Figure 5.4). However, evidence of photodegradation to the surface of composites was apparent in the spectra of UV-weathered samples (spectra (b) to (f) in Figures 5.5 and 5.6). The main spectral changes are seen at around 3300-3354 cm^{-1}, 1714-1738 cm^{-1}, and 1029-1033 cm^{-1} frequency ranges, which are characteristics to wood components [8].

Uncapped composite surface (Figure 5.5) experienced a fast and severe wood component loss after exposure to accelerated UV/water spray weathering than the coextruded counterparts (Figure 5.6). Unlike coextruded composite surface, a significant decrease in the intensity of peaks at 3300-3354 cm^{-1} (OH in cellulose) and 1029-1033 cm^{-1} (C–O in cellulose and primary alcohols of lignin) occurred on the surface uncapped composites even after only 192 h exposure and these peaks almost disappeared as the weathering exposure time increased. Wood index data listed in Table 5.2 support these findings. It is believed that water spray cycle during weathering washed away the loose wood components (lignin decay) and the presence of microcracks provided a channel for their fast removal on the surface of the uncapped composites.

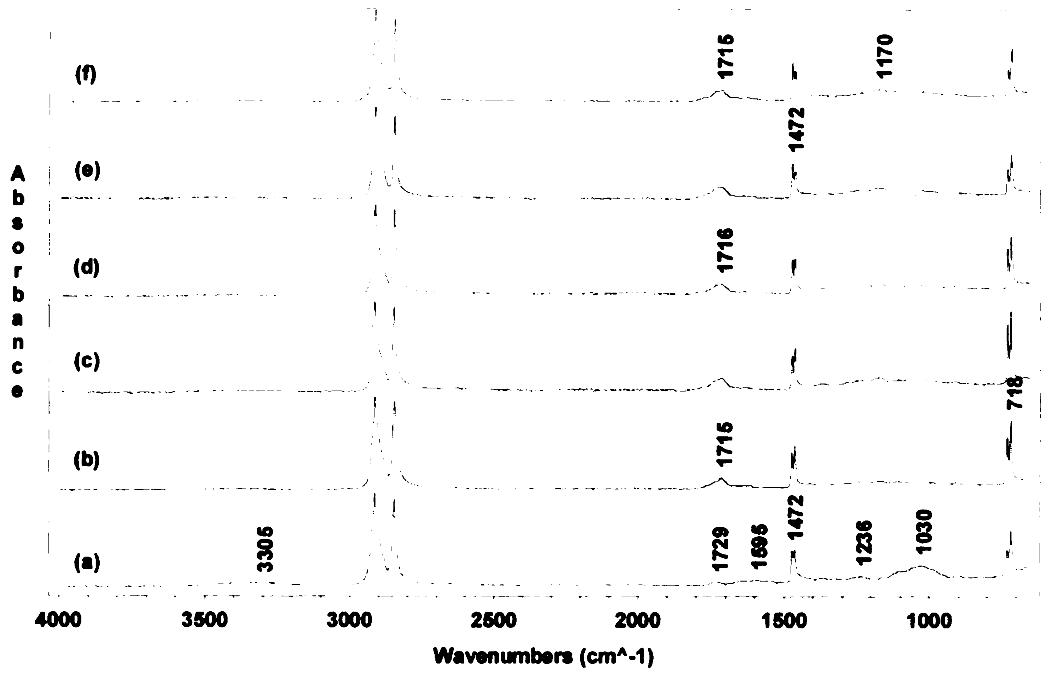

Figure 5.5. FTIR of the surface of uncapped WPCs as a function of weathering time (a) unexposed or control, (b) 192 h, (c) 432 h, (d) 744 h, (e) 1392 h, and (f) 1952 h.

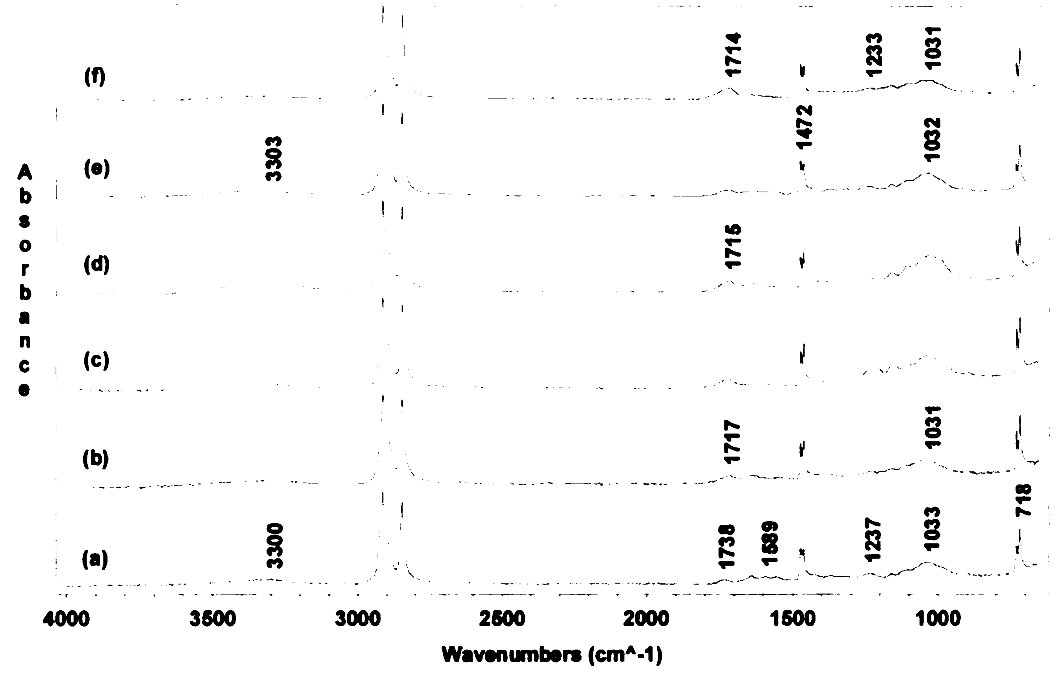

Figure 5.6. FTIR of the interface of coextruded WPCs as a function of weathering time (a) unexposed or control, (b) 192 h, (c) 432 h, (d) 744 h, (e) 1392 h, and (f) 1952 h.

Table 5.2. Concentrations of oxidative products on uncapped and coextruded WPCs.

Exposure times (h)	Wood index (%)		Carbonyl index (%)	
	Uncapped WPCs	Coextruded WPCs	Uncapped WPCs	Coextruded WPCs
0	21	30.8	6.6	8.8
432	0	36.4	16.4	11.9
1392	0	37.3	19.7	15.8
1952	0	26.7	18.8	19.0

Although there were cracks on the surface of coextruded composite as shown in Figure 5.2, the presence of a thin HDPE cap layer onto composite still prevented loose wood components from being removed by the water spray as indicated by the intensity peak at 1029-1033 cm^{-1} (Figure 5.6) and percent wood index (Table 5.2), which remained almost unchanged in coextruded composites. Two main reasons could account for the coextruded composite surface to undergo the least wood components loss: (i) the presence of HDPE cap layer reduced the oxygen available for oxidation at the interface between the inner and outer layers of coextruded composites and (ii) HDPE cap absorbed some UV energy (Figure 5.3 shows that $HDPE_{1.2}$ absorbed 15-25% light in the UVA-340 irradiance region) to cause photodegradation.

Furthermore, composites experienced surface oxidation, irrespective of the cap layer. This can be clearly seen by the increased carbonyl index (Table 5.2) and area under the absorption bands in the region 1650-1750 cm^{-1}, assigned to carbonyl groups in carboxylic acid, acetyl ester, or quinine (Figures 5.5 and 5.6). Photodegradation of lignin leads to the formation of these carbonyl groups and thus the increase in intensity of the carbonyl bands. Several authors have correlated the increased integrated area or peak height of this band and carbonyl index with the oxidative photodegradation of polymer [43, 44], wood [15-17], and wood-plastic composites [9 10, 14] due to the presence of oxygenated products.

The results obtained from XPS spectroscopy analysis provided supporting evidence of lignin decay and formation of oxygenated products on composite surfaces. Table 5.3 summarizes the atomic concentrations of oxidized carbons, i.e., carbon atoms connected to oxygen atoms (C2, C3, and C4) and unoxidized carbon (Cl) obtained from the assignment and ratios of various peak components calculated from the decomposed C_{1s} peak. The C1 atomic ratio decreased after weathering, indicating lignin decay on the surface of composites, which was accompanied by a significant increase in the concentration of oxidized carbon atoms (C2 + C3 + C4) or the degree of surface oxidation (C_{ox}/C_{unox}). These results suggest the presence of surface rich in oxygenated products such as functional carbonyl groups of wood particles detected in FTIR spectra (Figures 5.5 and 5.6). The degree of surface oxidation showed two distinct trends. For uncapped composites, it increased with exposure time, reaching a maximum value at 192 h, after which it decreased. This was expected because of wood components were washed away during weathering. In contrast, the degree of surface oxidation steadily increased in coextruded because the cap layer prevented removal of loose wood components on the surface of the samples.

Table 5.3 C1s peak analysis at WPCs surface and coextruded WPCs interface determined by high-resolution XPS scan.

Carbon types	Exposure times (h)					
	0	192	432	744	1392	1952
Uncapped WPC (control)						
C1	93.6	70.7	78.0	75.4	81.8	78.7
C2	4.5	15.8	12.8	13.4	11.0	15.3
C3	2.4	7.8	4.0	7.2	3.8	4.6
C4	-	5.7	3.2	4.0	3.5	1.4
C_{ox}/C_{unox}	0.08	0.42	0.26	0.33	0.22	0.27
Coextruded composites						
C1	90.5	87.1	86.9	86.6	83.8	82.4
C2	7.2	10.2	10.9	10.0	11.4	12.6
C3	2.3	2.0	2.1	2.8	3.4	3.4
C4	0	0.7	0.1	0.6	1.4	1.6
C_{ox}/C_{unox}	0.11	0.15	0.15	0.16	0.19	0.21

5.4.2 Color analysis

Figure 5.7 illustrates the visual appearance of uncapped and coextruded composites before and after weathering and Table 5.4 summarizes the color parameters measured on these samples.

Before weathering, the presence of cap layer did not affect the color of coextruded composites since both uncapped WPCs (control) and coextruded samples had similar visual appearance (Figure 5.7). The lightness (L*), red-green (a*) and yellow-blue (b*) color coordinates of unexposed samples confirm this observation since both uncapped and coextruded composites had similar lightness and chromaticity values (Table 5.4). The transparency of the thin $HDPE_{1.2}$ film coextruded onto the composites could account for the appearance similarities between the uncapped and coextruded composites before exposure to UV radiation. However, exposure to UV radiation resulted in two distinct trends in the visual appearances of the samples (Figure 5.7). The surface of uncapped WPC (control) lightened continuously upon UV radiation, as indicated by a constant increase in L* value and significant loss in both redness (a*) and yellowness (b*) (Figure 5.7 and Table 4). Conversely, the discoloration of coextruded composites occurred in two different stages. They first darkened up to approximately 744 h of UV exposure and then experienced lightening as the exposure time increased (Figure 5.7). The values of lightness, redness, and yellowness listed in Table 5.4 confirm this opposite trend. Darkness and yellowness observed in this stage of degradation of coextruded composites could be attributed to quinone chromophoric structures generated by the photodegradation of lignin [15, 45, 46] whereas redness is controlled by the extractive contents in wood [45].

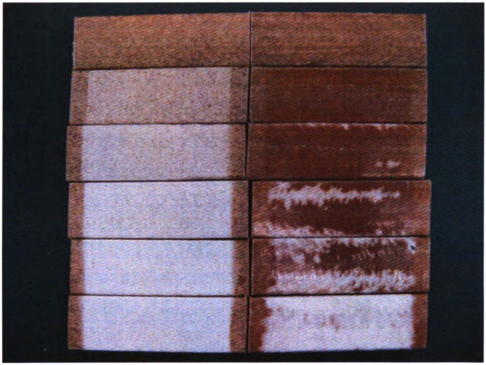

Figure 5.7. Visual appearance of uncapped WPCs (left column) and coextruded WPCs (right column) as a function of weathering exposure times (0, 192, 432, 744, 1392, 1952 h).

Table 5.4 Color parameters of control and coextruded samples before and after weathering.

Color parameters	Exposure times (h)					
	0	192	432	744	1392	1952
Uncapped WPC (control)						
L*	59.4	70.8	81.3	83.2	84.9	88.1
a*	7.0	4.7	2.8	2.1	0.9	1.1
b*	18.2	13.1	9.3	6.5	3.4	3.9
ΔE	-	12.6	24.0	27.0	30.1	32.3
Coextruded composites						
L*	55.7	50.6	50.4	49.2	51.8	62.9
a*	7.2	10.0	10.5	10.9	9.8	2.0
b*	17.8	20.5	19.2	17.9	13.3	5.6
ΔE		6.2	6.4	7.5	6.4	15.1

Color characteristics of solid wood (maple wood) and neat HDPE bars exposed to UV radiation and water condensation were measured to understand this opposite trend. Figure 5.8 illustrates the discoloration as well as the changes in lightness, yellowness, and redness of these samples as a function of UV radiation time. While UV radiation had a small influence on the discoloration of HDPE films, it significant impacted the surface of solid wood (Figure 5.8), suggesting that wood components made major contribution to the color changes in both uncapped and coextruded composites. Since the cap layer ($HDPE_{1.2}$) did not fade too much and the ultraviolet light penetrates the transparent film (Figure 5.3), discoloration of coextruded composites could have occurred at the interface between the wood plastic composites in the inner layer and the $HDPE_{1.2}$ in the outer layer.

Overall, the surface of uncapped composites (control) experienced a quick lightening with a loss of yellowness and redness and underwent more discoloration (ΔE) than coextruded counterparts (Table 5.4) due to the photodegradation of wood components (Figure 5.8). Uncapped composites experienced quicker lightening because water spray and condensation facilitated the removal of degraded wood component and formation of cracks, thus accelerating fading. The loss of degraded wood components on the surface of weathered composites could not be prevented due to poor adhesion between the filler and matrix [8].

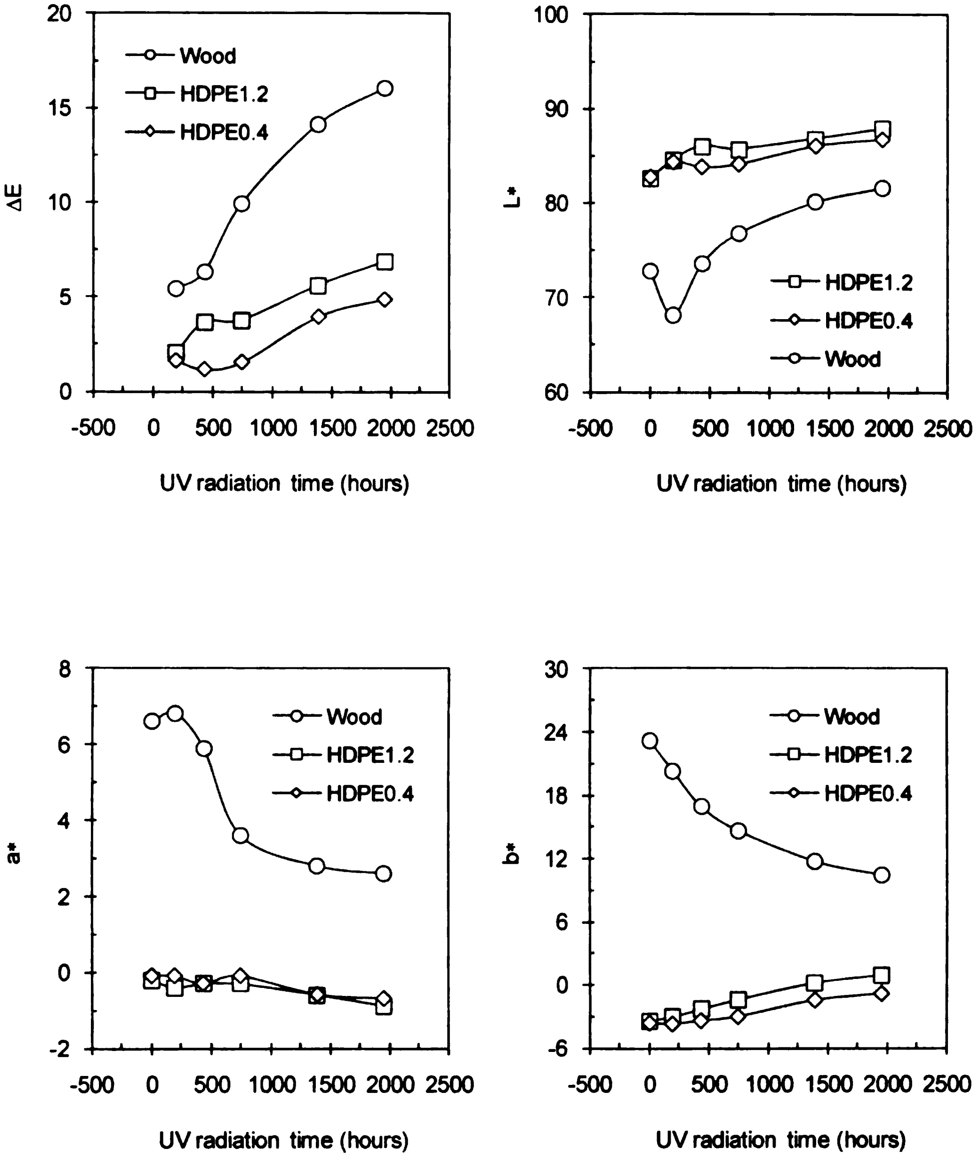

Figure 5.8. Color parameters for solid wood (maple), $HDPE_{0.4}$ and $HDPE_{1.2}$.

However, for coextruded composites, the cap layer prevented both the removal of both degraded wood components and wood flour from the surface of weathered samples. Consequently, color change of coextruded composites was mainly dependent on photochemistry reactions occurring at the interface, which resulted in darkening other than lightening. Moreover, the darkening of coextruded WPCs clarified the mechanism of fading observed in uncapped wood plastic composites (control). Photooxidation of wood components itself would not lead to the fading of uncapped composites since fading occurs primarily due to the loss of colored components at the surface as well as the increase in roughness [47, 48].

Conversely, the surface of coextruded composites initially darkened and then lightened with the failure of the cap layer. Darkening is due to the degradation of WPCs at the interface underneath the $HDPE_{1.2}$ cap layer since the hydrophobic HDPE cap layer prevented removal of degraded wood components by water spray. However, the cap layer experienced a quicker failure after 744 h weathering. Since water spray eroded the surface, tensile and compressive stresses would be induced to the cap layer due to the variation of temperature and relative humidity occurring during the wet weathering cycle test [49]. Stresses damaged the cap layer integrity and accelerated the photodegradation, resulting in the formation of cracks at the cap layer and delamination between the cap layer and the core layer (Figure 5.2). Moreover, after water entered the interface through cracks, it washed away the water-soluble degraded wood component, thus causing the fading of composites underneath the cap layer of coextruded samples.

Figure 5.9 shows the micrographs of HDPE cap layer in the "white" area and "brown" area at the surface of coextruded samples weathered for 1392 h. Large and deep cracks were present in "white" area (Figure 5.9(a)), implying that water could reach the interface through these cracks and wash away degraded wood components. It is believed that cracks at the surface of the HDPE cap layer caused light diffusion, resulting in a whitening effect. Therefore, both the cap layer and the interface made contributions to fading in the "white" area. By contrast, only small and narrow surface cracks were present in the "brown" area (Figure 9(b)), which made it difficult for water to penetrate the interface through these areas. Thus the color in these areas appeared brown instead of white because most of chromophoric compounds generated by photodegradation of lignin were not removed from the interface between the core and cap layers.

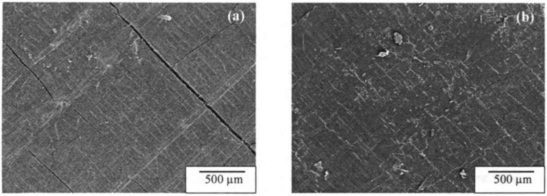

Figure 5.9. Micrograph of HDPE cap layer in "white" area (a) and "brown" area (b) at the surface of weathered coextruded samples.

5.4.3. Discoloration mechanisms of WPCs

The results of this study indicate that the discoloration mechanisms of WPCs depend on the degree of the encapsulation of the fiber by matrix and are related to whether the degraded wood components remain or not on the surface of WPCs upon UV weathering.

For uncapped WPCs, photooxidation of wood components combined with the loss of degraded wood components due to water spray constitute the main factors for fading, i.e., continuous lightening of WPCs during weathering. The increased roughness of surface due to the degradation of polymer matrix could also account for the continuous fading of uncapped WPCs.

Coextruded composites darken first because the hydrophobic cap layer over WPCs prevented water/moisture to penetrate the wood-plastic composites underneath the outer layer to wash away water soluble extractives from wood and/or other chromophoric compounds generated by photodegradation of lignin. This action reduces the negative effect of water on weathering. In contrast, as the exposure time increases, the cap layer cracks, water penetrates the interface washing away water soluble extractives from wood, leading to the lightening of the interface.

These results suggest that the discoloration of WPCs upon UV weathering is a combination of both chemical and physical changes. Chemical changes are induced by the photooxidation of wood components, which determines the initial color change. The composites become dark and yellow if the adhesion between fibers and matrix is strong to prevent surface erosion and removal of degraded wood components. Otherwise, the loss of degraded wood components could occur, and if combined with the degradation of polymer matrix which increases the roughness of WPC surface, leading to in fading of the WPC surface. Therefore, whether the degraded wood components remain on the surface of WPCs or not would determine the direction of the long-term color change of WPCs upon UV weathering.

Based on these proposed mechanisms, several weathering-induced discoloration phenomena reported in literature could be explained. Investigations have shown that PVC-based WPCs darken after UV radiation [6] whereas polyolefin-based WPCs lighten [11-13, 22]. Owing to PVC polarity, it is believed that the interfacial adhesion between wood fiber and polymer matrix is much better in PVC-based WPCs than that in polyolefin-based counterparts, making the removal of wood components more difficult on the surface of PVC-based WPCs during the weathering [6]. On the contrary, wood components are easily washed away on the surface of polyolefin-based WPCs upon UV radiation/water spray cycle, leading to fading. It appears that strong adhesion between wood fiber and polymer matrix would reduce the loss of wood components upon weathering. Consequently, the extent of wood fiber encapsulation by the polymer matrix is crucial for the discoloration of WPCs. Generally, lower the wood flour content, better the fiber encapsulation by the matrix, resulting in less fading for polyolefin-based WPCs [11-13, 22] or more darkening for PVC-based WPCs [6].

5.5. Conclusions

Both noncoextruded and coextruded WPCs with a clear HDPE cap layer were exposed to accelerated weathering cycles including UV radiation, water spray, and condensation. The color, functional groups, and degree of oxidation of samples before and after weathering were analyzed by chroma meter, FTIR-ATR, XPS, and UV vis. The following conclusions can be drawn from the experimental results:

The color of noncoextruded and coextruded WPCs upon weathering changed in different directions, revealing the discoloration mechanism of WPCs.

Overall, the surface of uncapped composites (control) experienced a quick lightening with a loss of yellowness and redness and underwent more discoloration (ΔE) than coextruded counterparts due to the photodegradation of wood components. Uncapped composites experienced quicker lightening because water spray and condensation facilitated the removal of degraded wood component and formation of cracks, thus accelerating fading. The loss of degraded wood components on the surface of weathered composites could not be prevented due to poor adhesion between the filler and matrix. This mechanism indicates the critical role of wood fiber-polymer matrix interface adhesion on the discoloration of WPCs.

Conversely, the surface of coextruded composites initially darkened and then lightened with the failure of the cap layer. Darkening is due to the degradation of WPCs at the interface underneath the HDPE cap layer since the hydrophobic HDPE cap layer prevented removal of degraded wood components by water spray. However, the cap layer experienced a quicker failure after 744 h weathering. Since water spray eroded the surface, tensile and compressive stresses would be induced to the cap layer due to the variation of temperature and relative humidity occurring during the wet weathering cycle test. Stresses damaged the cap layer integrity and accelerated the photodegradation, resulting in the formation of cracks at the cap layer and delamination between the cap layer and the core layer. Moreover, after water entered the interface through cracks, it washed away the water-soluble degraded wood component, thus causing the fading of composites underneath the cap layer of coextruded samples.

Overall, the hydrophobic cap also prevented wood fiber access to moisture/water, reducing the negative effect of water on weathering. Moreover, the cap layer absorbed some UV light and reduced the availability of oxygen at the interface of coextruded composites, thus decreasing the photodegradation rate. The decreased lignin degradation rate and the oxidation rate at the interface of coextruded WPCs were demonstrated by FTIR and XPS spectra, respectively.

5.5 Acknowledgements

The authors gratefully acknowledge the USDA-CSREES Grant-Advanced Technology Applications to Eastern Hardwood Utilization (Grant No. 2008-34158-19510) for the financial support for this research work.

5.6 References

1. J.M. Pilarski and L.M. Matuana, Durability of wood flour-plastic composites exposed to accelerated freeze-thaw cycling. Part I. Rigid PVC matrix, *Journal of Vinyl & Additive Technology*, **11**(1): 1-8 (2005).
2. J.M. Pilarski and L.M. Matuana, Durability of wood flour-plastic composites exposed to accelerated freeze-thaw cycling. II. High density polyethylene matrix, *Journal of Applied Polymer Science*, **100**(1): 35-39 (2006).
3. B. Dawson-Andoh, L.M. Matuana, and J. Harrison, Mold susceptibility of rigid PVC/wood-flour composites, *Journal of Vinyl & Additive Technology*, **10**(4): 179-186 (2004).
4. B. Dawson-Andoh, L.M. Matuana, and J. Harrison, Susceptibility of high density Polyethylene/wood-flour composite to mold discoloration, *Journal of the Institute of Wood Science*, **17**(2): 114-119 (2005).
5. J. Markarian, Wood-plastic composites need protection, *Plastics Engineering*, **63**(7):54-56 (2007).
6. L.M. Matuana and D.P. Kamdem, Accelerated ultraviolet weathering of PVC/wood-flour composites, *Polymer Engineering and Science*, **42**(8): 1657-1666 (2002).
7. L.M. Matuana, D.P. Kamdem, and J. Zhang, Photoaging and Stabilization of rigid PVC/wood-fiber composites, *Journal of Applied Polymer Science*, **80**(11): 1943-1950 (2001).
8. N.M. Stark and L.M. Matuana, Characterization of weathered wood–plastic composite surfaces using FTIR spectroscopy, contact angle, and XPS, *Polymer Degradation and Stability*, **92**(10): 1883-1890 (2007).
9. N.M. Stark and L.M. Matuana, Surface chemistry and mechanical property changes of wood-flour/high-density-polyethylene composites after accelerated weathering, *Journal of Applied Polymer Science*, **94**(6): 2263-2273 (2004).
10. N.M. Stark and L.M. Matuana, Surface chemistry changes of weathered HDPE/wood-flour composites studied by XPS and FTIR spectroscopy, *Polymer Degradation and Stability*, **86**(1): 1-9 (2004).
11. N.M. Stark, Effect of weathering cycle and manufacturing method on performance of wood flour and high-density polyethylene composites, *Journal of Applied Polymer Science*, **100**(4): 3131-3140 (2006).
12. N.M. Stark, L.M. Matuana, and C.M. Clemons, Effect of processing method on surface and weathering characteristics of wood–flour/HDPE composites, *Journal of Applied Polymer Science*, **93**(3): 1021-1030 (2004).
13. N.M. Stark and L.M. Matuana, Influence of photostabilizers on wood flour-HDPE composites exposed to xenon-arc radiation with and without water spray, *Polymer Degradation and Stability*, **91**(12): 3048-3056 (2006).

14. J.S. Fabiyi, A.G. McDonald, M. P. Wolcott, and P. R. Griffiths, Wood plastic composites weathering: visual appearance and chemical changes, *Polymer Degradation and Stability*, **93**(8): 1405-1414 (2008).

15. W.C. Feist and D.N.-S. Hon, *Chemistry of weathering and protection*, U.S. Department of Agriculture, Madison, (1984).

16. U. Müller, M. Ratzsch, M. Schwanninger, M. Steiner, and H. Zöbl, Yellowing and IR-changes of spruce wood as result of UV-irradiation, *Journal of Photochemistry and Photobiology B Biology*, **69**(2): 97-105 (2003).

17. K.K. Pandey, Study of the effect of photo-irradiation on the surface chemistry of wood, *Polymer Degradation and Stability*, **90**(1): 9-20 (2005).

18. K.K. Pandey, A note on the influence of extractives on the photo-discoloration and photo-degradation of wood, *Polymer Degradation and Stability*, **87**(2): 375-379 (2005).

19. H. Zweifel, *Plastic additives handbook*, Hanser Gardner, Cincinnati, (2000).

20. S. Girois, P. Delprat, and J. Verdu, Oxidation thickness profiles during photooxidation of non-photostabilized polypropylene, *Polymer Degradation and Stability*, **56**(2):169-177 (1997).

21. I. Yakimets, D. Lai, and M. Guigon, Effect of photo-oxidation cracks on behaviour of thick polypropylene samples, *Polymer Degradation and Stability*, **86**(1): 59-67 (2004).

22. N.M. Stark and S.A. Mueller, Improving the color stability of wood-plastic composites through fiber pre-treatment. *Wood and Fiber Science*, **40**(2): 271-278 (2008).

23. D. Ndiaye, E. Fanton, S. Morlat-Therias, L.Vidal, A. Tidjani, and J.L. Gardette, Durability of wood polymer composites: Part 1. Influence of wood on the photochemical properties. *Composites Science and Technology*, **68**(3): 2779-2784 (2008).

24. M. Muasher and M. Sain, The efficacy of photostabilizers on the color change of wood filled plastic composites, *Polymer Degradation and Stability*, **91**(5): 1156-1165 (2006).

25. N.M. Stark and L.M. Matuana, Ultraviolet weathering of photostabilized wood-flour-filled high density polyethylene composites, *Journal of Applied Polymer Science*, **90**(10): 2609-2617 (2003).

26. B. George, E. Suttie, A. Merlin, and X. Deglise, Photodegradation and photostabilisation of wood–the state of the art, *Polymer Degradation and Stability*, **88**(2): 268-274 (2005).

27. S.T. Chang and P.L. Chou, Photodiscoloration of UV-curable acrylic coatings and the underlying wood, *Polymer Degradation and Stability*, **63**(3): 435-439 (1999).

28. P.L. Chou, H.T. Chang, T.F. Yeh, and S.T. Chang, Characterizing the conservation effect of clear coatings on photodegradation of wood, *Bioresource Technology*, **99**(5): 1073-1079 (2008).

29. S.T. Chang and P.L. Chou, Photodiscoloration inhibition of wood coated with UV-curable acrylic clear coatings and its elucidation, *Polymer Degradation and Stability*, **69**(3): 355-360 (2000).

30. L. Long L, M.P. Wolcott, J. Zhang, and K. Englund. Flexural properties of surface reinforced wood/plastic deck board, *Polymer Engineering and Science*, **47**(3):281-288 (2007).

31. C. Rauwendaal, *Understand extrusion*, Hanser Gardner, Cincinnati, (1998).

32. H.J. Giles Jr., J.R. Wagner Jr., and E.M. Mount III, *Extrusion: The Definitive Processing Guide and Handbook*, William Andrew Publishing, New York, (2004).

33. S. Jin and L.M. Matuana, Coextruded PVC/wood-flour composites with WPC cap layers. *Journal of Vinyl & Additive Technology,* **14**(4):197-203 (2008).

34. S. Jin and L.M. Matuana, Improving water resistance of wood plastic composites Through coextrusion, *SPE ANTEC Papers*, **66**: 19-23 (2008).

35. S. Jin and L.M. Matuana, Wood plastic composites coextruded with multi-walled carbon nanotube filled rigid PVC cap layer. *Polymer International*, **59**(5): 648-657 (2010).

36. M.Tsuboi, Infrared spectrum and crystal structure of cellulose. *Journal of Polymer Science*, **25**(109): 159-171 (1957).

37. K.K. Pandey KK. A study of chemical structure of soft and hardwood and wood polymers by FTIR spectroscopy, *Journal of Applied Polymer Science,* 71(1): 1965-1975 (1999).

38. Colom X, Carrillo F, Nogues F, Garriga P. Structural analysis of photodegraded wood by means of FTIR spectroscopy. *Polymer Degradation and Stability,* **80**(3): 543-549 (2003).

39. Y. Kataoka and M. Kiguchi, Depth profiling of photo-induced degradation in wood by FT-IR, *Journal of Wood Science*, **47**(4): 325-327 (2001).

40. Ohkoshi M. FTIR-PAS study of light-induced changes in the surface of acetylated or polyethylene glycol-impregnated wood. *Journal of Wood Science*, **48**(5): 394-401 (2002).

41. G. Socrates, *Infrared and Raman characteristic group frequencies*, John Wiley and Sons, New York, (2004).

42. J.E. Mark, *Physical properties of polymers handbook*, Springer, New York, (2006).

43. S.S. Fernandoa, P.A. Christensena, T.A. Egerton, and J.R. White. Carbon dioxide evolution and carbonyl group development during photodegradation of polyethylene and polypropylene, *Polymer Degradation and Stability*, **92**(12): 2163-2172 (2007).

44. L. Guadagno, C. Naddeo, V. Vittoria, C. Giovanni, and C. Cagnani, Chemical and morphologial modifications of irradiated linear low density polyethylene (LLDPE). *Polymer Degradation and Stability,* **72**(1): 175-186 (2001).

45. L. Tolvaj and O. Faix. Artificial aging of wood monitored by DRIFT spectroscopy and CIE L*a*b* color measurements I: effect of UV light. *Holzforschung*, **49**(5): 397-404 (1995).

46. A.J. Ragauskas, Photoreactivity of ligninlike quinoid structures. In: *Photochemistry of lignocellusic materials*, ACS symposium series, 531. American Chemical Society, (1993).

47. D. Benavente, F. Martínez-Verdú, A. Bernabeu, V. Viqueira, R. Fort, M.A. García del Cura, C. Illueca, and S. Ordóñez. Influence of surface roughness on color changes in building stones. *Color Research & Application*, **28**(5): 343-351 (2009).

48. M. Yonehara, T. Matsui, K. Kihara, H. Isono, A. Kijima, and T. Sugibayashi, Experimental relationships between surface roughness, glossiness and color of chromatic colored metals. *Materials Transactions,* **45**(4): 1027-1032 (2004).

49. R.A. Ryntz. *Plastics and coatings: durability, stabilization, testing*, Hanser Gardner, Cincinnati (2001).

CHAPTER 6

Conclusions and Future Work

6.1 Conclusions

Durability and flexural properties are two key issues for application of WPCs. Because WPCs absorb water through the surface, photodegradation of WPCs is surface phenomenon, and surface layers of materials suffer the maximum tensile or compressive stress when materials are bent, a durable or reinforced surface layer can improve durability or flexural properties of composites. The main objective of this study was to improve the durability (in terms of resistance to water absorption and weathering) and flexural properties of WPCs via encapsulation of WPCs by a plastic surface-rich cap layer through a coextrusion process. The following conclusions were drawn from the experimental results.

1) Wood-plastic composites can be encapsulated by a neat rigid PVC or HDPE cap layer, or a PVC-based composites (wood flour or carbon nanotube filled rigid PVC) cap layer in a coextrusion process.

2) Coextrusion of a hydrophobic polymer surface-rich cap layer over WPCs significantly increased moisture resistance of composites. Coextruded WPCs absorbed less moisture and underwent a slower moisture sorption rate than noncoextruded counterparts. While moisture resistance of coextruded WPCs was insensitive to the cap layer thickness, moisture resistance was a strong function of the amount of wood flour in the cap layer. Moisture resistance decreased with wood flour content in the cap layer. Because the surface of coextruded samples was covered by a

hydrophobic polymer, the unprotected edges provided a shortcut for moisture to diffuse into composites.

3) Coextruding a rigid PVC surface-rich cap layer on WPCs significantly increased their flexural strength but decreased their flexural modulus compared to those of noncoextruded control. This can be attributed to greater strength but lower stiffness of rigid PVC compared to WPCs. The changes in flexural properties were dependent on both the thickness of the cap layer and its wood flour content. Increasing the cap layer thickness did not affect the strength but decreased the modulus. While increasing the wood flour content increased the modulus but did not influence the strength.

4) In order to obtain coextruded composites with better flexural properties than uncapped WPCs, a two-level factorial design was used to statistically evaluate the effects of material compositions and processing conditions on these properties. Material composition variables were the wood flour content in the core layer and the carbon nanotube (CNT) content in the cap layer of coextruded composites. The processing condition variable was the processing temperature profile for the core layer. Regression models indicated all main effects and two powerful interaction effects (processing temperature/wood flour content and wood flour content/CNT content interactions) as statistically significant. Factors leading to a fast fusion of the PVC-wood flour composites in the core layer, i.e. low wood flour content and high processing temperature, were effective material composition and processing condition parameters for improving the flexural properties of coextruded composites. Reinforcing the cap layer with CNTs also produced a significant improvement in the flexural properties of the coextruded composites, no matter the core layer composition and the processing temperature condition.

5) Coextruding a transparent hydrophobic HDPE cap layer over WPCs significantly decreased the discoloration of WPCs upon accelerated artificial weathering. The surface of coextruded WPCs initially darkened and then lightened with the failure of the cap layer. Darkening is due to the degradation of WPCs at the interface underneath the HDPE cap layer since the hydrophobic HDPE cap layer prevented removal of degraded wood components by water spray. However, the cap layer experienced a quicker failure after 744 h weathering. Since water spray eroded the surface, tensile and compressive stresses would be induced to the cap layer due to the variation of temperature and relative humidity occurring during the wet weathering cycle test. Stresses damaged the cap layer integrity and accelerated the photodegradation, resulting in the formation of cracks at the cap layer and delamination between the cap layer and the core layer. Moreover, after water entered the interface through cracks, it washed away the water-soluble degraded wood component, thus causing the fading of composites underneath the cap layer of coextruded samples. Overall, the hydrophobic cap also prevented wood fiber access to moisture/water, reducing the negative effect of water on weathering. Moreover, the cap layer absorbed some UV light and reduced the availability of oxygen at the interface of coextruded composites, thus decreasing the photodegradation rate. The decreased lignin degradation rate and the oxidation rate at the interface of coextruded WPCs were demonstrated by FTIR and XPS spectra, respectively.

6.2 Future work

Coextrusion of a hydrophobic HDPE or PVC cap layer over WPCs significantly decreased the moisture sorption, which is critical for microbial degradation and photodegradation of WPCs. The role of polymer-rich cap layer in the biological resistance of WPCs needs investigation. The influences of biocide concentration in the cap layer and fungal exposure types and duration on the decay resistance of both control and coextruded WPCs need to be evaluated to gain an in depth understanding of the role of encapsulation in the biological resistance of WPCs.

Although coextrusion of a transparent hydrophobic HDPE cap layer over WPCs reduced the discoloration rate compared to the noncoextruded counterparts upon accelerated artificial weathering, both HDPE cap layer and interface between cap layer and core layer experienced photodegradation. Thus it is necessary to add UV light stabilizers (UV absorbers and HALS) into cap layer to protect both the cap layer and interface underneath the cap layer against photodegradation.

Moreover, coextruded WPCs with UV light stabilizers or biocides filled cap layer should be compared to noncoextruded WPCs filled with UV lighter stabilizers or biocides in the entire composites in terms of weathering or decay resistance. The results of comparison would test whether providing a protective cap layer is more efficient to improve durability than adding preservatives to the entire composites.

In this study, we primarily focused on the properties of the cap and the core layer but the influence of the interface between the cap and the core layer on the properties of coextruded WPCs should not be ignored. The interface between the cap and the core layer was already found to provide a shortcut for water sorption. The role of the interface in flexural properties should be studied.